PhD degree in Systems Medicine (curriculum in Molecular Oncology)

European School of Molecular Medicine (SEMM),

University of Milan and University of Naples "Federico II"

Settore disciplinare: BIO/13

NANOPARTICLES FOR MUCOSAL VACCINE DELIVERY

Catarina Fortuna dos Remédios

IEO, Milan

Matricola n. R10760

Supervisor: Prof. Maria Rescigno

IEO, Milan

Anno accademico 2016-2017

TABLE OF CONTENTS

LIST OF ABBREVIATIONS

AF   Alexa Fluor

APC   Antigen-presenting cell

APRIL   Proliferation-inducing ligand

BAFF   B cell activating factor

CFSE   Carboxyfluorescein succinimidyl ester

CmgA   Chromogranin A

CSR   Class-switch recombination

CT   Cholera toxin

CX_3CR1 CX_3C chemokine receptor 1

DAPI   4',6-diamidin-2-fenilindolo

DC   Dendritic cell

DiD   1.1′-dioctadecyl-3,3,3′,3′-tetramethylindodicarbocyanine perchlorate

DMEM   Dulbecco's Modified Eagle Medium

DPPG   1,2-dipalmitoyl-sn-glycero-3-phosphatidylglycerol

DSS   Dextran sodium sulfate

EDTA   Ethylenediaminetetraacetic acid

FAE   Follicle-associated epithelium

FBS   Fetal bovine serum

FITC   Fluorescein isothiocyanate

Foxp3	Forkhead box P3
GALT	Gut-associated lymphoid tissue
GFP	Green fluorescent protein
GI	Gastrointestinal
GM-CSF	Granulocyte-macrophage colony stimulating factor
GP2	Glycoprotein 2
IFN	Interferon
Ig	Immunoglobulin
IL	Interleukin
ILF	Isolated lymphoid follicles
LPS	Lipopolysaccharides
LYS	Lysozyme
M-CSF	Macrophage-colony stimulating factor
MDP	Macrophage-dendritic cell precursor
mLN	Mesenteric lymph nodes
MUC	Mucin
NF-κB	Nuclear factor kappa B
NK	Natural killer
NLR	Nucleotide-binding domain and leucine-rich repeat containing receptor
NOD2	Nucleotide-binding oligomerization domain-containing protein 2
NP+	Polysaccharidic cationic nanoparticles
NPL	Polysaccharidic lipidated nanoparticles

OVA	Ovalbumin
PAMP	Pathogen-associated molecular pattern
PBMC	Peripheral blood mononuclear cell
PBS	Phosphate-buffered saline
PMA	Phorbol myristate acetate
PP	Peyer's patches
PrP^C	Cellular prion protein
PRR	Pattern Recognition Receptor
RA	Retinoic acid
RLR	Retinoic acid-inducible gene-I-like receptor
SDS-PAGE	Sodium dodecyl sulfate polyacrylamide gel electrophoresis
SED	Sub-epithelial dome
TGF-β	Transforming growth factor-β
Th	Helper T cell
TLR	Toll-like receptor
TNF	Tumor necrosis factor
Treg	Regulatory T cell
TRITC	Tetramethylrhodamine-5-isothiocyanate
TSLP	Thymic stromal lymphopoietin

FIGURES INDEX

TABLES INDEX

ABSTRACT

Influenza is a contagious respiratory disease often disregarded due to the mild symptoms associated with it. The economic burden that flu cases impose on health care systems is substantial, not only due to influenza pandemics, but also to required hospitalizations and the need for yearly revisions of seasonal influenza vaccines. The need for a universal influenza vaccine was already recognized by the Global Vaccine Action Plan.

Currently, injection-based vaccination is the most common method for influenza immunization. However, evidence has shown that mucosal immune responses, representing an important first line of defense at these sites, since most pathogens enter the body through mucosal tissues, are most efficiently induced by administration of vaccines onto mucosal surfaces than injected vaccines. From the different mucosal tissues, the gastrointestinal tract is an attractive route to be explored for vaccination; nonetheless, oral influenza vaccines are not available yet.

The intestinal homeostasis is tightly controlled by several components of the intestinal barrier, such as the mucus layer, epithelial cells with different functions and an underlying immune system that surveys the gut. Between microorganisms that normally inhabit our gut, food antigens constantly present in our diet and potential pathogens, the intestinal barrier has the difficult task of integrating external and internal signals received by different cells in order to establish the correct response, immunity or tolerance, according to the antigen. Hence, oral vaccines will encounter these same intestinal barrier components and face the same obstacles as any other oral antigen or gut microorganism.

The UniVacFlu consortium is currently working to develop a new mucosal universal vaccine against influenza, exploring different immunogens, immunization routes and delivery systems. This study was undertaken to understand the potential of the influenza vaccine candidate CTA1-3M2e-DD and polysaccharidic lipidated nanoparticles (NPL) when immunization occurs through the oral route.

We found that, while CTA1-3M2e-DD revealed a poor ability to cross the intestinal epithelium and target intestinal antigen-presenting cells, NPL were found to readily overcome the intestinal barrier and were found associated with both CX_3CR1^+ macrophages and $CD103^+$ dendritic cells. Two different routes of NPL uptake were identified: one depends on Goblet cell-associated passages that allow the transfer of high amounts of NPL from the lumen to the intestinal lamina propria; the second relies on the direct acquisition of NPL by CX_3CR1^+ macrophages in Peyer's patches by extension of trans-epithelial dendrites. Moreover, NPL as an oral vaccine vector was able to deliver the loaded antigen in the intestinal lamina propria and enhanced antigen presentation to $CD4^+$ T lymphocytes in different organs. Despite increasing the availability of antigen, NPL did not induce tolerance towards the formulated antigen and a Th1 immune response was found at the level of the Peyer's patches. We also identified the contribution of the starvation period in the immune response induced by the NPL formulation in our model of oral immunization. The full potential of NPL as a vaccine vector is currently being further investigated to understand its immunomodulatory properties.

1 INTRODUCTION

1.1 Intestinal homeostasis

The gastrointestinal (GI) tract is continuously challenged by a variety of environmental agents and has developed different mechanisms to maintain tissue homeostasis. Here, food antigens and microbes are introduced every day. In fact, 10^{14} bacteria are present in the human intestine, represented by approximately 1000 different species [1]. The intestinal microbiota has developed a symbiotic relationship with the host, benefitting from nutrients provided by the host and providing the host with degradation products and other dietary factors [2]. At the same time, the intestine also has to deal with pathogens and harmful agents introduced via the oral route. Such high antigen load represents a potent activation stimulus that the immune system has to tolerate or react against. To interact with all these agents, the organism has developed a complex barrier that protects from pathogens and simultaneously promotes tolerance towards the commensal microflora [2]. The different chemical and physical components of the intestinal barrier that allow such adaptability will be further detailed in the next sections.

1.1.1 The intestinal barrier

1.1.1.1 Mucus layer

The mucus layer is the first barrier separating the host from the external world at mucosal surfaces. Throughout the GI tract, the characteristics of the mucus layer fluctuate according to the physiology and environment of each region. For instance, the mucus layer lining the stomach is extremely thick, as it should protect the epithelium against the acidic pH; in the intestine, this layer is thinner, allowing the absorption of digested nutrients [3]. Variations in mucus properties also occur in the different intestinal segments. The small intestine presents a discontinuous and uneven mucus layer, whereas the colon, where the bacterial load is higher, is covered by a thicker mucus layer [3]. Here, a

compact inner layer is firmly attached to the epithelium and is sterile, while an outer and lose layer provides a colonization niche for the intestinal flora, by offering nutrients and preventing their clearance [4].

The mucus is formed by mucins, high molecular weight proteins produced and secreted by specialized epithelial cells, called Goblet cells. Mucus composition also includes other proteins, carbohydrates, salts, lipids, cellular debris, but mucin (MUC) 2 has been identified as the main component of intestinal mucus, both the inner and outer layers [4]. Being extensively glycosylated, MUC2 and other mucins confer gel-like properties to the mucus that protect against bacterial invasion and allow the concentration of various molecules (e.g. antimicrobial peptides and secretory immunoglobulin (Ig) A) close to the epithelium, helping to maintain sterility at this level [3,5].

As the first barrier encountered by microbes, the intestinal mucus layer has the dual function of providing a niche for the commensal microflora, while preventing tissue invasion by not only the later but also pathogens. The role of the mucus layer in maintaining intestinal homeostasis has been shown in MUC-deficient mouse models. Indeed, *Muc2*$^{-/-}$ mice develop spontaneous colitis at an early age [6] and are more susceptible to infectious colitis triggered by *Citrobacter rodentium* [7] and *Salmonella enterica* serovar Typhimurium [8]. Velcich and colleagues also demonstrated the contribution of MUC2 in colorectal cancer suppression [9]. Other than a barrier between the host and the intestinal flora, mucus can also exert an immunomodulatory function on intestinal antigen-presenting cells (APCs). In fact, MUC2 is able to bind dendritic cells (DCs) through galectin-3, Dectin-1 and FcγRIIB, impairing the expression of inflammatory signals via β-catenin activation and simultaneously increasing the production of tolerogenic signals leading to differentiation of regulatory T cells (Tregs) in response to lipopolysaccharides (LPS) stimulation [10].

1.1.1.2 Antimicrobial peptides

Antimicrobial peptides are small molecules able to restrain the bacterial burden in the intestine, as well as prevent an excessive contact between the epithelium and bacteria [2,11]. This group of molecules includes defensins, C-type lectins, cathelicidins, and lipocalins, which are mainly produced and secreted into the intestinal lumen by Paneth cells located at the base of intestinal crypts [11–13]. These peptides exert their function through different mechanisms, which confers flexibility in targeting different groups of bacteria. Defensins are often found to attach to the outer membrane of Gram-negative bacteria, forming a "pore-like" structure through enzymatic digestion, whereas lipocalins obstruct the acquisition of essential metals required for bacterial growth [11,14].

Production of antimicrobial peptides can occur in a constitutive manner, but can be also triggered by bacterial sensing. For example, germ-free mice are able to produce the same mature intestinal defensins as mice colonized by a normal microflora [15]. Nevertheless, production of other antimicrobial peptides has been shown to depend on recognition of bacterial factors through Toll-like receptors (TLRs) [13] or Nucleotide-binding oligomerization domain-containing protein 2 (NOD2) [16] on Paneth cells. Moreover, taking advantage of small intestine organoids, Farin and colleagues demonstrated that degranulation of Paneth cells is not entirely dependent on activation of Pattern Recognition Receptors (PRRs), but that interferon (IFN)γ produced by bacterial activated natural killer (NK) T and CD3$^+$ T cells is the trigger for lysozyme and defensin secretion [17].

Since many antimicrobial peptides share similar functions, their importance in maintaining intestinal homeostasis has been addressed using a variety of transgenic mouse models. In fact, mice depleted of Paneth cells or *Myd88*$^{-/-}$ mice (that present a decreased expression of intestinal antimicrobial peptides) show higher translocation of both commensal bacteria and pathogens, such as *S.* Typhimurium. Systemic spreading of this pathogen is also observed in these models [13]. Mice lacking the matrix metalloproteinase-7 encoding-gene (required for α-defensin proteolytic activation) also exhibit higher susceptibility to infection [18] and alterations in microbiota composition, but

not in total bacterial numbers [19]. Alterations in microbiota were found as well in transgenic mice expressing human defensin-5 [19], which seem to be more protected against *S.* Typhimurium infection [20].

1.1.1.3 Secretory IgA

The secretion of IgA, the most abundant Ig in mucosal secretions, acts as another line of defense in the intestine, controlling the translocation of bacteria across the epithelial barrier.

Induction of IgA-producing B cells occurs in different compartments of the gut-associated lymphoid tissue (GALT), namely Peyer's patches (PP), isolated lymphoid follicles (ILF) and lamina propria through various mechanisms [21]. IgA specific for the intestinal microbiota are produced upon stimulation of B cells by DCs that have sampled luminal bacteria in the PP [22] or directly from the gut lumen [23]. Also epithelial cells can induce class-switch recombination (CSR) by producing B cell activating factor (BAFF) belonging to the tumor necrosis factor (TNF) family and the proliferation-inducing ligand (APRIL) after TLR stimulation that are then recognized by their receptor on B cells [24].

T cell-independent IgA production by B cells was demonstrated by Macpherson and colleagues when DCs in the dome of PP sample the commensal flora and convey live bacteria to the draining mesenteric lymph nodes (mLN) [22]. This process allows the containment of the bacteria to the mLN, preventing bacterial dissemination through the lymphatic and blood systems. Induced IgA+ B cells can then recirculate through the mucosal tissues and home back to the gut as the result of their expression of gut homing-receptors [25]. Reaching the intestine, the IgA dimers are transported through the epithelium into the intestinal lumen via the polymeric Ig receptor present at the basolateral membrane of the epithelial cells. The "secretory" IgA is then released in the lumen by proteolysis of the extracellular domain of the polymeric Ig receptor [24].

The role of IgA in controlling intestinal microbiota has been investigated through a variety of approaches. Peterson and colleagues found that germ-free immunodeficient *Rag1*[-/-

mice administered with *Bacteroides thetaiotaomicron* show a more robust innate immune response compared to wild-type mice and to *Rag1*^{-/-} mice implanted with *B. thetaiotaomicron* specific IgA-producing hybridoma cells, suggesting the role of IgA in reducing intestinal pro-inflammatory signaling [26]. Moreover, mice deficient for Aicda and IgA present an expansion of anaerobic bacteria, including segmented filamentous bacteria, resulting in systemic hyperactivation of germinal center B cells [27,28].

1.1.1.4 Epithelium

The intestinal epithelium is a permeable barrier involved in the prevention of uncontrolled translocation of food antigens and bacteria, regulation of fluid absorption and secretion of various molecules. It is composed of a layer of columnar epithelial cells with intercellular tight junctions and adherens junctions located near the apical surface of the intestinal epithelial cells, that prevent paracellular traffic of certain molecules, whereas the brush border on the apical side avoids microbial attachment and invasion [11]. Different specialized cells are present in the epithelium and are involved in the maintenance of intestinal homeostasis. For instance, microfold cells (M cells), located in the follicle-associated epithelium (FAE) that line PP, colonic patches and ILF, are characterized by irregular microvilli on the apical membrane, and by a pocket-like microfold structure on the basal side in contact with T and B lymphocytes, macrophages and DCs [29]. The structure of these cells is consistent with their function to transport antigens. Other cells, include Goblet cells, important for the formation of the mucus layer, and Paneth cells, that produce antimicrobial peptides and have secretory functions.

The epithelium was considered for a long time just a mechanical barrier impeding the uncontrolled translocation of invading pathogens. But this limited view has been changed by the observation that the epithelium also takes an active part in immunological processes [30]. Indeed, these cells may recognize conserved pathogen-associated molecular patterns (PAMPs), which are shared by pathogenic and non-pathogenic bacteria, through expression of PRRs, sending signals to the underlying mucosa. PRRs

are classified in four main groups, namely TLRs, nucleotide-binding domain and leucine-rich repeat containing receptors (NLRs), retinoic acid-inducible gene-I-like receptors (RLRs) [31] and C-type lectin receptors (CLRs) [32]. The key mechanism to discriminate invasive pathogens, which can cross the epithelial monolayer, from the commensal microbiota, and to prevent responses to the bacterial components in the gut lumen, preserving the ability to mount responses against pathogens, is the compartmentalization of PRRs to the basolateral membrane or into the cytosol [30,33–35]. Indeed, *in vitro* studies have shown that when TLR9 is stimulated from the apical side, there is a defective activation of the nuclear factor kappa B (NF-κB) pathway and a different gene expression profile was found between cells stimulated apically and basolaterally [36]. Also, mouse models deficient for different TLRs were reported to spontaneously develop colon inflammation or increased susceptibility to experimental colitis [34,36–39].

Intestinal epithelial cells are also involved in conditioning the intestinal hypo-responsiveness of underlying APCs to harmless stimuli through the secretion of cytokines [30]. Such conditioning renders DCs "tolerogenic", that in turn induce tolerogenic T cell responses [40–42]. The opposite happens too, as in the presence of inflammatory signals, the intestinal epithelium releases inflammatory cytokines and chemokines that recruit non-educated DCs, initiating an inflammatory responses [30]. A variety of immune conditioning factors were found to be produced by epithelial cells, including transforming growth factor-β (TGF-β), retinoic acid (RA), prostaglandin E2 and thymic stromal lymphopoietin (TSLP), that have been shown to play a major role in the induction of tolerance [30].

1.1.1.5 Immune cells

The intestinal immune system, generally called GALT consists of lymphocytes scattered in the intestinal epithelium and lamina propria, as well as organized tissues, like PP, mLN and ILF, responsible for the induction of immune responses. PP and ILF can be found in the small intestine, whereas patches similar to ILF are found in the colon [43].

Between the different cell types that constitute the intestinal immune barrier, APCs play an important role in maintaining immune homeostasis. This group of cells is composed of a large number of mononuclear cells, including macrophages and DCs, and over recent years there was a growing interest in characterizing these different subpopulations of phagocytes and their role in regulating mucosal innate and adaptive immune responses, in both the steady-state and inflammatory conditions. In the small intestine lamina propria, two main populations of developmentally and functionally non-overlapping phagocytes have been described and can be distinguished by their expression of CX_3CR1 and CD103 [44,45] (Fig. 1.1). These two populations will be further described in the next sections.
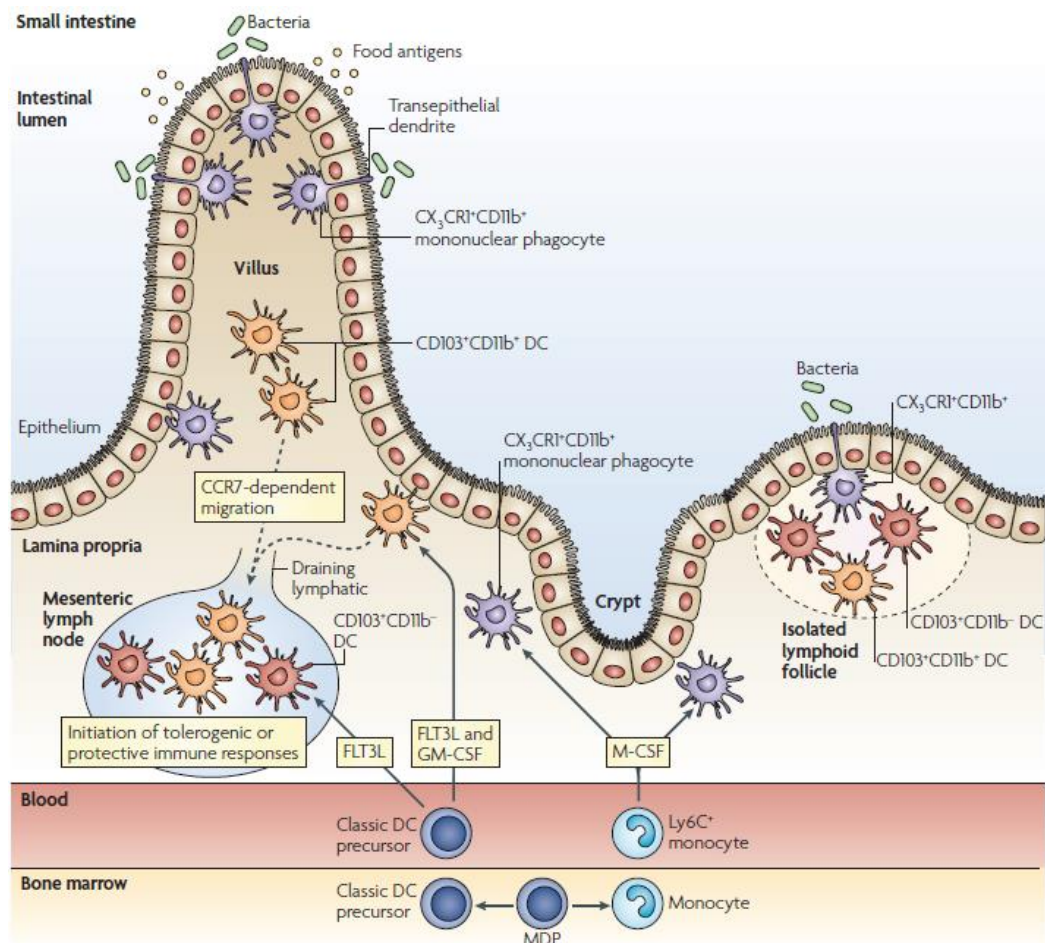
Figure 1.1. Origin, phenotype and function of the main subsets of intestinal APCs.

The common macrophage-dendritic cell precursor (MDP) gives rise to classic DC precursors and monocytes in the bone marrow. From these, classic DC precursors differentiate into CD103^{+} lamina propria DCs, that can give rise to a CD11b^{-} and a CD11b^{+} populations, and Ly6C^{+}

monocytes differentiate into CX_3C chemokine receptor 1 $(CX_3CR1)^+$ lamina propria mononuclear phagocytes. Adapted from *Varol et al., Nature Reviews Immunology, 2010* [46].

1.1.1.5.1 CX_3CR1^+ macrophages

CX_3CR1, also known as Fractalkine receptor, is mainly involved in leukocyte adhesion and migration and its main ligand CX_3CL1 is mostly expressed by epithelial and endothelial cells in the intestine [47,48]. The expression of this receptor has been associated with a subset of lamina propria phagocytes able to form trans-epithelial projections and capture luminal bacteria, such as *Salmonella enterica* [23,49–51]. This characteristic depends on the expression of the Fractalkine receptor and requires the involvement of epithelial cells forming tight junction-like structures, as demonstrated in experiments with bone marrow chimeras [50].

Initially, and due to the lack of specific markers to unequivocally classify DCs and macrophages in non-lymphoid tissues, these cells were thought to be DCs. However, a detailed characterization of these cells, both at the phenotypical and functional level, revealed that they share common features with macrophages [52]. The CX_3CR1^+ lamina propria population derives from $Ly6C^{high}$ blood monocytes and is dependent on macrophage-colony stimulating factor (M-CSF) for its development [45,53]. This population can be defined by expression of specific phenotypical markers ($F4/80^+$ $MHC-II^+$ $CD11c^+$ CX_3CR1^+ $CD103^-$ $CD11b^+$) [52,54,55]. CX_3CR1^+ cells are highly phagocytic [56], cannot migrate from the lamina propria to the mLN (due to lack of CCR7 upregulation) [44] and have poor ability in priming naïve T cells, though they were already reported to induce a helper T (Th) 1/Th17 cell differentiation [56]. Different levels of CX_3CR1 expression, however, are associated with different functional subsets in this population, as CX_3CR1^{int} cells were found to migrate, efficiently prime T cells and respond to Flt3 ligand, similarly to DCs [57]. Additionally, antibiotic-induced dysbiosis was shown to trigger CX_3CR1^{high} macrophages to migrate into the mLN in a CCR7-dependent manner [58].

Extension of dendrites and luminal sampling by this population have been shown to be induced by TLR ligands and bacteria, such as *Salmonella* [50], depending on the MyD88 signaling pathway [59]. These cells can also acquire antigens from the blood stream that are then cross-presented to CD8^{+} T cells, which in turn express interleukin (IL)-10, IL-13 and IL-9 and migrate to the intraepithelial compartment [60].

CX_3CR1^+ cells have been shown to play an important role in the establishment of oral tolerance. Indeed, F4/80[+] CX_3CR1^{high} macrophages produce high levels of IL-10 and acquire an anti-inflammatory phenotype when stimulated with LPS [54,61]. Moreover, mice lacking CX_3CR1 showed impaired local Treg expansion and failed to establish oral tolerance due to a reduced capacity of IL-10 production by CX_3CR1-expressing macrophages [62].

Inflammatory conditions, on the other hand, lead to the differentiation of E-cadherin^{+} F4/80^{int} CX_3CR1^{int} CD11b^{+} macrophages from Ly6C^{high} monocytes that are then able to produce pro-inflammatory cytokines, such as IL-12, IL-23 and TNF-α [54,63]. CCR2- and CX_3CR1-deficient mice (lacking two receptors needed for Ly6C^{high} monocyte recruitment to the inflamed tissue) are also less susceptible to colitis after dextran sodium sulfate (DSS) treatment [64,65].

1.1.1.5.2 CD103^{+} dendritic cells

CD103 (also called integrin $α_E$) is expressed by a subset of *bona fide* lamina propria DCs. These cells derive from pre-DCs and expand in response to Flt3 ligand and granulocyte-macrophage colony stimulating factor (GM-CSF) [44,45,53,66]. The best known ligand for CD103, E-cadherin, is mainly expressed by epithelial cells [67], which suggests its involvement in the maintenance of these cells (as well as CD103^{+} CD8^{+} T cells) in the intestinal tissue. They also express CCR7, allowing them to migrate to the mLN [44,53,68]. Migration can occur under steady state conditions, but TLR stimulation can further increase the traffic of these cells to mLN, as supported by studies showing that

after oral infection with *S.* Typhimurium, CD11b^{+} CD103^{+} DCs are the only DC subset in the draining mLN containing green fluorescent protein (GFP)-labeled *Salmonella* [53].

In the mLN, under steady state conditions, CD103^{+} DCs induce the differentiation of naïve CD4^{+} T cells into forkhead box P3 (Foxp3)[+] Tregs, through a mechanism dependent on RA and TGF-β [69,70], indicating their contribution in the maintenance of tolerance. They also induce the expression of gut homing molecules, such as CCR9 and $\alpha_4\beta_7$, on T lymphocytes [68,71,72]. This ability, as well as other tolerogenic properties of CD103^{+} DCs, are conditioned by vitamin A that is introduced through the diet [73]. Additionally, the expression of IDO, an enzyme involved in tryptophan catabolism, is also required for their induction of Tregs [74]. The inhibition of this enzyme results in a failure in the establishment of tolerance to fed antigens and increased susceptibility in colitis models.

As conventional DCs, intestinal lamina propria CD103^{+} DCs express CD11c and MHC-II and can be further subdivided into different populations by their expression of CD8α and CD11b [75]. CD8α^{high} CD11b^{-} cells are mainly found in PP and ILF [53]. However, this population still persists in Rorγt-deficient mice, which lack PP and ILF, suggesting that they are not exclusively found in these intestinal compartments [57]. Transcription factors, such as Id2 and IRF8, are critical for the development of CD8α^{high} CD11b^{-} cells [53,76] and, similarly to CD8α^{+} conventional DCs, these cells are highly efficient in cross-presentation of cell-associated antigens [54]. CD8α^{-} CD11b^{high} cells express TLR5 and 9 and, in response to flagellin, this subset induces a T cell-independent differentiation of naïve B cells to IgA^{+} B cells and polarization of T cells to a Th1/Th17 phenotype [75,77].

Under inflammatory conditions, the tolerogenic features of the CD103^{+} DCs are lost and they acquire a pro-inflammatory phenotype. Laffont and colleagues have shown that in a model of T cell-induced colitis, the ability to induce Foxp3^{+} Tregs is compromised in CD103^{+} DCs sorted from mLN and a Th1 phenotype is instead imprinted [78]. Furthermore, CD11b^{+} CD103^{+} DCs act as a first line of defense to bacterial infection, as upon flagellin stimulation, this population from the small intestine rapidly increases its

expression of IL-23 subunits IL-23p19 and IL-12p40 and mediates IL-22-dependent antimicrobial peptide secretion by epithelial cells [79].

1.1.2 Antigen uptake in the intestine

The different components of the intestinal barrier participate in a complex network of interactions in order to avoid the entry of harmful organisms and other environmental agents in the intestinal tissue, as described in the previous sections. Nevertheless, the intestinal immune system needs to respond adequately to the different stimuli present in the intestinal lumen. Harmless agents, as commensal bacteria and food antigens, have to be distinguished from detrimental ones, including pathogens, in order to mount tolerogenic or protective immune responses, accordingly. Sampling of intestinal antigens by APCs is the initiating step of such regulated immune responses that ensure a balanced intestinal homeostasis.
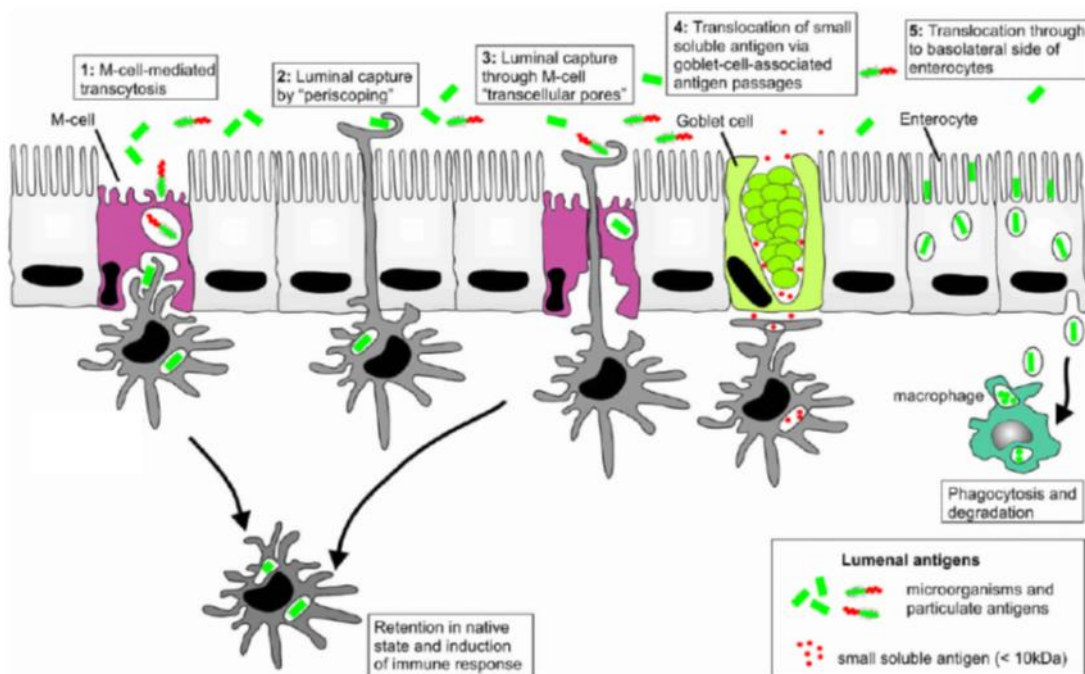
Figure 1.2. Routes of antigen uptake in the intestine.

Studies have identified different pathways for antigen uptake, including: (1) transcytosis by M cells in FAE; (2) extension of trans-epithelial dendrites by CX$_3$CR1$^+$ APCs; (3) extension of dendrites

through M cell transcellular pores by LysoDCs in PP; (4) transfer of small molecules by Goblet cells; and (5) transfer of antigen-containing endosomes by enterocytes. Adapted from *Mabbott et al., Mucosal Immunology, 2013* [80].

In the past few years, several mechanisms for transport of luminal antigens across the intestinal epithelium have been described, involving both epithelial cells and immune cells (Fig. 1.2).

M cells, abundantly present in the FAE, covering PP and ILF, are specialized transcytotic epithelial cells that greatly contribute to antigen transport into these inductive immune compartments. M cells are able to actively internalize particulate material through a number of mechanisms (macropinocytosis, endocytosis in clathrin-coated vesicles, actin-dependent phagocytosis), releasing it in basolateral "intraepithelial pockets", where APCs can take up the shuttled material [80,81]. The transcytotic function of M cells can be further enhanced by microbial products, increasing antigen uptake through the FAE [82]. In fact, several pathogens take advantage of this feature of M cells to breach the intestinal barrier. This process occurs due to the interaction between microorganisms and molecules that are specifically expressed on the apical surface of M cells. For instance, glycoprotein 2 (GP2) is highly expressed by M cells [83] and selectively binds to FimH, a component of the type I pili found on the membrane of bacteria, such as *S.* Typhimurium. The contribution of GP2 in M cell-mediated uptake was confirmed by a defective transcytosis of FimH+ bacteria, decreased bacterial load and antigen-specific immune responses in PP when GP2 was absent in the host [84]. Another receptor on M cells that is likely to contribute to the uptake of microorganisms by these specialized cells is the cellular prion protein (PrP^C) [85]. Nakato and colleagues have shown that *Brucella abortus* can interact with PrP^C on M cells and trigger its internalization by expressing heat shock protein 60 on the cell surface [86]. Moreover, expression of the complement C5a receptor on M cells allows the binding and uptake of *Yersinia enterocolitica* after oral infection, as this bacterium expresses an homologous protein to the Skp α1 domain of *Escherichia coli*, a ligand of C5a receptor [87]. Alternatively, an indirect uptake can also occur through M

cells, as they rely on secretory IgA to bridge the transport of intestinal antigens. This feature of M cells depends on their expression of an IgA-specific receptor, different from FcαRI [88], that binds to secretory IgA-antigen immune complexes of various sizes and enables their transference into PP [89].

Compared to M cells, other epithelial cells have a poor endocytic and transcytotic capacity. Still, high resolution imaging techniques revealed that FAE enterocytes are able to transport prions within large endosomes and exocytose their cargo into the extracellular space of the sub-epithelial dome (SED) [90]. Moreover, Ig-bound antigens can also be transported from the lumen to the lamina propria by villous epithelial cells expressing the neonatal Fc receptor, which is involved in both IgG secretion into the lumen and sampling of IgG-antigen complexes [91]. Epithelial cells with secretory functions, as is the case of Goblet cells, were also implicated in the trafficking of intestinal antigens. McDole and colleagues have demonstrated that different low molecular weight soluble antigens can enter the lamina propria through Goblet cell-associated passages and be directly delivered to CD103^{+} DCs [92]. In addition, the paracellular diffusion of antigens across the intestinal epithelium can be included in the mechanisms of antigen uptake, as small molecules may pass between adjacent epithelial cells due to the existence of pores in the tight junctions [93].

On the other hand, routes of antigen sampling that are not mediated by epithelial cells and rely on the direct uptake by intestinal APCs have also been described. In PP, Lelouard and colleagues have found that CD11c^{+} CX$_3$CR1^{+} cells expressing lysozyme M, named LysoDCs, capture inert particles and *S.* Typhimurium by extending dendrites through M cell specific transcellular pores. This process is accompanied by recruitment of M cell junctional adhesion molecule A and epithelial cell adhesion molecule [94]. In the villous lamina propria, CD11c^{+} APCs were also found to directly sample luminal antigens. However, differently from the previous case, extension of dendrites by these cells does not involve transcellular pores. Instead, their dendrites cross the epithelial barrier in a paracellular way without disruption of its integrity and relies on the formation of tight junctions between epithelial cells and APC's protrusions [23]. Furthermore, these trans-

epithelial extensions were identified mainly in the proximal jejunum, presenting a "balloon" shape, and their discreet presence in the terminal ileum was markedly increased after infection with different *Salmonella* strains [50]. Another study further characterized these cells as CX_3CR1^+ APCs, showing the involvement of CX_3CR1 in the formation of trans-epithelial dendrites through experiments with mice lacking this chemokine receptor [49].

1.1.3 Oral tolerance

Immune tolerance is considered a state of unresponsiveness of the immune system towards a particular antigen that has the potential to trigger an immune response. As described in the previous sections, the intestinal mucosa is permanently in contact with many different antigens, including harmless food antigens and commensal microorganisms. Hence, in order to maintain tissue homeostasis and prevent exacerbated immune responses against such antigens, the intestinal immune system developed mechanisms that allow the induction of tolerance, both in the intestine and systemically, upon encounter with these antigens, known as oral tolerance [93].

Oral tolerance is mainly induced in the draining mLN. Different studies have shown that in mice devoid of mLN [95] or subjected to mesenteric lymphadenectomy [96], induction of oral tolerance to food antigens fails. Additionally, PP may also function as an induction site for oral tolerance, since mice treated with lymphotoxin β-receptor Ig fusion protein *in utero* (lacking PP) are not able to mount oral tolerance to ovalbumin (OVA) [97]. Nevertheless, the contribution of PP to oral tolerance establishment is still controversial, as other studies have pointed in the opposite direction. Indeed, Enders and colleagues have shown that rats subjected to surgical removal of PP present a similar response to control animals [98]. Despite strong evidence supporting the role of the GALT in the induction of oral tolerance, some studies have revealed that this immune response can also be attained through other tissues. By intraperitoneal injection of serum from tolerized mice (expected to contain processed antigen), Kagnoff was able to demonstrate the

induction of tolerance in recipient animals [99]. In addition, antigen delivery directly in the hepatic portal vein can have similar effects to oral delivery [100]. These observations suggest that the establishment of oral tolerance relies on the transport of antigens to the GALT, as well as on their systemic dissemination and transport to the liver through portal circulation [101].

Besides the induction site, the establishment of oral tolerance relies on a complex interaction of different factors. The dose and frequency of antigen administration can dictate tolerance induction, as high doses of antigen can lead to anergy and deletion of antigen-reactive T cells [102,103], whereas repeated low doses of antigen might induce Tregs [104]. The differentiation of Tregs is indeed an essential step in mounting tolerance to orally delivered antigens. This process depends on antigen uptake by intestinal APCs, particularly DCs endowed with migratory capacity, that then transport the processed antigen to the draining mLN. Here, DCs present their cargo to T cells and induce their differentiation towards a regulatory phenotype, as well as expression of gut-homing receptors that allow Treg migration to the intestine where their regulatory function can be exerted. The induction of tolerogenic characteristics on T cells is shaped by different aspects, including the local environment from where APCs migrate and the innate features of the various APC subsets presenting the antigen (as described in sections 1.1.1.5.1 and 1.1.1.5.2).

Tregs control and suppress effector immune responses against specific antigens. These cells encompass different subsets of both CD4$^+$ and CD8$^+$ T cells, but two main subsets are usually recognized according to their origin: naturally occurring CD4$^+$ CD25$^+$ Tregs and inducible Tregs. The first originate in the thymus and suppress self-reactive T cells in the periphery; the second differentiate in peripheral tissues upon antigen presentation by APCs in the absence of co-stimulatory signals and/or in the presence of tolerogenic cues.

Among the different inducible Tregs, Tregs expressing the transcription factor Foxp3 have been linked to the occurrence of oral tolerance [62]. Adoptive transfer of naïve OVA-specific T cells into congenic recipients has confirmed the conversion of OVA-specific

CD4$^+$ Foxp3$^+$ T cells in the intestinal lamina propria and mLN after oral administration of this antigen [70]. CD4$^+$ Foxp3$^+$ T cells can be induced by specific subsets of DCs in the presence of RA and TGF-β [69,70]. IL-2 was also shown to be required for the differentiation of Foxp3$^+$ Tregs [105]. Furthermore, the expression of gut-homing receptors, such as α$_4$β$_7$, and the correct environment for Foxp3$^+$ Tregs expansion are fundamental for their function in oral tolerance. Indeed, Hadis and colleagues have shown that oral tolerance is compromised in β$_7$-deficient mice [62] and, along with other studies, have demonstrated the role of IL-10 produced by lamina propria APCs in the induction of Tregs and in the maintenance of Foxp3 expression [61,62,106].

1.2 Vaccination

The introduction of vaccination is regarded as the most effective intervention for protection against infectious diseases and has contributed significantly to an increase in life expectancy [107]. Mass vaccination programs have spared millions from the morbidity and mortality associated with such diseases and resulted in the total eradication of smallpox [108]. However, for some infectious diseases, further improvement is still required in vaccine research and development to provide complete protection against them. Numerous pathogenic bacteria and viruses colonize and invade the host at mucosal surfaces, being instrumental the generation of a first line of defense at the site of infection, including induction of pathogen-specific secretory IgA [109,110].

1.2.1 Influenza vaccination

Influenza is a contagious respiratory disease often disregarded due to the mild symptoms associated with it, including cough, sore throat and fatigue that go away in few days. However, susceptible human populations (young children, elderly adults, people with chronic medical conditions, pregnant women) are at high risk of developing serious flu complications, resulting sometimes in death. Circulating influenza viruses undergo

antigenic drift, i.e. small changes in their genetic material that happen gradually as the virus replicates [111]. Accumulation of these genetic changes over time leads to antigenically diverse viruses. Once this happens, the immune system might not be able to fight the virus anymore, as the antibodies generated upon previous encounters cannot recognize the "new" virus. For this reason, every year the composition of flu vaccines has to be reviewed and updated in order to keep up with the evolving viruses and adequately protect the population. Less frequently, human type A influenza viruses (or animal influenza viruses) can also undergo antigenic shift, a major change that results in new hemagglutinin or hemagglutinin and neuraminidase combinations [111]. In such cases, most people do not have immunity to the virus and, as happened in 2009 when a H1N1 virus emerged, an influenza pandemic occurs, causing a considerable death toll.

The economic burden that flu cases impose on health care systems is substantial, not only due to influenza pandemics, but also to required hospitalizations and the need for yearly revisions of seasonal influenza vaccines. Moreover, the global production and distribution capacity of both seasonal and pandemic influenza vaccines cannot keep up with demand, and developing countries are affected by vaccine shortage [112]. The need for a universal influenza vaccine – a vaccine eliciting long-lasting broader immune responses against a wider range of influenza viruses and that eradicates the necessity for annual updates of seasonal vaccines and production of new vaccines upon advent of influenza pandemics – was already recognized by the Global Vaccine Action Plan, that aims to generate one by 2020.

1.2.1.1 CTA1-3M2e-DD: a universal influenza vaccine candidate

In an attempt to abolish cholera toxin (CT) toxicity while maintaining its adjuvanticity, the fusion protein CTA1-DD was generated [113]. This fusion protein is composed of an enzymatically active CT A1 subunit (CTA1) genetically fused through its C-terminal end to a dimer of the D region (DD) of *Staphylococcus aureus* protein A, an Ig-binding domain. CTA1-DD was found to target B cells *in vivo* [113] and to bind to both Fc and Fab

fragments and to different Ig classes, preferentially to the various IgG subclasses [113,114]. Immunization with CTA1-DD generates a Th1/Th2 response, resulting in increased T cell proliferation, germinal center formation and antibody production as well as cytotoxic T lymphocyte activity [113,115–117]. Moreover, this fusion protein has been combined with different antigens and has been shown to confer protective responses in different disease models including chlamydia, rotavirus, influenza and *Helicobacter pylori* [118–122].

Amongst the different approaches to generate a universal influenza vaccine, M2e-based vaccines have been extensively studied [123]. M2e (the extracellular domain of matrix protein 2) is highly conserved among all human influenza A viruses [124] and, as such, is highly attractive as a viral antigen. The interest in M2e for universal vaccines has been supported by studies showing that vaccines carrying this antigen elicit a high degree of protection upon virus challenge that correlates with production of anti-M2e antibodies [125–127].

When M2e was incorporated as a three tandem repeat into the CTA1-DD adjuvant, the universal influenza vaccine candidate CTA1-3M2e-DD was able to protect against a lethal dose of live influenza virus upon intranasal immunization and promoted high M2e-specific serum IgG and mucosal IgA antibody titers [121]. Recently, it has also been shown that CTA1-3M2e-DD-induced protection after mucosal immunization relies not only on M2e specific antibodies, but also M2e-specific memory CD4$^+$ T cells that are found in the lungs, rapidly expanded upon viral challenge infection and present a Th17 phenotype [128].

1.2.2 Mucosal vaccination *vs* parenteral vaccination

The majority of pathogens enter the body through mucosal surfaces. Thus, mounting a first line of defense at these sites to protect from pathogen invasion and infection is fundamental. It is now generally accepted that mucosal vaccination, that includes oral, nasal, sublingual, and genital tract vaccination, is the most effective way to achieve

successful protective immune responses in mucosal tissues [109,110]. This is explained by the ability of mucosal vaccines to induce both humoral and cell-mediated immune protection at the level of mucosal surfaces, but also systemically [109,110]. Indeed, mucosal vaccines are taken up by APCs at the immunization site and are then presented to B and T cells in the draining lymph nodes, where they acquire tissue-specific homing receptors. This enables antigen-specific memory and effector immune cells to exit the draining lymph nodes, enter the blood circulation and settle in the mucosal tissue [110]. Moreover, mucosal vaccination can trigger antigen-specific IgA production not only at the tissue of immunization, but also in distal mucosal surfaces [109]. Mucosal surfaces are also densely equipped with APCs, as they are constantly in contact with the external world and vulnerable to invading pathogens, improving the uptake of vaccines at these sites.

Nevertheless, most vaccines in use today are administered by parenteral injection. This vaccination route is not the most effective, as it generally fails to elicit a pathogen-specific mucosal immunity and, for many pathogens, optimal protection requires both mucosal and systemic immune effectors. This is due to the systemic homing specificity of effector lymphocytes activated in the peripheral lymph nodes. Moreover, subcutaneous tissue and muscle contain very low numbers of APCs [129].

The advantages of mucosal vaccines over parenteral vaccines are observed at many other levels. For instance, administration of mucosal vaccines is easier and does not require professionals with medical training or a clinical setting, as it eliminates the use of needles and syringes, and prevents concerns regarding their reuse and disposal that often leads to vaccination-related infections and environmental hazards. This also renders mucosal vaccines more suitable for mass vaccination and prevention of pandemic spread of infections [110]. Better compliance is achieved with mucosal vaccines, since parenteral vaccines often cause pain, local swelling and stiffness. Moreover, regulatory requirements for the production of mucosal vaccines are less stringent and consequently production is cheaper [130]. This is due to the fact that mucosal surfaces, such as the intestine, already present high numbers of bacteria, which eliminates the necessity to purify oral vaccines from bacterial by-products to the same level as vaccines injected parenterally [110].

Considering these advantages, few licensed mucosal vaccines are currently available in the market, including vaccines for poliovirus, *S.* Typhimurium, *Vibrio cholerae* and rotavirus [110]. Several studies involving oral vaccines have been delayed due to the challenges that this route imposes. In fact, as with any other orally delivered antigen or pathogen, oral vaccines face many obstacles in the GI tract. These include an extremely variable pH throughout the GI tract, dilution of the vaccine dose in mucosal secretions, entrapment in the mucus layer, exclusion by epithelial barriers, and enzymatic degradation by digestive proteases, just to mention a few [109]. To overcome some of these obstacles, high doses of vaccine are required; however, the dose that is actually taken up by the host through the intestinal mucosa cannot be precisely quantified. Another important hurdle that oral vaccines face is the induction of oral tolerance, which completely compromises the overall goal of vaccination. Indeed, if taken up, soluble non-adherent antigens, as is the case of some oral vaccines, usually induce immune tolerance [131].

1.2.3 Particulate vaccines for mucosal immunization

In recent years, different delivery strategies have been studied in order to address the challenges described above. These include the development of particulate vaccines that protect the antigen and incorporate features shared by mucosal pathogens that are successful in invading the host.

Indeed, different studies have demonstrated protection from degradation of protein, peptide and DNA vaccines after inclusion in microparticles, liposomes or proteasomes [132–134]. Such delivery systems have also proven to retain the vaccine antigens on mucosal surfaces, increasing their uptake across the epithelium [135,136]. Particulate delivery systems also have the advantage of being easily transcytosed by M cells and this characteristic can be further enhanced by coupling ligands and antigens that target PP [136–138]. Importantly, particulate-based vaccine delivery systems not only have the potential to increase the uptake of their cargo, but can also act as vaccine adjuvants, as

some have been shown to efficiently modulate immune responses [139,140]. A summary of the different strategies to overcome the challenges that mucosal immunization imposes using particulate material is presented in Table 1.1.

Table 1.1. Mucosal vaccination challenges and solutions from particle-based vaccine research.

Adapted from *Sahdev et al., Pharmaceutical Research, 2014* [141]**.**

	Challenges	Solutions	References
Site of administration	Induction of mucosal immunity via oral and intranasal administration	Nanoparticles coated with or composed of mucoadhesive biopolymers	[142–144]
		Use of pH-responsive particles for protection of antigens from stomach acids and subsequent release in lower digestive tract	[145,146]
Antigen delivery to lymph nodes	Instability of particles *in vivo*	Increasing stability of lipid vesicles via interbilayer crosslinking	[147–150]
	Ineffective lymphatic transport of particles	Design of small (< 100 nm) and PEGylated nanoparticles for enhanced lymphatic drainage	[151–156]
		Direct intranodal injection of particle vaccines	[157]
Activation of APCs	Promotion of APC activation and maturation to avoid immune tolerance	Co-delivery of antigens and danger signals within particles	[146,158,159]
		Use of intrinsically immunostimulatory material as building blocks	[153,154,160,161]
Intracellular antigen release	Antigens trapped in lysosomes are degraded	Cell-penetrating peptides for cytosolic antigen delivery	[162–164]
		pH-responsive polymers for endosome escape	[165–170]
		Reduction-sensitive conjugation of antigens to particles	[153–156,167–169,171]
Vaccine preparation	Loss of antigenicity and immunogenicity during particle synthesis	Antigen loading into polymeric particles in aqueous conditions via self-healing process	[172,173]
		Use of cell membrane-decorated particles for adsorption and inactivation of bacterial toxin	[174]

2 AIM OF THE STUDY

Although mucosal vaccines can elicit a more complete protective immune response, injected vaccines are still the most common ones. The oral route, particularly, offers many advantages in vaccination, but simultaneously many challenges, as the environment throughout the GI tract presents different threats to the stability of vaccines. Taking this in consideration and in the framework of the UniVacFlu project, whose overall goal is to develop a new universal influenza vaccine that is administered on a mucosal surface, the main aim of this project was to investigate the potential of an influenza vaccine candidate and nanoparticulate vaccine vectors generated in our consortium as an oral vaccine/delivery system.

Thus, we proceeded through the following steps:

- Characterization of the vaccine candidate/vaccine vector uptake in the small intestine;

- Identification of the small intestine lamina propria APC subsets responsible for vaccine candidate/vaccine vector uptake, focusing on CX_3CR1^+ macrophages and $CD103^+$ DCs;

- Assessment of the effect of the vaccine vector on antigen delivery and antigen-specific immune responses in a model of oral immunization;

- Identification of conditions that might impact the outcome of immunization in this model;

- Manipulation of the gastric pH for optimal function of the vaccine vector through the oral route.

3 MATERIALS AND METHODS

3.1 Mice

Six- to ten-week-old C57BL/6J and C57BL/6-Ly5.1 (B6.SJL-*Ptprc*ª*Pepc*ᵇ/BoyCrl) mice were purchased from Charles River. *Cx3cr1*ᴳᶠᴾ/ᴳᶠᴾ (B6.129P-*Cx3cr1*ᵗᵐ¹ᴸⁱᵗᵗ/J) mice, expressing GFP under the control of the endogenous *Cx3cr1* locus [175], and OT II (B6.Cg-Tg(TcraTcrb)425Cbn/J) mice, expressing the mouse α-chain and β-chain T cell receptor that pairs with the CD4 co-receptor and specifically recognizes chicken OVA$_{323-339}$ peptide in the context of I-Aᵇ [176], were purchased from Jackson Laboratory. The heterozygous *Cx3cr1*ᴳᶠᴾ/⁺ mouse colony was obtained by *Cx3cr1*ᴳᶠᴾ/ᴳᶠᴾ males × C57BL/6J females mating. Mice were bred and maintained at the Animal Facility of the IFOM-IEO campus (Milan, Italy) under specific pathogen-free conditions. All experiments were performed in accordance with the Italian Laws (D.lgs. 26/2014), which enforce Directive 2010/63/EU (Directive 2010/63/EU of the European Parliament and of the Council of 22 September 2010 on the protection of animals used for scientific purposes).

3.2 Fusion protein preparation

The fusion protein CTA1-3M2e-DD (carrying three copies of the extracellular domain of the influenza virus M2 protein; amino acid sequence: SLLTEVETPIRNEWGSRSNDSSD) was produced by MIVAC Development AB (Gothenburg, Sweden), according to what was previously described [121,128], and provided by Prof. Nils Lycke's laboratory (University of Gothenburg, Sweden). Briefly, the fusion protein was expressed in *E. coli* DH5 cells, which were grown in 500 mL cultures overnight in SYPPG medium with 100 µg/mL carbenicillin, at 37°C. The fusion protein, produced as inclusion bodies, was washed before extraction by treatment with 8 M urea. After refolding of the protein by slow dilution

in Tris-HCl pH 7.4 at 4ºC, the fusion protein was purified by ion exchange and size exclusion chromatography, concentrated and submitted to sterile filtration. Protein analysis was performed with sodium dodecyl sulfate polyacrylamide gel electrophoresis (SDS-PAGE) and protein concentration was determined using the DC Protein Assay (Bio-Rad), according to the manufacturer's instructions. The purified fusion protein was stored at -80ºC until use and it was routinely tested for the presence of endotoxin using the Limulus amebocyte lysate Endochrome assay (Charles River Endosafe). CTA1-3M2e-DD was conjugated with Alexa Fluor (AF) 488 or AF647 using the Antibody Labeling Kit (Thermo Fisher Scientific) and following the manufacturer's instructions.

3.3 Vaccine vector preparation
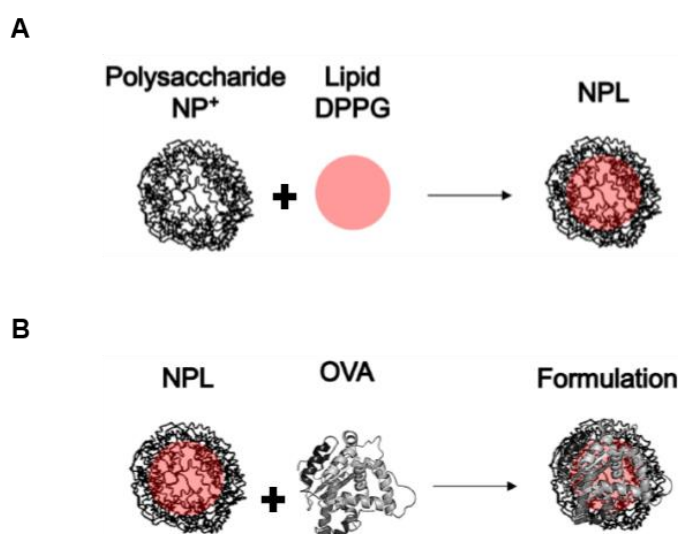
Figure 3.1. Schematic representation of composition and preparation of NPL formulations. **(A)** NP+ are loaded with the anionic lipid DPPG to form NPL. **(B)** An antigen of interest (for example, OVA) is then loaded into NPL, obtaining an antigen:vaccine vector formulation. Adapted from *Bernocchi et al.*, *Journal of Controlled Release*, *2016* [177].

Polysaccharidic lipidated nanoparticles (NPL) were produced (Fig. 3.1), characterized and conjugated as described previously [177,178] and provided by Prof. Didier Betbeder's

laboratory (University of Lille, France). Briefly, maltodextrin (Roquette) was dissolved in water and a mixture of epichlorohydrin and glycidyltrimethylammonium chloride (Sigma-Aldrich) in basic medium was added to the cationic polysaccharide, forming a gel. The gel was neutralized with acetic acid and crushed with a high pressure homogenizer, obtaining polysaccharidic cationic nanoparticles (NP+) that were then purified by tangential flow ultra-filtration to remove oligosaccharides, low-molecular weight reagents and salts, and freeze dried. Lyophilized NP+ were resuspended in a 70% (w/w) aqueous solution of the anionic lipid 1,2-dipalmitoyl-sn-glycero-3-phosphatidylglycerol (DPPG, Lipoid), which was incorporated by the nanoparticles, obtaining NPL. For OVA:NPL formulations, OVA (Sigma-Aldrich) was purified by gel filtration, the concentration of protein was evaluated using the Micro BCA Protein Assay Kit (Thermo Fisher Scientific), following the supplier's instructions, and 1 mg/mL of protein was loaded into sterile NPL (5 mg/mL) by mixing both, obtaining a 1:5 (w/w) OVA:NPL formulation. The characterization of the size (Z-average), Zeta potential and polydispersity index of NPL and OVA:NPL formulations was performed with Zetasizer Nano ZS (Malvern Instruments) and is presented in Table 3.1. The analysis of the protein association to NPL was performed by native-PAGE, followed by silver nitrate staining to detect the unbound protein and measure the amount of associated protein.

Table 3.1. Characterization of size, polydispersity index and Zeta-potential of empty NPL and OVA:NPL formulation used in this study.

Adapted from *Bernocchi et al., Journal of Controlled Release, 2016* [177].

	Z-average (nm)	Polydispersity index	Zeta-potential (mV)
NPL	76.07	0.211	+44.2 ± 10.15
OVA:NPL 1:5 w/w	62.39	0.236	+33.47 ± 8.417

When necessary, NPL and OVA were fluorescently labeled. For NPL detection, NP+ were covalently labeled with fluorescein isothiocyanate (FITC, Sigma-Aldrich). FITC was added to NP+ (NP+:FITC mass ratio of 10), solubilized in 0.1 M bicarbonate buffer pH 9.5, and the solution was mixed for 6h at room temperature and protected from light. NP+/FITC were then lipidated, as described above, to obtain NPL/FITC. Alternatively, the phospholipids of DPPG encapsulated in NP+ were labeled with 1.1′-dioctadecyl-3,3,3′,3′-tetramethylindodicarbocyanine perchlorate (DiD, Thermo Fisher Scientific). DiD (1 mg/mL in ethanol) was added to NPL at a final concentration of 0.7% (w/w of DPPG) and mixed for 30 min at room temperature in order to obtain NPL/DiD. Conjugation of OVA with tetramethylrhodamine-5-isothiocyanate (TRITC, Thermo Fisher Scientific) was performed following the same protocol used for NP+ labeling. After organic solvent evaporation, fluorescent NPL formulations were kept in the dark at 4ºC until use.

3.4 Isolation of human peripheral blood mononuclear cells

Human peripheral blood mononuclear cells (PBMCs) were isolated from heparinized blood from healthy donors. Approximately 40 mL of a buffy coat suspension were washed twice in phosphate-buffered saline (PBS) and the serum was discarded. The remaining volume of buffy coat was mixed with PBS up to a final volume of 35 mL by inverting the tube. The buffy coat suspension was gently layered on 15 mL of Ficoll (Biocol) and centrifuged at 1200 rpm for 30 min without brake. The PBMC ring was collected and washed three times with PBS.

3.5 *In vitro* CTA1-3M2e-DD binding

Mouse splenocytes were isolated from C57BL/6J mice as described in section 3.11. Human PBMCs were obtained as described in section 3.4. Increasing doses (0-2 µg) of

CTA1-3M2e-DD/AF488 were incubated for 1h at 4°C with 10^6 mouse splenocytes or human PBMCs in 100 μL of 2% fetal bovine serum (FBS) in PBS. Cells were extensively washed in PBS to remove the unbound fusion protein and CTA1-3M2e-DD binding to B cells was detected by flow cytometry after staining mouse splenocytes and human PBMCs with anti-B220 (clone RA3-6B2, BD Pharmingen) and anti-CD19 (clone LT19, Miltenyi Biotech) antibodies, respectively.

3.6 Ligated intestinal loop

C57BL/6J and *Cx3cr1*GFP/+ mice were starved overnight (while allowing continuous access to water) in order to reduce the intestinal content and avoid competition of the injected agent with food antigens and feces. The next day, mice were anesthetized with 2.5% Avertin for the entire duration of the experiment. An incision was made on the skin to expose the peritoneum and another incision in the peritoneal wall allowed access to the intestine. A 3-4 cm segment of the small intestine was exposed, ligated at both extremities with surgical thread and fluorescently labeled CTA1-3M2e-DD (5-100 μg), NPL (50 μg), OVA:NPL (10 μg OVA:50 μg NPL) or PBS (vehicle) alone were injected into the loop in a volume of 100 μL. Mice were sutured, maintained in a recovery rack and sacrificed after 1 or 2h for resection of the intestinal loops. Tissues were processed for confocal microscopy analysis.

3.7 Intraduodenal administration

C57BL/6J, *Cx3cr1*GFP/+ and C57BL/6-Ly5.1 mice were starved overnight. The next day, mice were anesthetized with 2.5% Avertin for the duration of the surgery. An incision was made on the skin and peritoneal wall, and CTA1-3M2e-DD or NPL formulations were

injected directly into the duodenum in a volume of 200 µL. Mice were sutured and maintained in a recovery rack until awake.

3.8 Human intestinal specimens and *ex vivo* organ culture model

Human intestinal (ileum) specimens were obtained from the healthy tissue of patients undergoing surgery for tumor resection. The tissue was placed in Hanks' Balanced Salt Solution medium supplemented with 100 IU/mL penicillin and 100 µg/mL streptomycin at 4°C immediately after resection. To study whether NPL could be taken up in the human intestine, an *ex vivo* organ culture model allowing the maintenance of tissue polarization developed in our laboratory [179,180] (Fig. 3.2) was followed, with some modifications. Briefly, the intestinal explants were gently washed in Dulbecco's Modified Eagle Medium (DMEM), the mucosa was separated from the submucosa and the former was cut in approximately 1 cm^2 pieces. With the apical side of the mucosa facing upwards, a plastic cloning cylinder (BellCo) was attached with surgical glue to the luminal surface of the explant. The explant was then placed on a metal grid positioned in a center-well organ culture dish (BD Falcon) filled with DMEM containing 15% FBS, 2 mM L-glutamine, 200 ng/mL epidermal growth factor (Peprotech) and 10 µL/mL Insulin-Transferrin-Selenium-X (Gibco). To mimic physiological conditions, reconstitution of the mucus layer was allowed by placing the intestinal explant in a regular cell culture incubator without medium on the luminal side of the tissue. After 1h, 50 µL of supplemented medium alone or containing 20 µg NPL/FITC was applied inside the cylinder, covering the luminal surface of the explant delimited by the cylinder, and incubation continued under the same conditions for an additional hour. The explants were then processed for confocal microscopy analysis after removal of the cylinder.
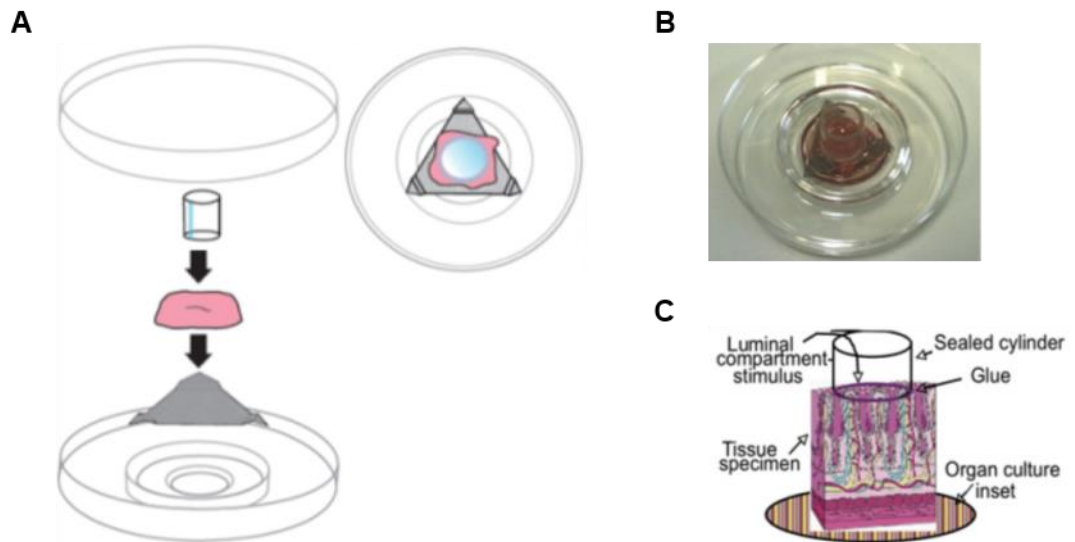
Figure 3.2. *Ex vivo* **organ culture model.**

(A) Schematic representation of the technical setting viewed from the side and from the top. The intestinal explant is placed on a metal grid and a plastic cylinder is sealed on the luminal surface of the tissue. **(B)** Photograph of the assembled components of the organ culture model. **(C)** The stimulus is placed inside the cylinder, maintaining tissue polarization and mimicking physiological conditions, as the stimulus is only in contact with the luminal surface and does not enter through the basolateral surface. Adapted from *Tsilingiri et al.*, *Gut*, *2012* [179] and *Tsilingiri et al.*, *JoVE*, *2013* [180].

3.9 Immunofluorescence and confocal microscopy

Tissues were fixed overnight in 1% paraformaldehyde, 0.1 M L-Lysine pH 7.4 and 0.16% $NaIO_4$ in P-buffer (0.02 M NaH_2PO_4 and 0.08 M Na_2HPO_4) pH 7.4. After washing in P-buffer, tissues were dehydrated in 20% sucrose for at least 4h, included in optimum cutting temperature compound (Sakura Finetek) and frozen at -80° C. Ten µm-thick sections were cut, placed onto Superfrost Ultra Plus microscope slides (Thermo Scientific) and rehydrated with 0.1 M Tris-HCl pH 7.4. When staining for specific markers was performed, cryosections were blocked for 30 min with 2% FBS, 0.3% Triton X-100 in 0.1 M Tris-HCl pH 7.4, followed by overnight incubation at 4°C with the following primary

antibodies: polyclonal anti-MUC2 (Santa Cruz Biotechnology), polyclonal anti-chromogranin A (Abcam), polyclonal anti-lysozyme (Dako). Cryosections were extensively washed before incubation at room temperature with the appropriate fluorophore-conjugated secondary antibodies for 2h. Nuclei were counterstained with 4',6-diamidin-2-fenilindolo (DAPI) and coverslips were applied after adding Vectashield mounting medium (Vectorlabs) on the cryosections. Confocal microscopy was performed on a Leica TCS SP5 laser confocal scanner mounted on a Leica DMI 6000B inverted microscope (Leica Microsystem) and images were acquired with a 40x or 63x oil immersion objective, using Leica Application Suite AF software (Leica Microsystem). Images were analyzed and processed using ImageJ software.

3.10 Isolation of cells from small intestine lamina propria

Small intestines from *Cx3cr1*$^{GFP/+}$ mice were resected, cut longitudinally after removal of PP and connective tissue and extensively washed in PBS to eliminate feces. The tissue was cut in 1 cm pieces and incubated twice in separation medium (PBS, 10% FBS, 1 mM dithiothreitol, 1 mM ethylenediaminetetraacetic acid (EDTA)) for 15 min at 37°C and under gentle shaking to remove mucus. The tissue was then minced and incubated in digestion medium (Minimum Essential Medium α, 10% FBS, 0.5 mg/mL collagenase type VIII (Sigma-Aldrich), 5 U/mL DNase I (Roche Diagnostics), 100 IU/mL penicillin and 100 µg/mL streptomycin) for 30 min at 37°C under gentle shaking. The obtained single cell suspension was passed through a strainer, to eliminate tissue debris, and centrifuged. Cells were washed in PBS, blocked with anti-FcR antibody (clone 24G2, BD Biosciences) and stained for flow cytometry with the following primary antibodies: anti-CD45.2 (clone 104, BD Biosciences), CD11c (clone HL3, BD Pharmingen), IA/IE (clone M5/114.15.2, BD Biosciences), CD103 (clone M290, BD Pharmingen), CD11b (clone M1/70, BD Pharmingen). DAPI or Fixable Viability Stain (BD Biosciences) were added to exclude

dead cells. Samples were acquired using FACSCanto II (BD Biosciences) and analyzed with FlowJo software (Treestar).

3.11 Isolation of cells from lymphoid organs

PP were resected and digested in RPMI-1640 medium containing 10% FBS, 1 mg/mL collagenase D (Roche), 5 U/mL DNase I, 100 IU/mL penicillin and 100 µg/mL streptomycin for 20 min at 37°C. Spleens, mLN and the remaining tissue of PP were crushed onto a strainer with a syringe plunger to obtain a single cell suspension. Cells were centrifuged and, in the case of spleens, red blood cells were lysed with a hypotonic lysis buffer.

When naïve $CD4^+$ T cells were required for adoptive transfer experiments, spleens and lymph nodes from OT II mice were resected and cells were obtained as described above. Naïve $CD4^+$ T cells were isolated using the $CD4^+$ T Cell Isolation Kit (Miltenyi Biotec) together with biotinylated anti-CD25 antibody (Miltenyi Biotec), according to the manufacturer's instructions. To obtain a higher purity, cells were passed twice in the separation column. Cells were labeled with 5 µM carboxyfluorescein succinimidyl ester (CFSE) for 10 min at 37ºC, followed by one wash in 10% FBS in PBS and extensive washing in PBS alone. Cell purity was evaluated by flow cytometry and typically ≥92% purity was achieved.

When staining for flow cytometry was required, the obtained cell suspensions were incubated with anti-FcR antibody and stained with the following primary antibodies: anti-CD45.2 (clone 104, BD Biosciences), CD45.1 (clone A20, eBioscience), CD3 (clone 145-2C11, Biologend), CD4 (clone RM4-5, BD Pharmingen), CD62L (clone MEL14, BD Pharmingen), CD25 (clone PC61, BD Pharmingen). Fixable Viability Stain was added to exclude dead cells.

3.12 Staining for Tregs and cytokines

For intracellular staining of Foxp3, surface staining was performed as described in section 3.11, cells were fixed and permeabilized with Fix-Perm Buffer (eBioscience) and subsequently stained in Permeabilization Buffer (eBioscience) with anti-Foxp3 (clone FJK-16s, eBioscience) antibody, following the manufacturer's instructions. When detecting Th1 and Th2 responses, cells were incubated in complete RPMI-1640 medium (10% FBS, 1% L-glutamine, 100 IU/mL penicillin and 100 µg/mL streptomycin) at 37ºC and stimulated for 4h with 50 ng/mL phorbol myristate acetate (PMA, Sigma-Aldrich), 500 ng/mL ionomycin (Sigma-Aldrich) and 0.7 µL/mL Golgi Stop (BD Biosciences). Surface staining was performed as described in section 3.11, cells were fixed and permeabilized as above and intracellular cytokines were stained with anti-IFNγ (clone XMG1.2, BD Biosciences) and IL-4 (11B11, BD Biosciences) antibodies.

3.13 Adoptive transfer and immunizations

CFSE-labeled naïve CD4$^+$ T cells from OT II mice, obtained as described in section 3.11, were transferred into C57BL/6-Ly5.1 mice by intravenous injection (2×10^6 cells/mouse). Mice were starved. The following day, NPL formulations or OVA alone were given to the recipients by intraduodenal injection or intragastric administration using a feeding needle, in a volume of 200 µL. When indicated, intragastric administration of NPL formulations was buffered with 5% NaHCO$_3$.

3.14 Omeprazole treatment and GI tract pH measurement

Mice were treated intragastrically with 200 µL Omeprazole (40 mg/Kg body weight, Sigma-Aldrich) diluted in 0.2% $NaHCO_3$ and 0.5% methylcellulose. Untreated and treated mice were sacrificed, the stomach and intestine were excised and cut longitudinally, and the pH of their content was measured by placing a pH indicator stripe (GE Healthcare Life Sciences) on the mucosal surface of the tissues.

3.15 Statistics

Results are represented as mean±SEM. Statistical significance between two groups was determined by the unpaired Student's t-test. When more than two groups were compared, One-way ANOVA followed by Bonferroni post-test was performed. In all the cases, GraphPad Prism software was used to perform the statistical test. $*p<0.05$, $**p<0.01$, $***p<0.001$.

4 RESULTS

4.1 Studies on the universal influenza vaccine candidate CTA1-3M2e-DD

4.1.1 Validation of CTA1-3M2e-DD targeting ability

The influenza vaccine candidate CTA1-3M2e-DD has already been shown to elicit strong protective immunity against influenza virus challenge in mice as an intranasal vaccine [121,128]. Before assessing its potential as an oral vaccine, we performed *in vitro* binding experiments to confirm the targeting ability of CTA1-3M2e-DD in our hands.

The adjuvant fusion protein CTA1-DD is able to bind to different Ig isotypes through the DD moiety, targeting splenic B cells in mice after intravenous injection [113]. Since CTA1-3M2e-DD carries the same Ig-binding domain, we firstly assessed its targeting capability by incubating different amounts of fluorescently-labeled CTA1-3M2e-DD with mouse splenocytes, followed by staining for the B cell marker B220. Flow cytometric analysis revealed that CTA1-3M2e-DD binds to mouse splenic B cells, in a dose-dependent manner (Fig. 4.1).

The targeting of human B cells by CTA1-DD was also previously reported [181]. Similarly, when incubating human PBMCs with CTA1-3M2e-DD conjugated with AF488, we observed a dose-dependent binding of this fusion protein to $CD19^+$ B cells (Fig. 4.2). Moreover, as shown for CTA1-DD binding to human B cells by Eriksson and Lycke [181], CTA1-3M2e-DD also exhibited a bimodal binding pattern to this cell population in our assays, with one subpopulation of $CD19^+$ cells showing higher fluorescence and another $CD19^+$ subpopulation showing lower fluorescence (Fig. 4.2).

Figure 4.1. CTA1-3M2e-DD binds to mouse splenic B cells.

Flow cytometric analysis of the binding ability of CTA1-3M2e-DD/AF488 to freshly isolated splenocytes from C57BL/6 mice after 1h of incubation with the indicated amounts of fusion protein (μg), followed by staining for a B cell marker (B220). Histogram representations show AF488 fluorescence intensity of B220^{+} cells in the presence (colored histograms) or absence (shaded histogram) of CTA1-3M2e-DD. The geometric mean fluorescence intensity for each condition is reported inside the histograms. Data are representative of two independent experiments.

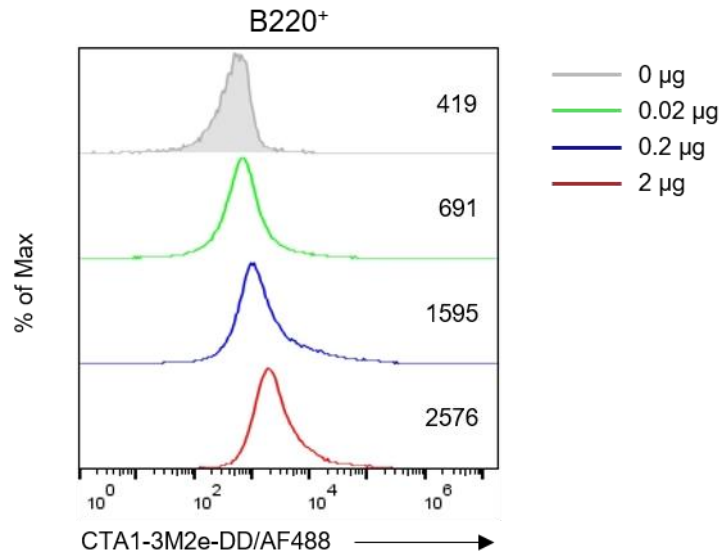**Figure 4.2. CTA1-3M2e-DD binds to human B cells.**

Flow cytometric analysis of the binding ability of CTA1-3M2e-DD/AF488 to freshly isolated human PBMCs after 1h of incubation with the indicated amounts of fusion protein (μg), followed by staining for a B cell marker (CD19). Histogram representations show AF488 fluorescence intensity of

CD19^{+} cells in the presence (colored histograms) or absence (shaded histogram) of CTA1-3M2e-DD. The geometric mean fluorescence intensity for each condition is reported inside the histograms. Data are representative of two independent experiments.
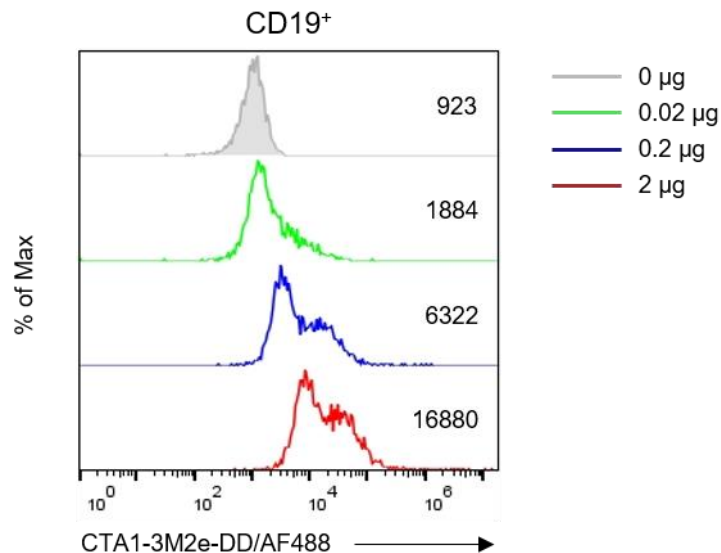
We therefore confirmed that the targeting function of the DD region is maintained in the influenza vaccine candidate CTA1-3M2e-DD, based on what was previously published for the fusion protein CTA1-DD.

4.1.2 Characterization of CTA1-3M2e-DD uptake in the small intestine

One of the most challenging aspects of designing mucosal vaccines is overcoming the harsh environment that they will encounter: degradation by proteases in mucosal secretions, entrapment by gel-forming mucins, and exclusion by epithelial barriers are some examples. When exploring the GI tract as a potential immunization route for a new vaccine, it is important to understand whether it can escape these hurdles and be available to immune cells.

We continued our studies by investigating whether CTA1-3M2e-DD, as an oral vaccine, can reach the lamina propria of the small intestine and be accessible to APCs. In order to do so, and at the same time avoid degradation by gastric enzymes and dilution throughout the GI tract, but still mimicking an oral immunization, CTA1-3M2e-DD was directly administered in the small intestine. C57BL/6 mice were subjected to intestinal ligation and different amounts of CTA1-3M2e-DD conjugated with AF647 were injected into the intestinal loops. Two hours later, the loop was resected and processed for imaging analysis.

As depicted in Figure 4.3, administration of increasing doses of CTA1-3M2e-DD/AF647 in ligated intestinal loops revealed that high amounts of protein were required for its detection, as only intestinal loops treated with 100 µg of CTA1-3M2e-DD/AF647 allowed a clear visualization of the fusion protein. Regarding CTA1-3M2e-DD localization, 2h after

| PBS | 5 µg | 50 µg | 100 µg |
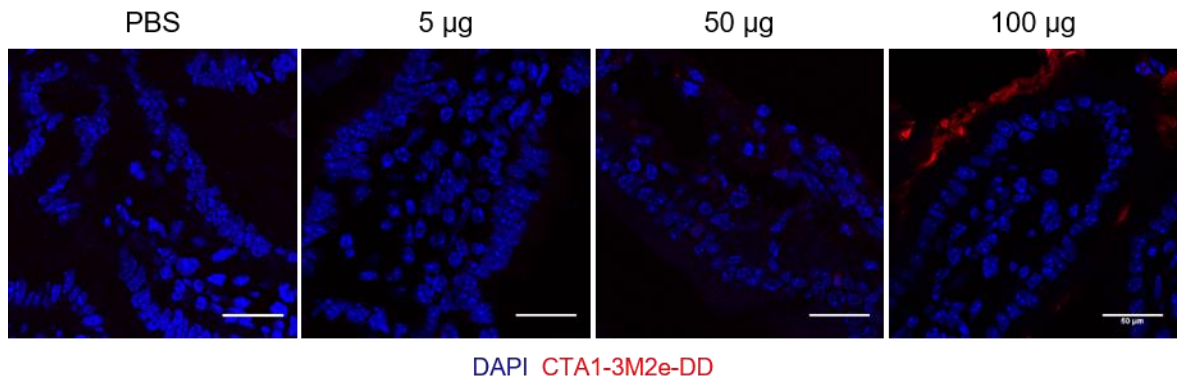
DAPI CTA1-3M2e-DD

Figure 4.3. CTA1-3M2e-DD remains in the intestinal lumen 2h after administration.

The small intestine of C57BL/6 mice was exposed, an intestinal loop was formed and the indicated amounts of CTA1-3M2e-DD conjugated with AF647 or PBS (vehicle) were injected into the loop. Two hours later, the loop was resected and processed for confocal microscopy. Cryosections were stained with DAPI. Confocal images of intestinal villi showing CTA1-3M2e-DD (red) and nuclei (blue). n=3 mice/group. Scale bars: 50 µm.

injection, the fusion protein remained in the intestinal lumen, surrounding the epithelium, and did not reach the lamina propria.

4.1.3 Characterization of CTA1-3M2e-DD uptake by intestinal APCs

Although CTA1-3M2e-DD failed to cross the intestinal epithelial barrier after 2h of its administration, we wondered if the fusion protein could still target intestinal APCs present in the small intestine lamina propria after an extended period of treatment.

To evaluate which subset of lamina propria APCs was able to take up CTA1-3M2e-DD, we took advantage of $Cx3cr1^{GFP/+}$ mice. These heterozygous knock-in mice carry a gene coding for GFP under the control of the CX_3CR1 promoter [175], allowing us to efficiently distinguish CX_3CR1^+ cells, a marker used to discriminate an important subset of macrophages in the small intestine, which otherwise would be difficult as the commercially available antibodies for CX_3CR1 have proven to be far from effective. $Cx3cr1^{GFP/+}$ mice were administered 100 µg of CTA1-3M2e-DD/AF647 (or vehicle alone) through

intraduodenal injection and 4h later the entire small intestine was collected and processed for flow cytometric analysis in order to quantify the uptake of CTA1-3M2e-DD.

The expression of CX_3CR1 and CD103 is typically used to identify the two main APC subsets in the small intestine, CX_3CR1^+ macrophages and $CD103^+$ DCs. Thus, the cells isolated from small intestines were stained with antibodies for CD45.2, IA-IE, CD11c, CD103 and CD11b. As shown in Figure 4.4, after excluding dead cells and gating $CD45.2^+$ $IA-IE^+$ $CD11c^+$ cells, the two main APC subsets were distinguished through their expression of CX_3CR1 and CD103. CX_3CR1^+ macrophages were further divided based on their intermediate and high expression of CX_3CR1 (CX_3CR1^{int} and CX_3CR1^{high}, respectively). Gating on $CD103^+$ DCs and separating them by their expression of CD11b allowed us to identify two other subsets, $CD103^+$ $CD11b^-$ and $CD103^+$ $CD11b^+$.
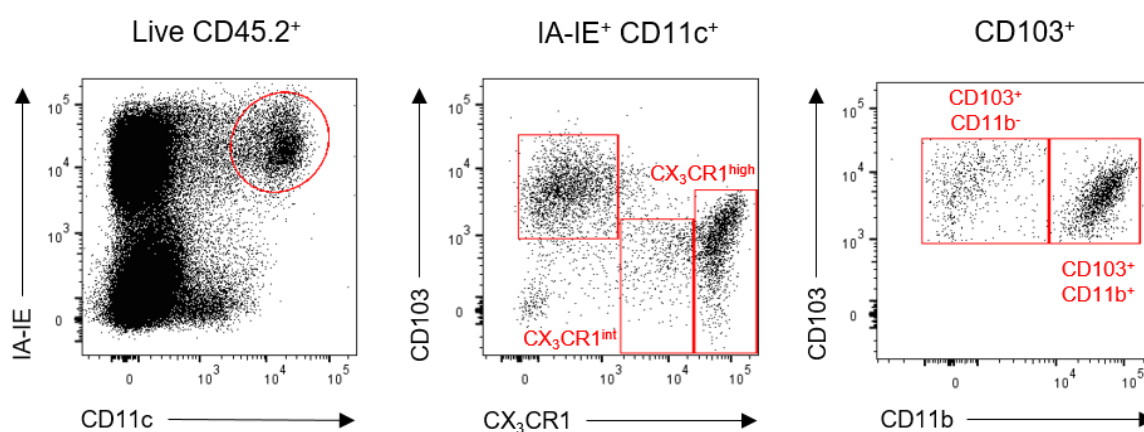
Figure 4.4. Gating strategy to define the main subsets of APCs in the small intestine lamina propria.

The small intestine of a *Cx3cr1*$^{GFP/+}$ mouse was processed to obtain a single-cell suspension. Cells were stained with a viability marker and antibodies for CD45.2, CD11c, IA-IE, CD103 and CD11b, and subsequently analyzed by flow cytometry. After exclusion of dead cells and epithelial cells ($CD45.2^-$), $IA-IE^+$ $CD11c^+$ cells were gated and three APC subsets can be identified: $CD103^+$ DCs, $CX3CR1^{int}$ and $CX3CR1^{high}$ macrophages. $CD103^+$ cells were further divided based on their expression of CD11b, distinguishing $CD103^+$ $CD11b^-$ and $CD103^+$ $CD11b^+$ DC populations.

A

B
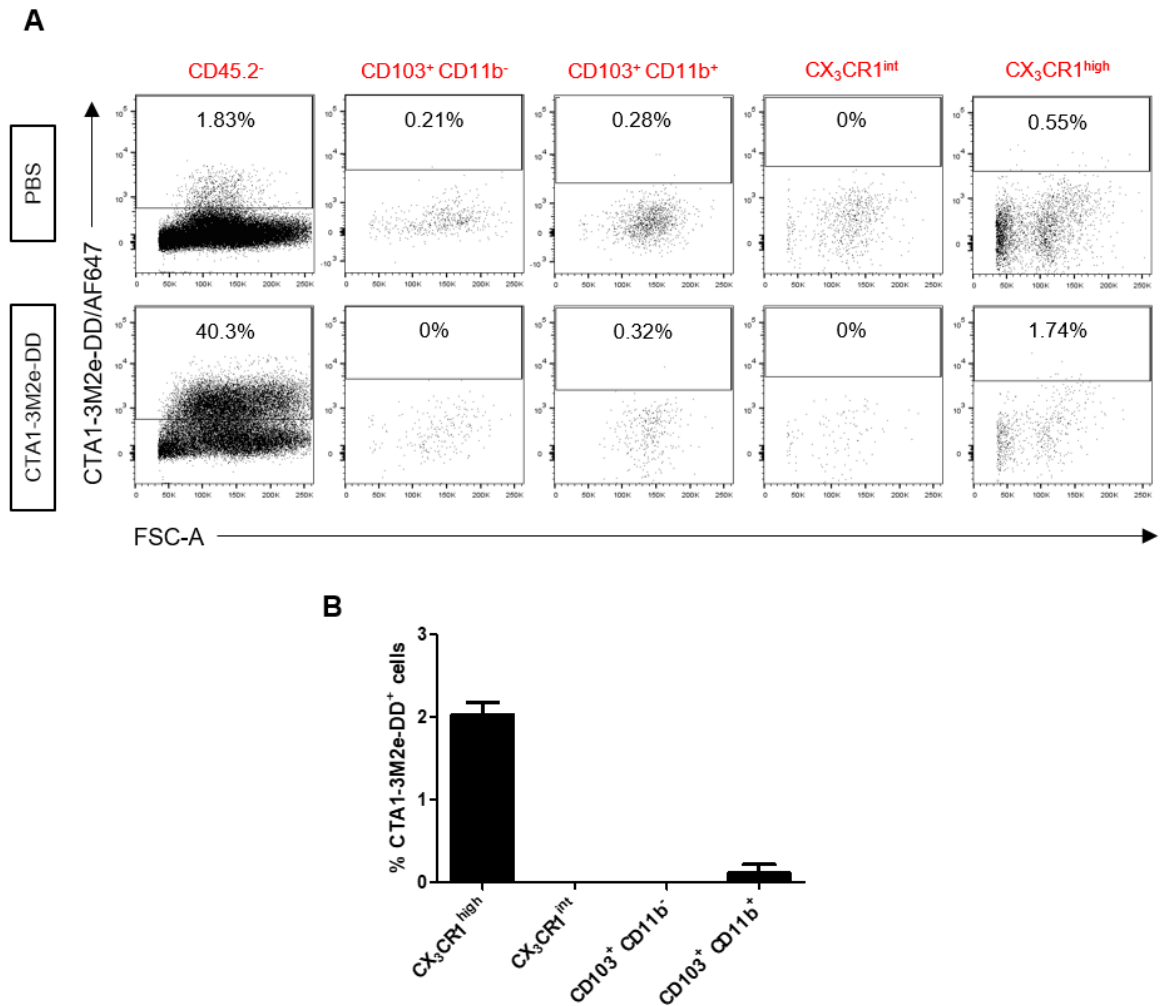
Figure 4.5. CTA1-3M2e-DD is poorly taken up by small intestine lamina propria APCs.

PBS (vehicle) or 100 µg of CTA1-3M2e-DD/AF647 were injected in the duodenum of $Cx3cr1^{GFP/+}$ mice. After 4h, the small intestines were processed and cells were isolated for flow cytometric analysis. **(A)** Representative dot plots show the percentage of CTA1-3M2e-DD⁺ cells found in CD45.2⁻ cells and in each subset of APCs. **(B)** Percentage of CTA1-3M2e-DD⁺ cells in CX₃CR1^high, CX₃CR1^int, CD103⁺ CD11b⁻ and CD103⁺ CD11b⁺ subsets. Data are shown as mean±SEM and are representative of two independent experiments, n=3 mice/group.

Four hours following CTA1-3M2e-DD administration, we observed that the protein was mainly associated with CD45.2⁻ cells, most likely intestinal epithelial cells (Fig. 4.5A). In the different subsets of APCs that were analyzed, only a small percentage of CTA1-3M2e-DD⁺ cells were found in CX₃CR1^high macrophages, while the fusion protein was virtually absent in the remaining subsets (Fig. 4.5A-B).

These results suggest that CD45.2$^-$ epithelial cells are a major contributor for CTA1-3M2e-DD uptake in the small intestine. However, and based on our initial observation through imaging analysis, due to the retention of the protein in the lumen and attachment to the luminal surface of the epithelium for at least 2h after administration, CTA1-3M2e-DD$^+$ CD45.2$^-$ cells observed by flow cytometry can reflect surface association and not necessarily internalization of the protein by epithelial cells. The fact that CTA1-3M2e-DD was found associated with CX_3CR1^{high} phagocytes, which are endowed with the ability of extending trans-epithelial dendrites [49], might indicate the direct uptake of the protein by this population.

4.2 Studies on the vaccine delivery system NPL

4.2.1 Characterization of NPL uptake in the small intestine

Given the low capacity of CTA1-3M2e-DD to penetrate the intestinal barrier and target APCs in the lamina propria, we turned our attention to the nanoparticle-based vaccine vectors that are being developed in our consortium to achieve enhanced targeting of immune cells in mucosal tissues. Cationic polysaccharide nanoparticles with a lipidic core, NPL, have already been characterized [182] and tested as vaccine vectors for mucosal immunization, namely intranasal delivery of vaccines [177]. Thus, we decided to investigate the behavior of NPL as a potential vaccine delivery system for oral vaccines.

To understand whether NPL could overcome the different components of the intestinal barrier, and identically to what was done with the influenza vaccine candidate, we performed intestinal loops in C57BL/6 mice, injected 50 µg of FITC-labeled NPL and analyzed their uptake by confocal microscopy.

After only 1h of its administration, NPL crossed the epithelial barrier in the intestine, as we were able to visualize them not only in the lumen, but also filling a few epithelial cells (highlighted by filled arrowheads) and most importantly in the lamina propria (highlighted by empty arrowheads) (Fig. 4.6).

PBS   NPL

DAPI NPL
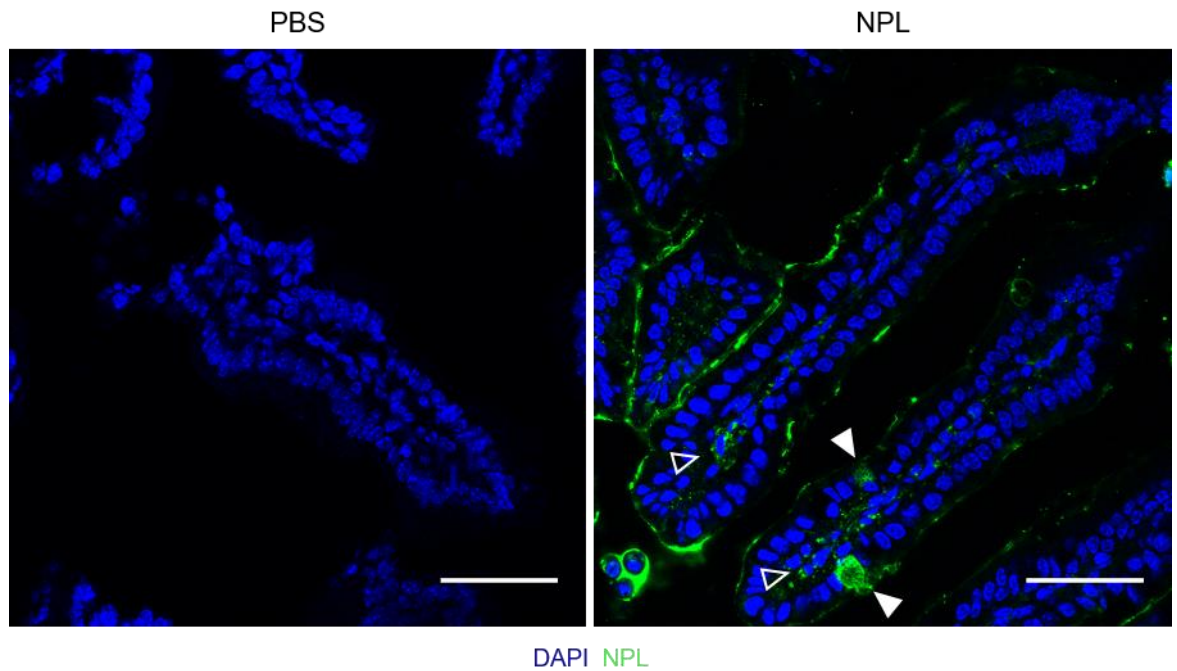
Figure 4.6. NPL cross the intestinal epithelium and reach the mouse intestinal lamina propria.

The small intestine of C57BL/6 mice was exposed and 50 µg of NPL/FITC or PBS (vehicle) were injected into an intestinal loop. After 1h, the loop was resected and processed for confocal microscopy. Cryosections were stained with DAPI. Confocal images of intestinal villi showing NPL (green) and nuclei (blue). Filled arrowheads and empty arrowheads highlight localization of NPL within epithelial cells and in the lamina propria, respectively. Images are representative of two independent experiments, n=3-4 mice/group. Scale bars: 50 µm.

Since the goal of our consortium is to generate a human influenza vaccine, we questioned whether NPL were also taken up in the human intestine. We took advantage of an *ex vivo* organ culture model developed a few years ago in our group to study the human intestine [179,180]. This model allows studying the response of intestinal tissue in a way that resembles the physiologic situation, as the polarization of the tissue is maintained and the stimulus of interest is solely in contact with the luminal surface and does not reach the basolateral side. Explants of human intestine (ileum) were cultured and, after allowing mucus reconstitution for 1h in order to mimic the *in vivo* situation, 20 µg of NPL/FITC or medium alone (vehicle) were added to the luminal surface of the tissue for another hour.

NT	Medium	NPL

DAPI NPL
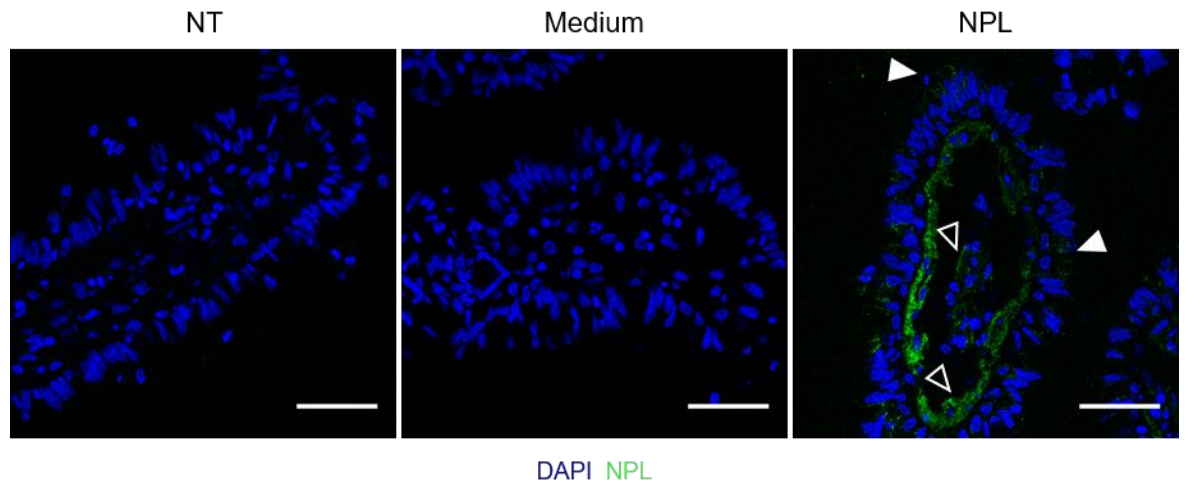
Figure 4.7. NPL cross the epithelium and reach the lamina propria in an *ex vivo* human intestine culture model.

Explants of human ileum were fixed upon arrival (not treated, NT) or were maintained in culture with 20 µg of NPL/FITC or medium alone (vehicle) in contact with the luminal surface for 1h. The cultured explants were then processed for confocal microscopy and cryosections were stained with DAPI. Confocal images of intestinal villi showing NPL (green) and nuclei (blue). Filled arrowheads and empty arrowheads highlight localization of NPL within epithelial cells and in the lamina propria, respectively. Representative images of four surgically resected ileal specimens. Scale bars: 50 µm.

Confocal analysis showed that the culture process did not affect tissue integrity, by comparing the villi morphology in cultured explants with the same in a piece of the specimen that did not undergo culture and was immediately fixed upon arrival (Fig. 4.7). Similarly to what was found *in vivo* in mice, NPL crossed the epithelial barrier in the human intestine, with NPL found within some epithelial cells (highlighted by filled arrowheads) and concentrated in the lamina propria (highlighted by empty arrowheads).

We therefore validated the ability of NPL to cross epithelial barriers in two different models (mouse and human) that enable us to study their behavior as a vaccine delivery system for oral immunization.

4.2.2 Identification of NPL-filled intestinal epithelial cells

Depending on the size and nature of intestinal antigens, these are sampled from the lumen and transferred into the lamina propria by different mechanisms [81]. Some of these mechanisms depend on intestinal epithelial cells that are specialized precisely in antigen sampling, particularly M cells [80–82,84,86,87,89]. However, epithelial cells with other functions, such as enterocytes that are specialized in nutrient absorption or Goblet cells that produce and secrete mucins, may also contribute to antigen transfer into the lamina propria or directly to specific immune cells [90,92,183].

High amounts of NPL were found within some epithelial cells in the intestines of mice (Fig. 4.6) and human intestinal explants (Fig. 4.7). These cells are unlikely to be enterocytes, as these are the most abundant epithelial cells in the intestine and we observed NPL^{+} epithelial cells with much less frequency in our experiments. Because these cells seem to facilitate the entrance of NPL into the lamina propria, we proceeded with their identification. Cryosections from intestinal loops of C57BL/6 mice treated with 50 µg of NPL/FITC for 1h were stained with antibodies for markers of different epithelial cells that exist in the epithelium at low frequencies. These epithelial cells include mucus-secreting Goblet cells, identified by the presence of MUC2; Paneth cells, identified by lysozyme (LYS), one of the antimicrobial enzymes secreted by these cells in the intestinal crypts; and enteroendocrine cells, which production of the neuroendocrine protein chromogranin A (CmgA) allows its visualization.

As shown in Figure 4.8, the distribution of NPL in the distinct mouse intestinal epithelial cells varies greatly. We found that small clusters of NPL were present inside LYS^{+} Paneth cells, whereas CmgA^{+} enteroendocrine cells did not take up NPL. Nonetheless, the cells initially detected as entry passages for NPL were identified as MUC2^{+} Goblet cells, as this marker co-localizes with the presence of high amounts of NPL in the epithelium.
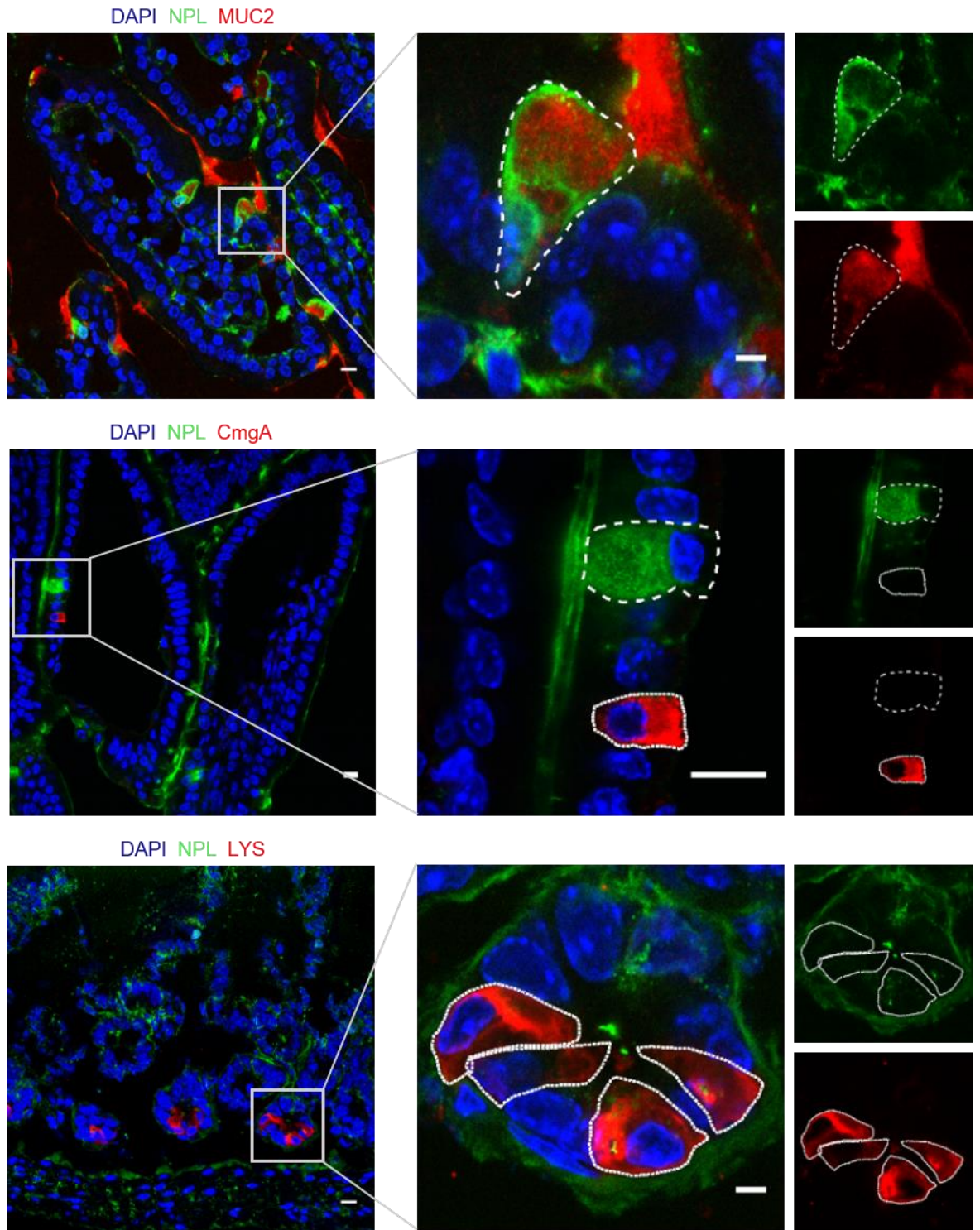
Figure 4.8. Goblet cells in the mouse small intestine transfer high amounts of NPL into the lamina propria.

Intestinal loops of C57BL/6 mice were injected with 50 μg of NPL/FITC and resected 1h later, followed by tissue processing for confocal microscopy. Cryosections were stained with DAPI and antibodies against different epithelial cell markers: MUC2 for Goblet cells; CmgA for enteroendocrine cells; LYS for Paneth cells. Confocal images of intestinal villi show NPL (green),

nuclei (blue) and the different epithelial cells (red). Square inset is shown on the right of each image with single channels for NPL and the different epithelial cells. Dashed lines represent the contour of NPL-filled epithelial cells and/or epithelial cells identified by each marker. Images are representative of two independent experiments, n=3-4 mice/group. Scale bars: 10 μm.

As NPL were also visualized within a few epithelial cells of human intestinal explants following our *ex vivo* experiments for NPL uptake, we wondered if these NPL^{+} cells were also Goblet cells. Cryosections from explants cultured with 20 μg of NPL/FITC for 1h were consequently stained for MUC2. In accordance to what was found in the mouse intestinal epithelium, NPL co-localized with MUC2^{+} cells in the epithelium of the human intestine (Fig. 4.9).
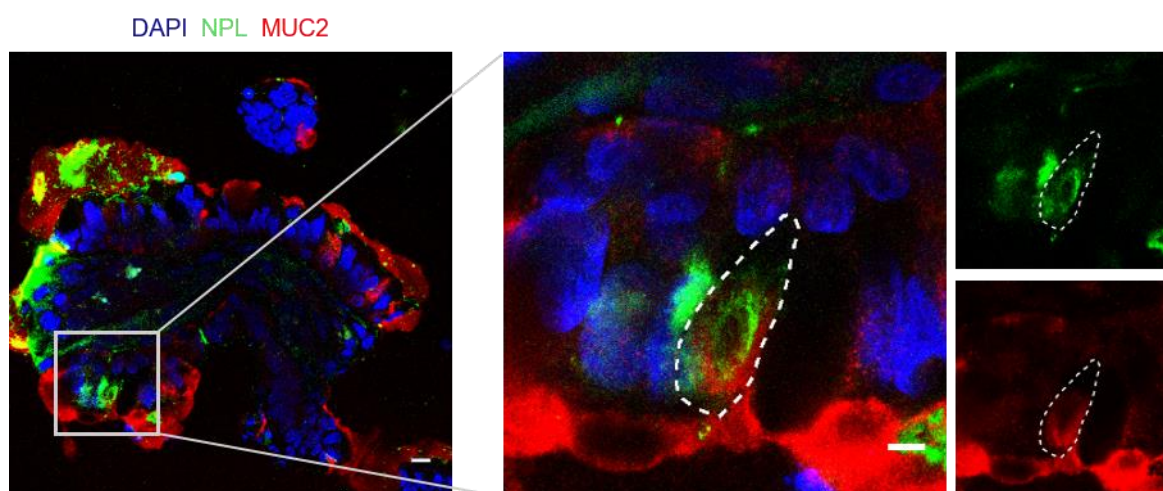
Figure 4.9. Goblet cells in the human intestine transfer high amounts of NPL into the lamina propria.

Explants of human ileum were maintained in culture with 20 μg of NPL/FITC in contact with the luminal surface for 1h, followed by tissue processing for confocal microscopy. Cryosections were stained with DAPI and anti-MUC2 antibody. Confocal images of intestinal villi showing NPL (green), nuclei (blue) and MUC2 (red). Square inset is shown on the right of the image with single channels for NPL and MUC2. Dashed line represents the contour of a MUC2^{+} Goblet cell transferring NPL. Representative images of four surgically resected ileal specimens. Scale bars: 10 μm.

Together, these results suggest that Goblet cells are a major contributor in the intestinal epithelium for NPL uptake and transfer from the lumen to the lamina propria.

4.2.3 Characterization of NPL uptake by intestinal APCs

Taking into account that NPL succeeded in traversing the epithelial barrier at the level of the intestine and were found in the lamina propria (where they were available for phagocytosis by immune cells), as shown by imaging analysis, we next wondered which intestinal APCs were able to take up NPL.
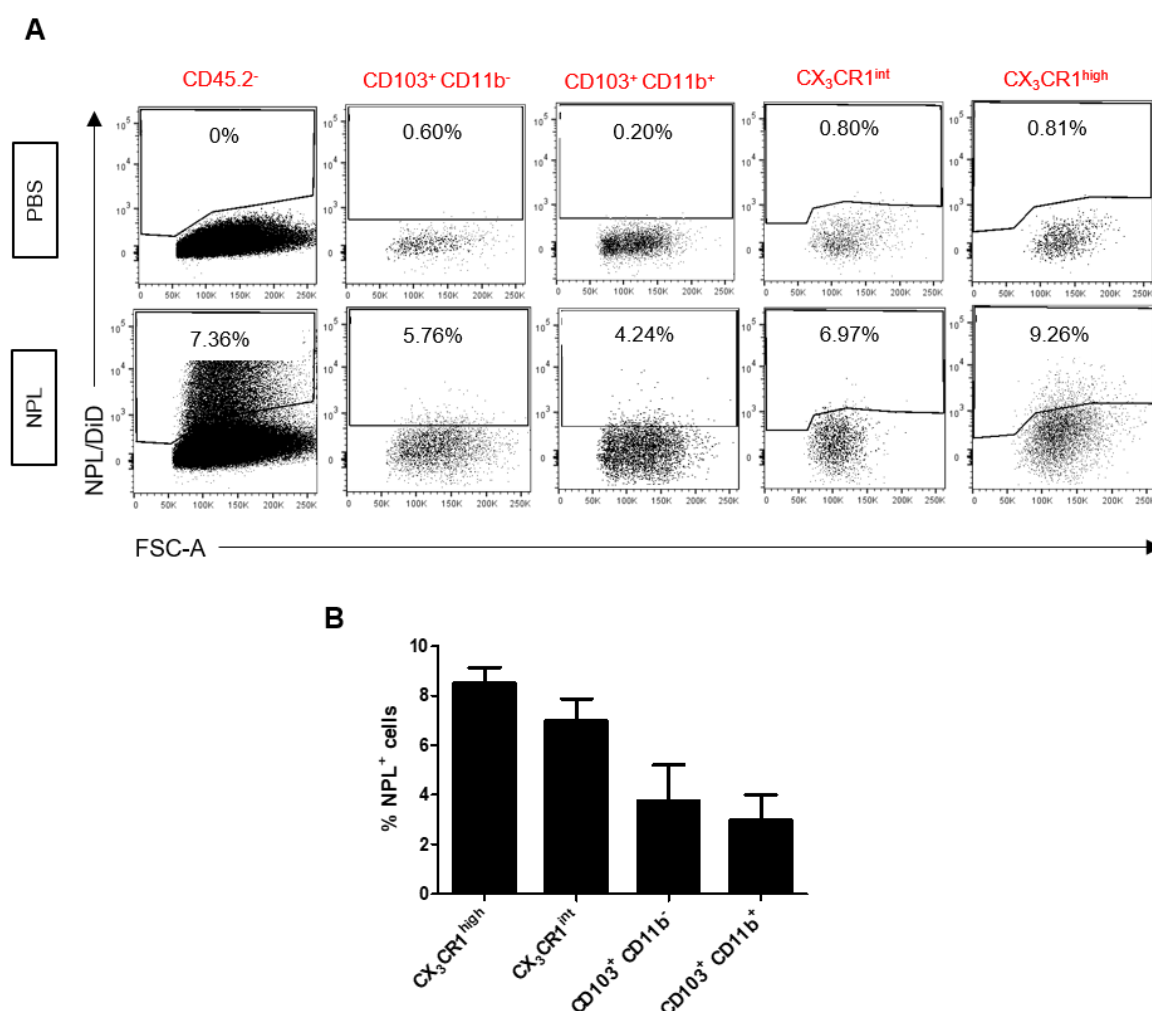
Figure 4.10. NPL are taken up by different subsets of intestinal lamina propria APCs.

PBS (vehicle) or 250 µg of NPL/DiD were administered to $Cx3cr1^{GFP/+}$ mice through intraduodenal injection. Two hours later, the small intestines were processed and cells were isolated for flow

57

cytometric analysis. **(A)** Representative dot plots show the percentage of NPL$^+$ cells found in CD45.2$^-$ cells and in each subset of APCs. **(B)** Percentage of NPL$^+$ cells in CX$_3$CR1^{high}, CX$_3$CR1^{int}, CD103$^+$ CD11b$^-$ and CD103$^+$ CD11b$^+$ subsets. Data are shown as mean±SEM and are representative of two independent experiments, n=3-4 mice/group.

Once more, we identified the main subsets of APCs by flow cytometric analysis (Fig. 4.4) and quantified the uptake of DiD-labeled NPL in the small intestine lamina propria of *Cx3cr1*$^{GFP/+}$ mice 2h after its administration directly in the duodenum. NPL were present in CD45.2$^-$ cells, presumably epithelial cells, which confirms our results from confocal microscopy analysis, but, most importantly, they were distributed across all the main APC subsets (Fig. 4.10A). The four analyzed subsets were able to internalize NPL to different extents, with CX$_3$CR1$^+$ macrophages showing a slightly higher percentage of NPL$^+$ cells than CD103$^+$ DCs (Fig. 4.10B).

The previous findings further support the aptness of NPL as vaccine carriers for oral delivery, as they are able not only to cross the intestinal epithelial barrier, but also target different types of intestinal APCs.

4.2.4 NPL uptake by CX$_3$CR1$^+$ macrophages

From the previous results, we determined that NPL are transferred to the lamina propria through Goblet cells, where different APCs internalize them. One of these subsets of APCs, CX$_3$CR1$^+$ macrophages, have the capacity to directly acquire antigens from the intestinal lumen by extending protrusions across the epithelium [49]. We therefore asked whether the uptake of NPL by these cells was also a result of this feature.

To answer that, we injected 50 µg of NPL/DiD into intestinal loops of *Cx3cr1*$^{GFP/+}$ mice and processed the tissue for confocal microscopy in order to visualize the possible formation of trans-epithelial protrusions by CX$_3$CR1$^+$ cells. As depicted in Figure 4.11, we confirmed the localization of NPL within CX$_3$CR1$^+$ cells, 1h after NPL administration, but no CX$_3$CR1$^+$ protrusions were found at the level of the villi. When looking at PP, however, NPL were
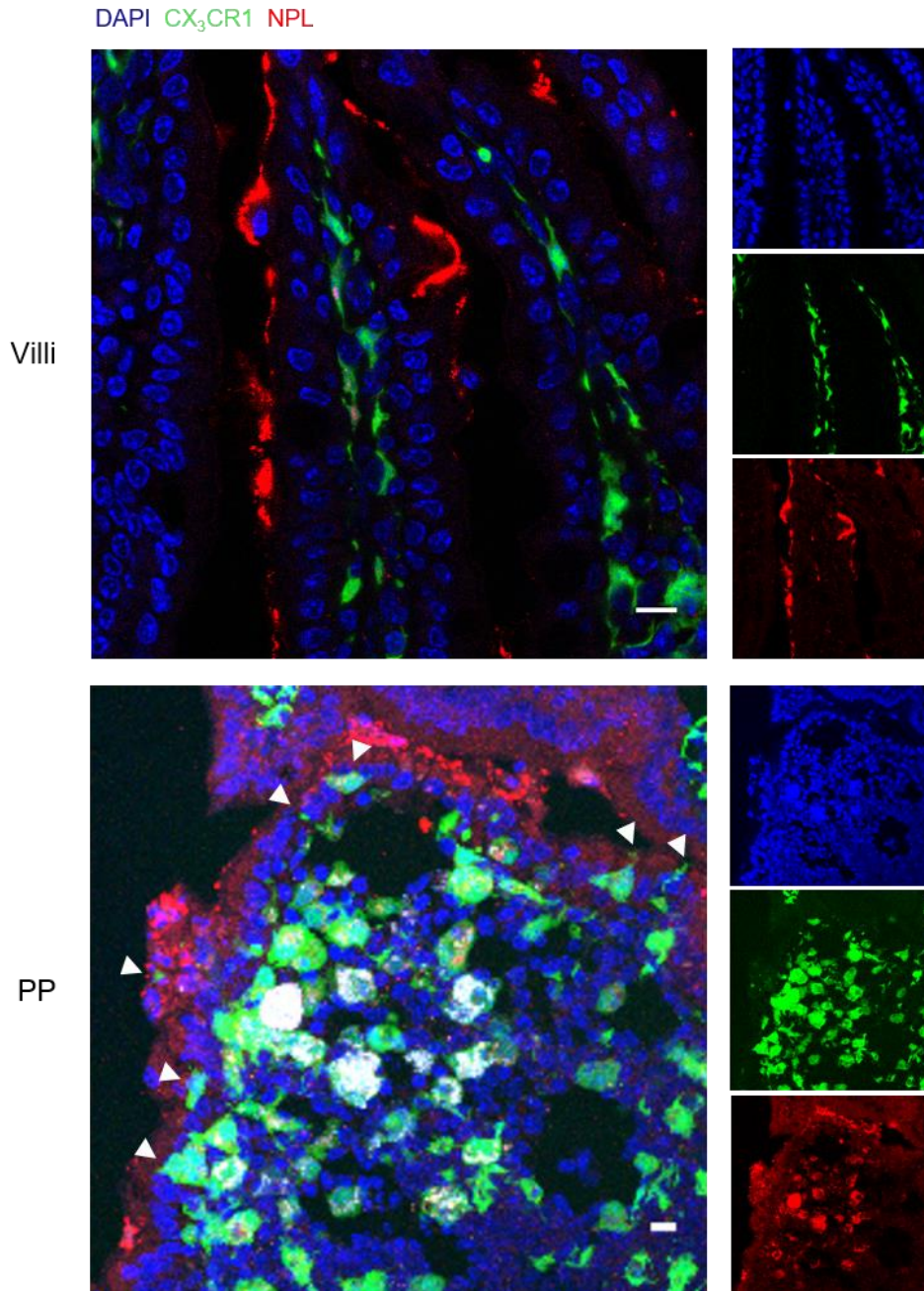
Figure 4.11. CX$_3$CR1$^+$ cells in PP directly acquire NPL from the lumen.

The small intestine of *Cx3cr1*$^{GFP/+}$ mice was exposed and 50 µg of NPL/DiD were injected into an intestinal loop containing a PP. After 1h, the loop was resected and processed for confocal microscopy. Cryosections were stained with DAPI. Confocal images of intestinal villi and PP showing CX$_3$CR1 (green), NPL (red) and nuclei (blue). Single channels for DAPI, CX$_3$CR1 and NPL are shown on the right of each image. Arrowheads highlight localization of CX$_3$CR1$^+$ cells or their protrusions crossing the FAE. Images are representative of two independent experiments, n=3 mice/group. Scale bars: 10 µm.

also found within CX_3CR1^+ cells and their dendrites or even the entire cell body was visualized crossing the FAE and sampling NPL from the lumen (highlighted by arrowheads).

This confirms that, at least in PP, the uptake of NPL by CX_3CR1^+ macrophages occurs directly and not merely due to epithelial transfer of NPL.

4.2.5 Characterization of antigen delivery by NPL in the small intestine

Vaccine delivery systems should be able to protect the vaccine against degradation and release it in the target tissue or cell. Studies have shown that loading NPL with OVA as a model antigen and giving this formulation by intranasal administration in mice extends the time of residence of the protein in the nose as compared to administering the protein alone [177].

To test the ability of NPL to protect the loaded antigen in the intestine and deliver it in the lamina propria, we used NPL and OVA in formulation, each conjugated with different fluorochromes. C57BL/6 mice were then treated with this formulation through injection in intestinal loops and the distribution of both OVA and NPL was visualized by confocal microscopy. Similarly to what was observed before in experiments with NPL alone, we were able to visualize some epithelial cells filled with OVA:NPL, as well as clusters of the formulation inside the lamina propria (highlighted by yellow arrowheads) (Fig. 4.12). Nevertheless, OVA alone was also found in epithelial cells and lamina propria (highlighted by white arrowheads).

This suggests that NPL can protect the formulated antigen from intestinal degradation, but probably a mechanism of antigen-NPL dissociation takes place when the vaccine vector is transferred through the epithelium, delivering some of the antigen by itself.
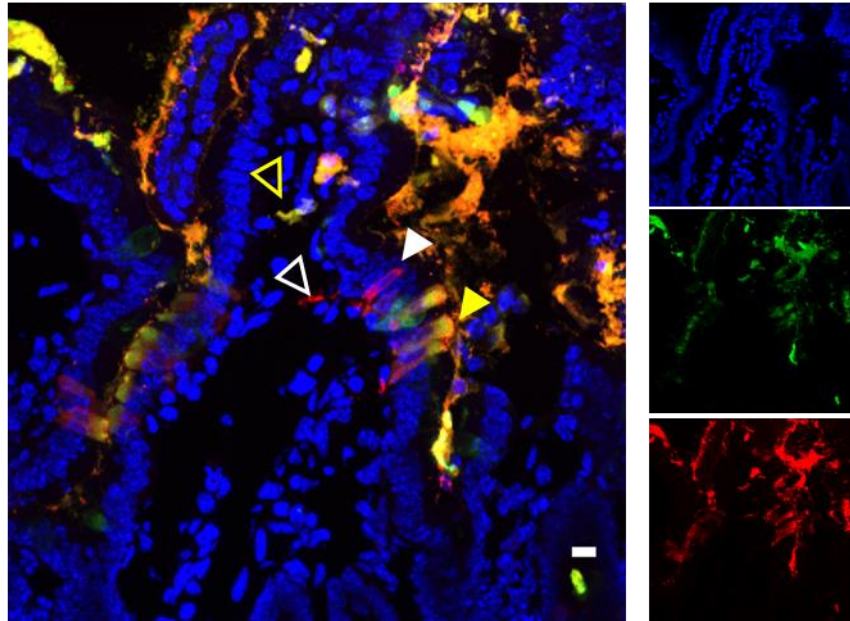
Figure 4.12. Antigen loaded into NPL reaches the lamina propria both in free form and associated with the vaccine vector.

Intestinal loops were performed in C57BL/6 mice and NPL/FITC loaded with OVA/TRITC (10 μg OVA:50 μg NPL) were injected in the loop. One hour later, the tissue was resected and processed for confocal microscopy. Cryosections were stained with DAPI. Confocal images of intestinal villi showing NPL (green), OVA (red) and nuclei (blue). Single channels for DAPI, NPL and OVA are shown on the right of the image. White and yellow arrowheads indicate localization of OVA alone and OVA:NPL, respectively. Filled and empty arrowheads highlight localization of the latter in epithelial cells and lamina propria, respectively. n=3 mice. Scale bars: 10 μm.

4.2.6 Effect of starvation and immunization time in the immune response of OVA:NPL treated mice

We next evaluated if formulating an antigen with NPL would be advantageous for antigen delivery/presentation in the small intestine, compared to administration of the antigen alone. We assessed that by choosing OVA as a model antigen and taking advantage of OT II mice, that express a transgenic T cell receptor able to recognize $OVA_{323-339}$ when presented by IA-IE on APCs. This allows us to measure and compare antigen-specific T cell activation after presentation of the antigen when this is delivered alone or formulated

with the vaccine vector. Thus, we isolated naïve CD4$^+$ T cells from lymphoid organs of OT II (Ly5.2) mice and, after labeling them with CFSE (that enables the measurement of cell proliferation, as it is equally distributed by daughter cells when cells divide), they were transferred into C57BL/6 (Ly5.1) mice through intravenous injection (Fig. 4.13). The next day, recipient mice were immunized with NPL alone (no antigen), OVA alone or OVA formulated with NPL by intraduodenal injection. Five days later, different organs were collected from the immunized mice and we assessed CD4$^+$ T cell proliferation in the OVA-specific Ly5.2$^+$ population by flow cytometry.

We observed that NPL-immunized mice showed virtually no proliferation in this cell population, as expected, as no antigen was present, whereas mice immunized with OVA alone or in combination with NPL presented higher proliferation (Fig 4.14). When comparing the OVA and OVA:NPL immunized groups, no significant advantage was given by the formulated treatment. However, we noticed that proliferation of OVA-specific CD4$^+$ T cells in the group receiving OVA:NPL reflected high variability.
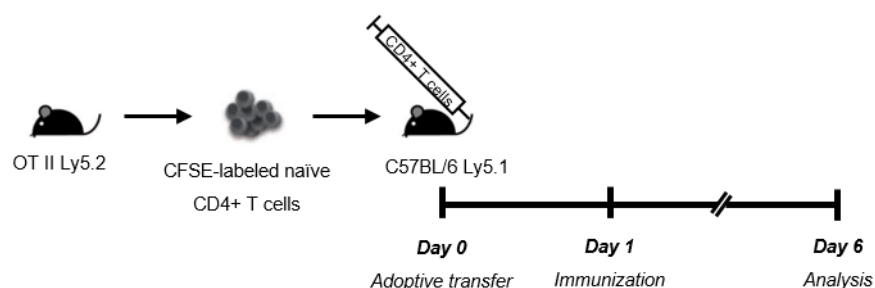
Figure 4.13. Scheme of the adoptive transfer and immunization schedule.

Spleens and lymph nodes from OT II Ly5.2 mice were collected and CD25$^-$ CD4$^+$ T cells were isolated. After labeling with CFSE, these cells were transferred into C57BL/6-Ly5.1 mice (2x10^6 cells/mouse) through intravenous injection. The following day, the recipient mice were immunized and 5 days later organs were collected, processed for flow cytometry and OVA-specific CD4$^+$ T cell proliferation was evaluated as CFSE dilution.
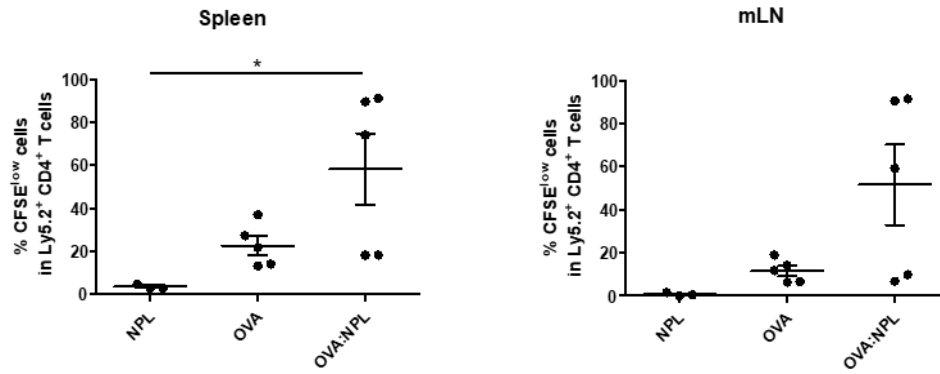
Figure 4.14. *In vivo* proliferation of antigen-specific CD4+ T cells after immunization with NPL formulation.

C57BL/6-Ly5.1 mice were adoptively transferred with naïve OT II Ly5.2+ CD4+ T cells and the next day were subjected to intraduodenal immunization with NPL alone (1 mg), OVA (200 µg) or formulation OVA:NPL (200 µg OVA:1 mg NPL). Five days later, proliferation of OT II Ly5.2+ CD4+ T cells in indicated organs was measured by flow cytometry. Each data point represents an individual mouse. Data are shown as mean±SEM, n=3-5 mice/group. One-way ANOVA followed by Bonferroni test was used to evaluate statistical significance. *p<0.05.

Since immunization relied on a procedure that takes some time to perform, as it includes subjecting the mice to anesthesia, surgery and intraduodenal injection, we hypothesized that this variability could be explained by different times of immunization. Accordingly, we plotted the percentage of OT II CD4+ proliferating T cells from this experiment with the time at which the immunization occurred for each mouse (Fig. 4.15). Indeed, from these preliminary results, we noticed a trend in the group immunized with OVA:NPL, in which mice subjected to immunization in the morning presented lower percentage of antigen-specific proliferating cells than mice from the same group immunized in the afternoon. In the case of OVA-treated mice, the immunization occurred in a shorter window of time and this trend couldn't be confirmed.
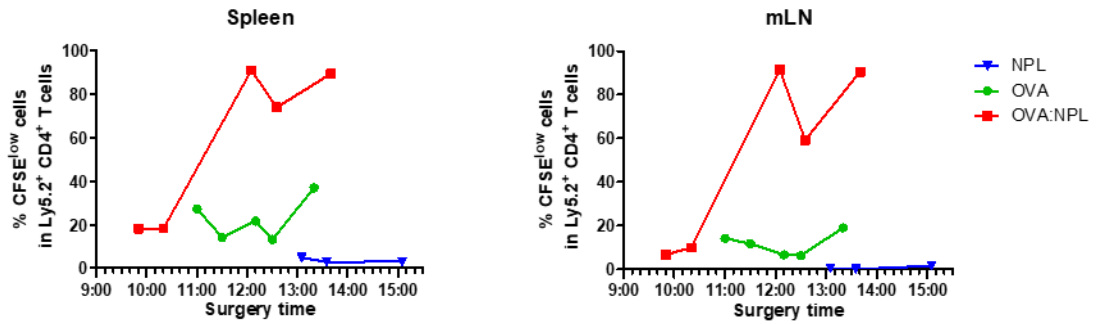
Figure **4.15***. OVA-specific CD4$^+$ T cell proliferation according to the time of immunization.*
The percentage of OVA-specific CD4$^+$ proliferating T cells presented in Figure 4.14 was plotted against the corresponding immunization time for each mouse. Each data point represents an individual mouse.

Based on these preliminary results, we thought about two possible factors that could influence the outcome of the immune response in this setting. In order to decrease the intestinal content, so it does not pose an important source of material competing with the immunization treatment, in our experiments the food is removed from the cages the evening before immunization. This means that mice undergo starvation during the night and until the moment of immunization and the ones that receive the treatment in the morning are less starved than the ones receiving it in the afternoon. As such, the period of starvation before immunization could play an important role. The other possibility is that the time of immunization itself shapes the immune response and mice immunized in the afternoon show a better response than the ones immunized in the morning.

Before deepening the investigation on the advantage of antigen presentation when it is formulated with NPL and to obtain more reliable results (addressed in sections 4.2.7 and 4.2.8), we decided to understand if the two factors mentioned above could really impact our experiments, in order to exclude this source of variability. We therefore uncoupled these two factors, immunization time and starvation, and evaluated the individual contribution of each.

A

Spleen

mLN

PP

B

Spleen

mLN

PP

Figure 4.16. Effect of immunization time on the immune response after OVA:NPL immunization.

C57BL/6-Ly5.1 mice were adoptively transferred with naïve OT II Ly5.2$^+$ CD4$^+$ T cells and the next day were subjected to intraduodenal immunization with OVA:NPL (200 µg OVA:1 mg NPL) in the morning (around 10 am) or in the afternoon (around 1 pm) without previous starvation. Five days later, the immune response in the OT II Ly5.2$^+$ CD4$^+$ T cell population of the indicated organs was analyzed by flow cytometry. **(A)** Percentage of proliferating OT II CD4$^+$ T cells. **(B)** Percentage of Foxp3$^+$ cells in OT II CD4$^+$ T cells. Each data point represents an individual mouse. Data are shown as mean±SEM, n=5 mice/group. Unpaired Student's *t*-test was used to evaluate statistical significance.

To understand the role of immunization time, we performed a similar experiment without previous starvation and immunizing the mice with OVA:NPL (the treatment in which we observed variability). In one group of mice, immunization occurred in a short window of time in the morning (around 10 am), whereas the other group of mice was immunized in the afternoon (around 1 pm). By assessing the proliferation of OVA-specific CD4$^+$ T cells in spleens, mLN and PP, we determined that the immunization time alone was not modulating the immune response, as T cell activation in both groups was comparable

(Fig. 4.16A). Additionally, we also performed staining for Foxp3 on these cells in order to understand if morning or afternoon immunizations could influence Treg cell conversion and therefore tolerance induction. Similarly, time of immunization did not significantly affect the occurrence of OVA-specific Tregs (Fig. 4.16B).
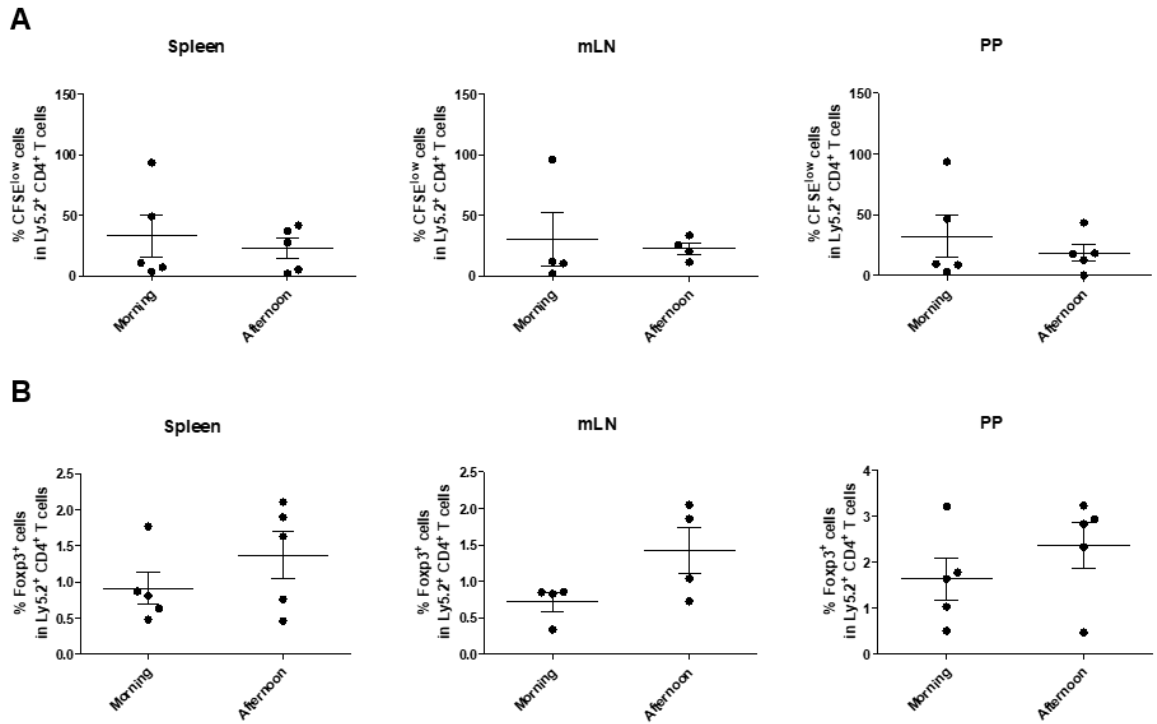

Figure 4.17. Effect of starvation on the immune response after OVA:NPL immunization.

C57BL/6-Ly5.1 mice were adoptively transferred with naïve OT II Ly5.2$^+$ CD4$^+$ T cells and the next day were subjected to intraduodenal immunization with OVA:NPL (200 µg OVA:1 mg NPL) after previous starvation during a long (19h) or short (16h) period. Five days later, the immune response in the OT II Ly5.2$^+$ CD4$^+$ T cell population of the indicated organs was analyzed by flow cytometry. **(A)** Percentage of proliferating OT II CD4$^+$ T cells. **(B)** Percentage of Foxp3$^+$ cells in OT II CD4$^+$ T cells. Each data point represents an individual mouse. Data are shown as mean±SEM and are pooled from four independent experiments. Unpaired Student's *t*-test was used to evaluate statistical significance. *p<0.05.

The sole contribution of the starvation period was subsequently assessed. To do so, a group of mice was immunized after 16h of starvation (short starvation) and another group after 19h (long starvation) (the duration of starvation of mice showing lower and higher proliferation, respectively, in the preliminary experiment, Fig. 4.15), and immunization with OVA:NPL occurred at random time of the day. Interestingly, we observed that long starvation induced significantly higher proliferation of OT II CD4$^+$ T cells in spleen and mLN, with PP showing a similar trend (Fig. 4.17A). Despite the increase in antigen presentation, a long starvation period did not induce Tregs in this population in any of the analyzed organs (Fig. 4.17B).
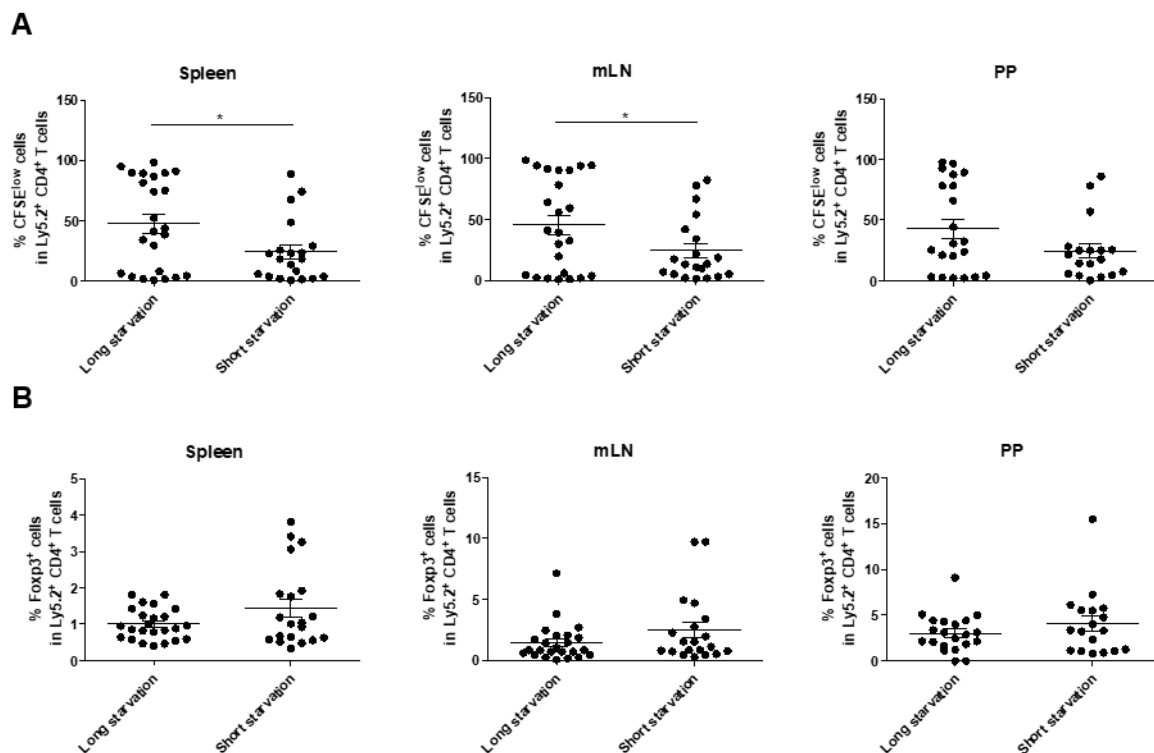
A

B
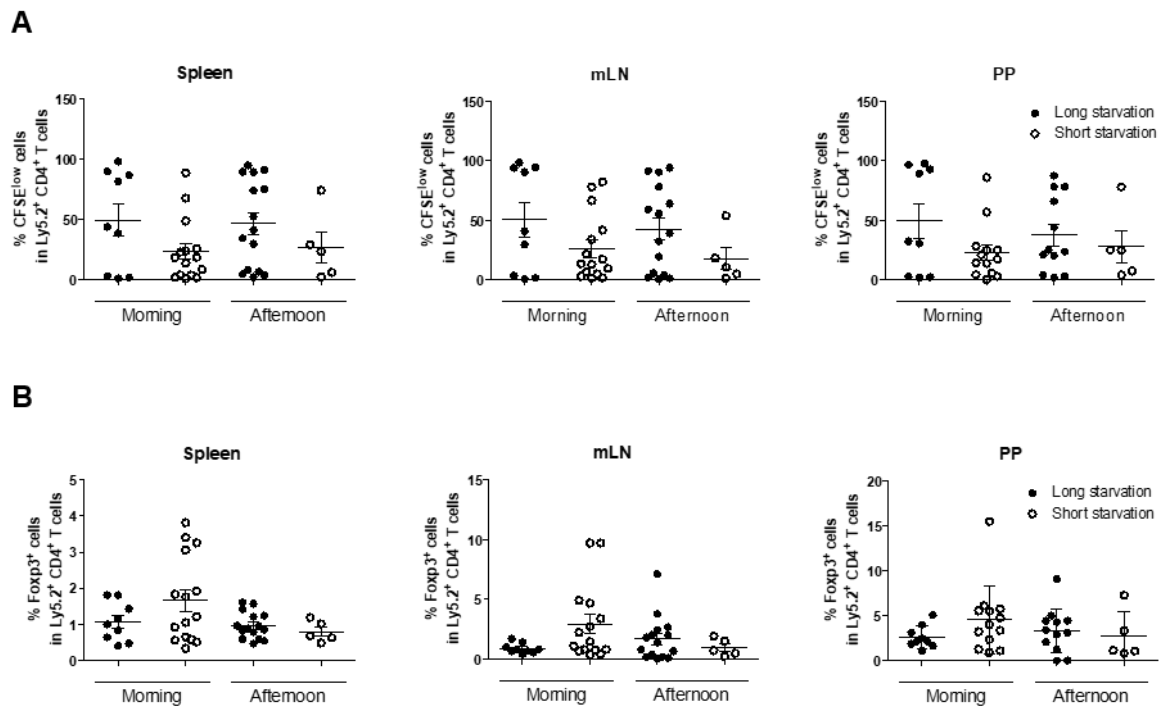
Figure 4.18. Combined effect of starvation and immunization time on the immune response after OVA:NPL immunization.

C57BL/6-Ly5.1 mice were adoptively transferred with naïve OT II Ly5.2$^+$ CD4$^+$ T cells and the next day were subjected to intraduodenal immunization in the morning (around 10 am) or afternoon (around 1 pm) with OVA:NPL (200 µg OVA:1 mg NPL) after previous starvation during a long (19h) or short (16h) period. Five days later, the immune response in the OT II Ly5.2$^+$ CD4$^+$ T cell population of the indicated organs was analyzed by flow cytometry. **(A)** Percentage of proliferating OT II CD4$^+$ T cells. **(B)** Percentage of Foxp3$^+$ cells in OT II CD4$^+$ T cells. Each data point

represents an individual mouse. Data are shown as mean±SEM and are pooled from two independent experiments. One-way ANOVA followed by Bonferroni test was used to evaluate statistical significance.

Finally, we sought to understand if both starvation period and immunization time could have a combinatorial effect on this setting. We immunized (with OVA:NPL) a group of mice in the morning and another in the afternoon, and further divided each group by the starvation period that each underwent, either long or short. As shown in Figure 4.18A, the four groups presented comparable OVA-specific CD4$^+$ T cell activation in spleen, mLN and PP, and no specific immunization time-starvation period combination resulted in a different response. Noteworthy, the effect of starvation was noticed here too, as groups immunized at different time of the day and under long starvation showed a trend to present higher proliferation than their counterpart. Again, Tregs in the OT II CD4$^+$ T cell population were not affected by the different combinations of immunization time-starvation period, as similar percentages of Foxp3$^+$ CD4$^+$ T cells were found in all tissues (Fig. 4.18B).

We determined that, from the possible factors, according to our data, that could affect the outcome of the immune response in this immunization setting, starvation plays an important role and should be considered to avoid artifacts in this types of experiments.

4.2.7 NPL enhance antigen presentation without establishment of oral tolerance

Acknowledging the important effect of starvation, we proceeded our investigation on the function of NPL as an oral vaccine vector. Using the same experimental setting, but performing the immunization to all the differently treated groups under the same starvation period (19h), we compared the OVA-specific CD4$^+$ T cell response in mice immunized with NPL, OVA and OVA:NPL. Five days after immunization, a significantly higher percentage of OT II CD4$^+$ proliferating T cells was found in the spleen and mLN of mice

receiving OVA formulated with NPL, relatively to the group receiving OVA alone (Fig. 4.19A). The same was not observed in PP, as both treatments induced similar proliferation of this T cell population. When looking at the OVA-specific Foxp3$^+$ CD4$^+$ T cell population, no conversion of Tregs was observed in the different treatments, despite the greater antigen presentation in OVA:NPL immunized mice (Fig. 4.19B).
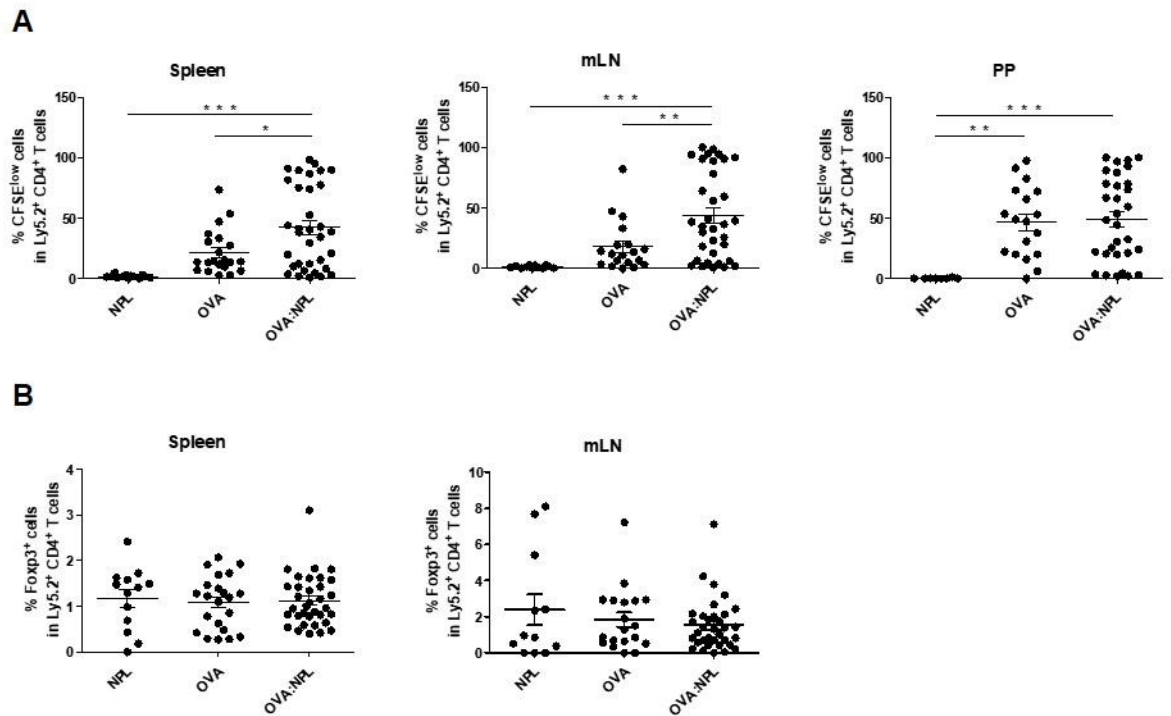
Figure 4.19. Advantage of NPL formulation in antigen-specific CD4$^+$ T cell response after immunization.

C57BL/6-Ly5.1 mice were adoptively transferred with naïve OT II Ly5.2$^+$ CD4$^+$ T cells and the next day were subjected to intraduodenal immunization with NPL alone (1 mg), OVA (200 µg) or formulation OVA:NPL (200 µg OVA:1 mg NPL) after previous starvation during a long (19h) period. Five days later, the immune response in the OT II Ly5.2$^+$ CD4$^+$ T cell population of the indicated organs was analyzed by flow cytometry. **(A)** Percentage of proliferating OT II CD4$^+$ T cells. **(B)** Percentage of Foxp3$^+$ cells in OT II CD4$^+$ T cells. Each data point represents an individual mouse. Data are shown as mean±SEM and are pooled from five independent experiments (in the case of spleens and mLN) or four independent experiments (in the case of PP). One-way ANOVA followed by Bonferroni test was used to evaluate statistical significance. *p<0.05, **p<0.01, ***p<0.001.

Altogether, this suggests that NPL have the potential to increase presentation of the loaded antigen without prompting tolerance, two fundamental aspects of a successful vaccine.

4.2.8 Antigen delivery by NPL induces a Th1 response in PP
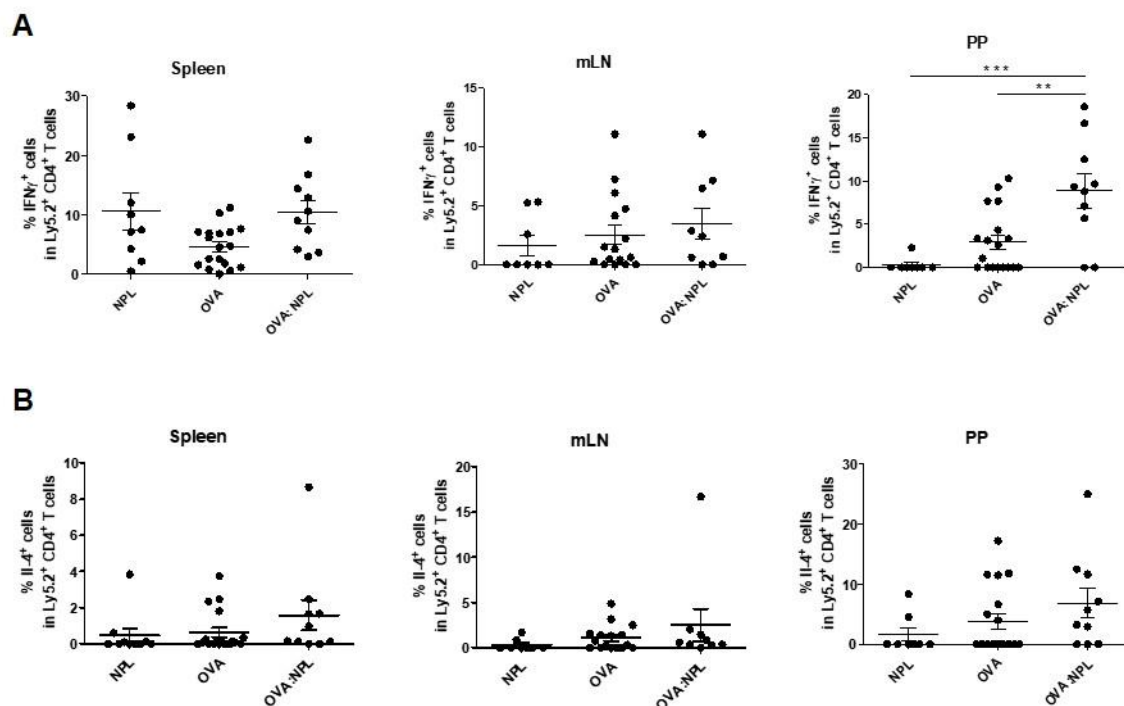
Figure 4.20. Th1 and Th2 immune responses after immunization with NPL formulation.

C57BL/6-Ly5.1 mice were adoptively transferred with naïve OT II Ly5.2+ CD4+ T cells and the next day were subjected to intraduodenal immunization with NPL alone (1 mg), OVA (200 µg) or formulation OVA:NPL (200 µg OVA:1 mg NPL) after previous starvation during a long (19h) period. Five days later, the cytokine production ability in the OT II Ly5.2+ CD4+ T cell population of the indicated organs was analyzed by flow cytometry, after *in vitro* stimulation with PMA and ionomycin for 4h. **(A)** Percentage of IFNγ-producing cells in the OT II CD4+ T cell population. **(B)** Percentage of IL-4-producing cells in the OT II CD4+ T cell population. Each data point represents an individual mouse. Data are shown as mean±SEM and are pooled from two independent experiments. One-way ANOVA followed by Bonferroni test was used to evaluate statistical significance. **p<0.01, ***p<0.001.

Since immunization with particulate adjuvants often results in enhanced protective immune responses, we questioned whether NPL have such ability. Immunization with NPL, OVA or OVA:NPL was performed on mice under long starvation in the same experimental setting. At the time of analysis, cells from spleen, mLN and PP were isolated and stimulated *in vitro* with PMA and ionomycin, and IFNγ- and IL-4-producing cells in the OT II CD4$^+$ T cell population was quantified by flow cytometry. As depicted in Figure 4.20A, the percentage of OVA-specific CD4$^+$ T cells able to produce IFNγ in PP was significantly higher when mice were immunized with OVA formulated with NPL than with the antigen alone. This Th1 response was only observed in this tissue though, as in spleen and mLN the IFNγ-producing population was similar between all groups. As for IL-4 production, no real difference was observed between the different immunization groups (Fig. 4.20B).

4.2.9 Protection of NPL from the stomach acidic pH

One of the main challenges when dealing with oral vaccines is maintaining their stability throughout the GI tract, as great pH fluctuations are present and digestive enzymes can also modify them. The stomach, in particular, poses one of the biggest threats with its extremely acidic pH. The stability of NPL formulations in the stomach were next evaluated. During our investigation, we adopted the intraduodenal administration as a surrogate for oral immunization so we could study both the vaccine and NPL without the putative degradation/modification in the stomach. Taking advantage of the experimental setting used in the previous studies, and having validated the vaccine vector function of NPL in increasing the immune response towards the loaded antigen, we tested whether this function is maintained when its administration was closer to an oral immunization, i.e. through intragastric administration.

As shown in Figures 4.21A and B, the advantage of NPL formulation was completely abrogated when OVA:NPL was administered in the stomach, showing similar percentages of OVA-specific CD4$^+$ T cell proliferation to what was found in mice immunized with OVA

A

B

C
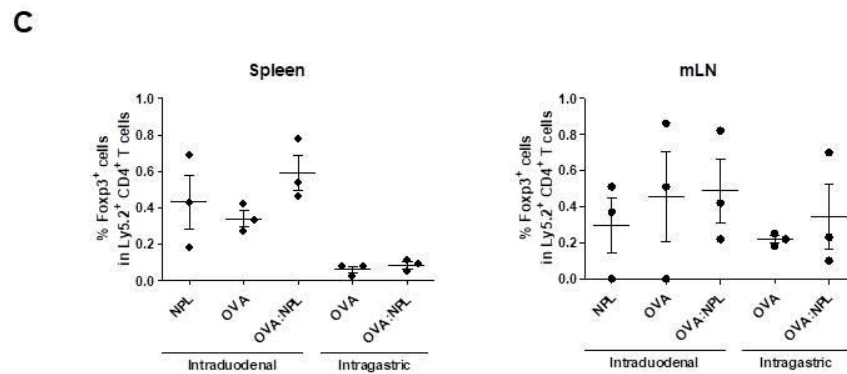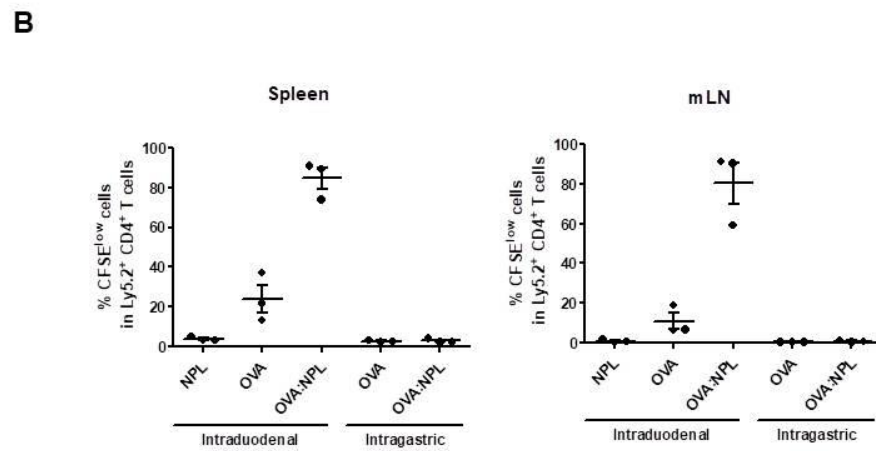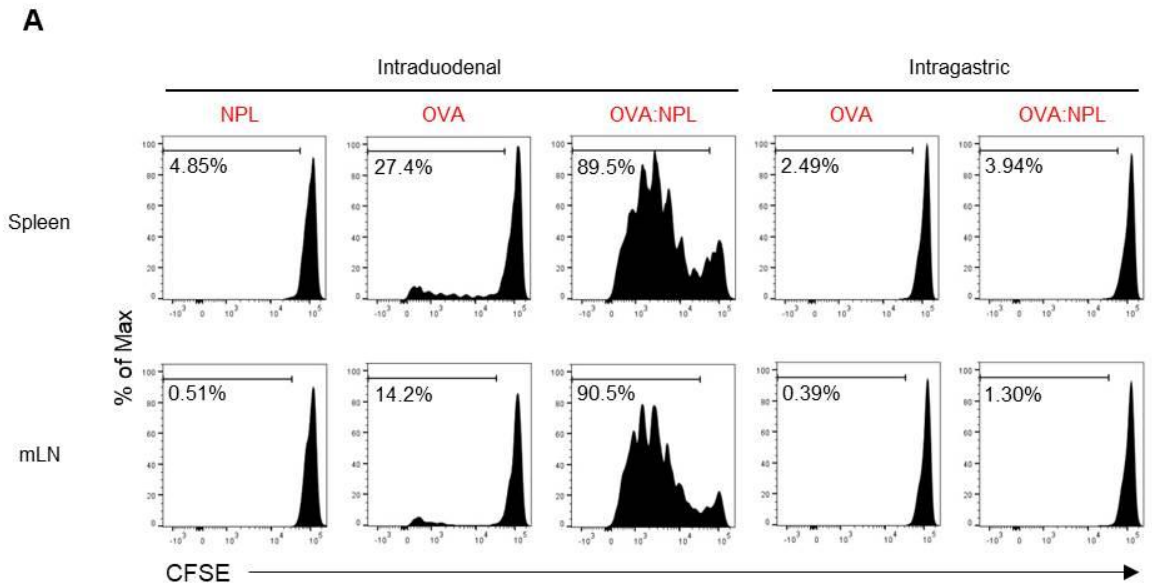
Figure 4.21. Comparison of antigen-specific CD4+ T cell response after intraduodenal and intragastric immunization.

C57BL/6-Ly5.1 mice were adoptively transferred with naïve OT II Ly5.2+ CD4+ T cells and the next day were subjected to immunization by intraduodenal injection or intragastric administration with NPL alone (1 mg), OVA (200 µg) or formulation OVA:NPL (200 µg OVA:1 mg NPL) after previous starvation during a long (19h) period. Five days later, the immune response in the OT II Ly5.2+

CD4$^+$ T cell population of the indicated organs was analyzed by flow cytometry. **(A)** Representative histograms showing cell division of OT II CD4$^+$ T cells in the different treatment groups and the respective percentage of CFSE^{low} cells. **(B)** Percentage of proliferating OT II CD4$^+$ T cells. **(C)** Percentage of Foxp3$^+$ cells in OT II CD4$^+$ T cells. Each data point represents an individual mouse. Data are shown as mean±SEM, n=3 mice/group.

alone given intragastrically or even when the antigen was absent. The percentage of OVA-specific Treg cells did not seem to vary between differently immunized groups either by intraduodenal injection or intragastric administration in both organs (Fig. 4.21C), the only exception being the spleen, in which less Tregs were found in the groups immunized intragastrically with OVA and OVA:NPL compared with OVA:NPL immunized mice by injection in the duodenum. Still, this difference does not indicate that more OVA-specific Tregs are induced by OVA in formulation and delivered by intraduodenal injection, as the percentage of this cell population in this group is similar to the one found when OVA is not present. However, due to the reduced number of mice in each group, a statistical analysis was not performed and no significant differences between the different groups can be inferred. Despite the reduced number of mice, it was clear though through this experiment that administration of NPL formulation by oral gavage puts at risk its vaccine vector function, our main question in this experiment.

Trying to overcome the effect of the environment of the stomach, in order to protect NPL formulations in its use as an oral delivery system for future experiments, we then immunized one group of mice by intragastric administration with the formulation OVA:NPL prepared in 5% NaHCO$_3$ (a buffer used for intragastric administration of bacteria, etc.) to neutralize stomach acidity. At the same time, another group of mice was immunized with the formulation in the regular vehicle by intraduodenal injection, serving as a positive control for OVA:NPL induced-immune responses. Still, protection of NPL formulation with sodium bicarbonate was not efficient, as mice receiving this treatment in the stomach presented a lower response in all organs compared to mice that were immunized bypassing the stomach (Fig. 4.22A). Also in this case, statistical analysis was not

performed due to the reduced number of mice in each group, but the difference in OVA-specific T cell proliferation was striking between mice immunized by intraduodenal injection and intragastric administration together with 5% NaHCO₃. Regarding OVA-specific Treg conversion, only a trend was observed with mice immunized by intraduodenal injection showing a higher percentage of Tregs (Fig. 4.22B).

Figure 4.22. Effect of sodium bicarbonate in the protection of NPL from stomach acidity.

C57BL/6-Ly5.1 mice were adoptively transferred with naïve OT II Ly5.2$^+$ CD4$^+$ T cells and the next day were subjected to immunization with OVA:NPL (200 µg OVA:1 mg NPL) by intraduodenal injection or intragastric administration buffered with 5% NaHCO₃ after previous starvation during a long (19h) period. Five days later, the immune response in the OT II Ly5.2$^+$ CD4$^+$ T cell population of the indicated organs was analyzed by flow cytometry. **(A)** Percentage of proliferating OT II CD4$^+$ T cells. **(B)** Percentage of Foxp3$^+$ cells in OT II CD4$^+$ T cells. Each data point represents an individual mouse. Data are shown as mean±SEM, n=3 mice/group.

As sodium bicarbonate failed to protect NPL formulation in the stomach, we decided to test a more effective and lasting method to manipulate the stomach pH. Omeprazole is a

proton pump inhibitor that blocks the activity of H^+/K^+-ATPase in parietal cells, preventing the formation of an acidic pH in the stomach [184]. Since its effect is transient and varies between species, we measured the pH of the stomach content (under starvation, in order to mimic the conditions of mice undergoing immunization) before and after different time points of Omeprazole treatment (Fig. 4.23). Additionally, we also measured the pH in the duodenum of untreated mice (under the same starvation condition) to comprehend the pH level that one should aim for so as to efficiently protect NPL formulations. As expected, the transient effect of Omeprazole was observed and a gastric pH similar to that in the duodenum was obtained 4h after treatment. We decided to choose this post-Omeprazole treatment time point to immunize the mice intragastrically and not sooner, so both oral administrations were far apart and this procedure would not cause additional stress in the animals.
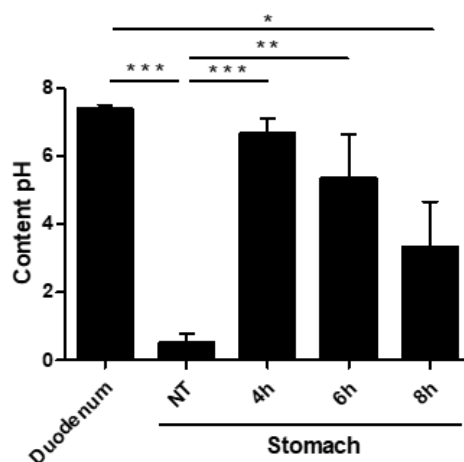
Figure 4.23. Omeprazole treatment increases stomach pH.

Starved C57BL/6 mice were treated with Omeprazole (40 mg/Kg body weight) in 0.2% $NaHCO_3$ and 0.5% methylcellulose by intragastric administration and the pH of the stomach content was measured after different time points. The pH of stomach and duodenum contents of not treated (NT) mice are also reported. Data are shown as mean±SEM, n=3-4 mice/group. One-way ANOVA followed by Bonferroni test was used to evaluate statistical significance. *p<0.05, **p<0.01, ***p<0.001.
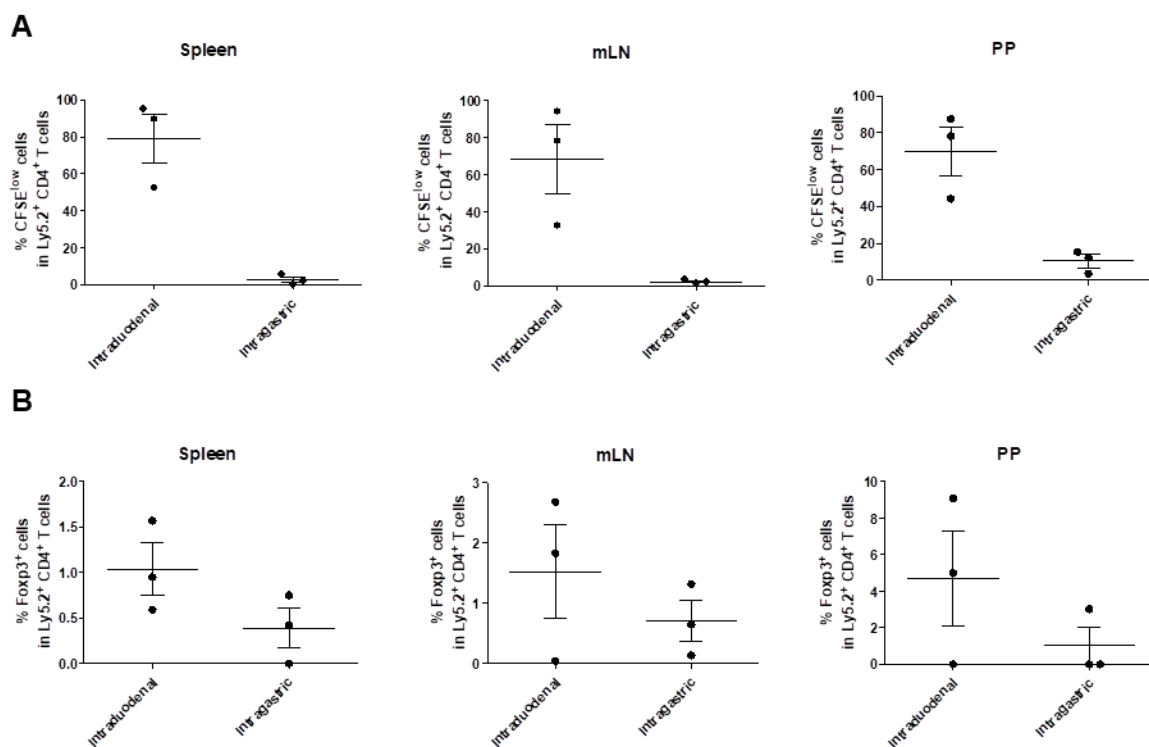
A

Spleen

PP

B

Spleen

PP
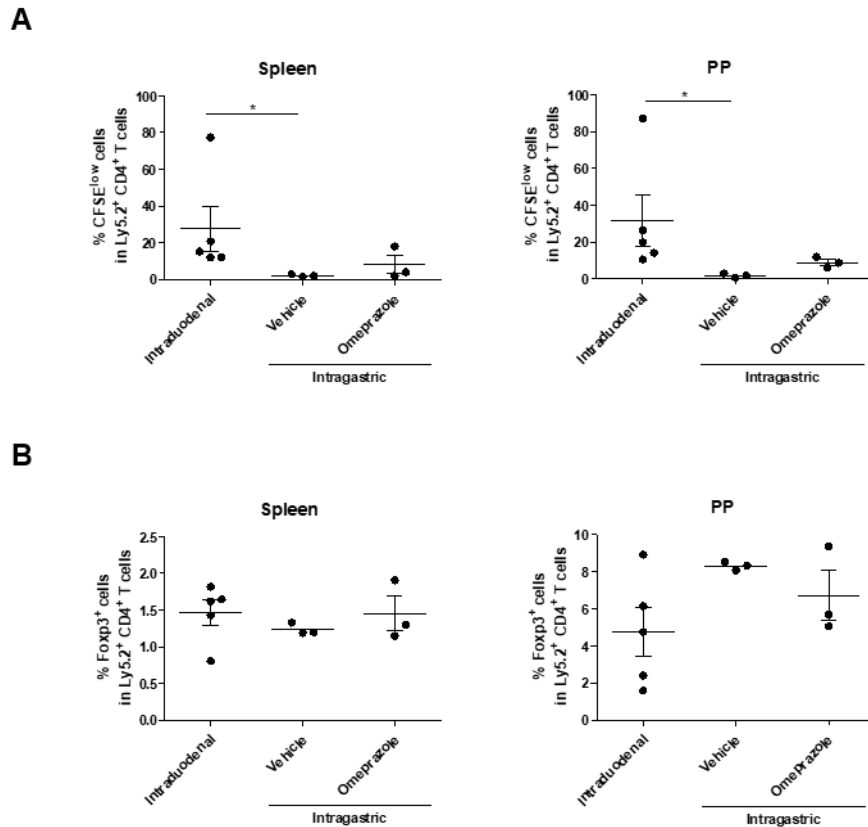
Figure 4.24. Effect of Omeprazole in the protection of NPL from stomach acidity.

C57BL/6-Ly5.1 mice were adoptively transferred with naïve OT II Ly5.2$^+$ CD4$^+$ T cells and the next day were subjected to immunization with OVA:NPL (200 µg OVA:1 mg NPL) by intraduodenal injection or intragastric administration 4h after treatment with Omeprazole or vehicle alone after previous starvation during a long (19h) period. Five days later, the immune response in the OT II Ly5.2$^+$ CD4$^+$ T cell population of the indicated organs was analyzed by flow cytometry. **(A)** Percentage of proliferating OT II CD4$^+$ T cells. **(B)** Percentage of Foxp3$^+$ cells in OT II CD4$^+$ T cells. Each data point represents an individual mouse. Data are shown as mean±SEM, n=3-5 mice/group. One-way ANOVA followed by Bonferroni test was used to evaluate statistical significance. *$p < 0.05$.

In the same experimental setting that included adoptive transfer of OVA-specific CD4$^+$ T cells, mice were then treated with Omeprazole or the vehicle alone and 4h later OVA:NPL was administered intragastrically. Pre-treatment with Omeprazole partially recovered the OVA-specific immune response found in mice immunized with the formulation directly in the duodenum, but its effect was not enough to induce a significantly higher response

than the one observed in mice treated with the vehicle alone and subjected to intragastric immunization (Fig. 4.24A). Again, the percentage of OVA-specific Foxp3$^+$ T cells did not vary significantly between groups (Fig. 4.24B).

Hence, although NPL exhibit some qualities that make them a good candidate for an oral delivery system, vulnerability to the stomach environment still needs to be addressed.

5 DISCUSSION

Oral vaccination holds great promise for immunization in developing countries, elimination of bio-hazardous waste and pandemic preparation, nevertheless no oral influenza vaccine is commercially available so far. Designing a successful oral vaccine is not an easy task, as the antigen might get trapped in the mucus, digested or never cross the epithelial barrier and the administration dose is not necessarily the dose that reaches the mucosal tissue due to dilution in mucosal secretions. Moreover, a serious challenge, particularly when dealing with oral immunization, is the induction of tolerance against the delivered antigen [131].

5.1 CTA1-3M2e-DD as an oral vaccine

We started our investigation by confirming the targeting ability of the universal influenza vaccine candidate, since our collaborators reported the binding of the adjuvant protein CTA1-DD (carrying the same targeting region) to B cells [113,181]. Thus, we replicated our collaborators' *in vitro* experiment using CTA1-3M2e-DD, which showed that the targeting function of the DD region in this fusion protein was maintained, being able to bind to both mouse and human B cells, as observed before for CTA1-DD [113,181].

Following the validation of CTA1-3M2e-DD targeting ability, we addressed our main question, whether this fusion protein is endowed with key features of an effective oral vaccine, i.e., to be able to cross the intestinal barrier and to be internalized by intestinal phagocytes *in vivo*. Although its functionality was preserved, CTA1-3M2e-DD showed a poor potential as an oral vaccine. The prolonged time that CTA1-3M2e-DD remained in the intestinal lumen overlying the epithelium, showed by imaging analysis of intestinal loops treated for 2h with the fusion protein, and the association mainly with $CD45.2^-$ cells, revealed by flow cytometry 4h after its intraduodenal administration, suggest that the fusion protein was trapped in the mucus layer. In fact, CTA1-3M2e-DD comprises the Ig-

binding domain DD that was shown to bind to different Ig isotypes, including IgA [113], the predominant Ig in mucosal secretions and one of the molecules that is found in the mucus layer. One explanation for the retention of CTA1-3M2e-DD in the lumen is that it might bind to IgA present in the intestinal mucus layer, getting trapped for a long period and being prevented from crossing the epithelium. By attaching to the mucus layer, CTA1-3M2e-DD has mucoadhesive properties, which are desirable for mucosal vaccines, but in this case further translocation across the epithelium did not occur. Not only was CTA1-3M2e-DD excluded by the epithelial barrier, but also its uptake by the APC populations of interest in this setting was reduced. The fact that CTA1-3M2e-DD was almost exclusively taken up by a small percentage of CX_3CR1^{high} macrophages also supports the inability of this fusion protein to enter the lamina propria, as CX_3CR1^+ macrophages have the capacity to extend dendrites across the epithelium and capture luminal content [23,44,50].

5.2 NPL as a delivery system for oral vaccines

As CTA1-3M2e-DD was found to be unsuitable as an oral vaccine, we continued our studies on the nanoparticulate vaccine delivery system generated in our consortium to understand whether it could be of value to deliver antigens by the oral route. Contrarily to CTA1-3M2e-DD, confocal microscopy revealed that NPL quickly crossed the epithelial barrier, both in the mouse and human intestine. Moreover, NPL were found in $CD103^+$ $CD11b^-$, $CD103^+$ $CD11b^+$, CX_3CR1^{high} and CX_3CR1^{int} lamina propria APCs. Further investigation into the route of NPL entry in the intestine identified two different mechanisms by which NPL are taken up.

5.2.1 Role of intestinal epithelial cells as a gateway for NPL

On one hand, specific epithelial cells were found to contribute to the transport of high amounts of NPL. When staining NPL-treated intestinal tissue for markers of different epithelial cells, we observed that NPL-filled cells were $MUC2^+$ Goblet cells. Antigen

sampling by Goblet cells is not a novelty. However, contrarily to what was once considered [80], not only small soluble antigens can pass through Goblet cell-associated passages. According to McDole et al., soluble antigens, such as dextrans, can fill Goblet cells, but there is a molecular weight exclusion limit for Goblet cell uptake, as 0.02 to 1 μm beads were excluded [92]. Nevertheless, NPL, which are approximately 76 nm in diameter [177], were taken up by Goblet cells. Moreover, Nikitas et al. reported that *Listeria monocytogenes* is able to cross the intestinal barrier by preferentially adhering to luminal accessible E-cadherin on Goblet cells, which in turn internalize the bacteria and release it in the lamina propria by exocytosis [183]. This suggests that rather than size, other characteristics are determinant for uptake by Goblet cells. Besides mechanisms depending on Goblet cell-specific targeting, it is possible that the chemical nature of the antigen plays an important role, since dextrans of different molecular weights (up to 2000 kD) readily fill Goblet cells [92] and NPL, also composed of polysaccharides, behave similarly.

The contribution of Goblet cells to NPL transport into the lamina propria might also explain the presence of NPL in the four lamina propria APC subsets and not in one in particular. NPL-containing Goblet cells probably release the vaccine vector indiscriminately in the lamina propria where NPL are then available to be phagocytosed by different APCs. However, the direct transfer of antigen from Goblet cells to specific APCs, such as CD103^{+} DCs, has been reported for low molecular weight antigens [92].

Although NPL transfer from the lumen to the intestinal lamina propria was mainly associated with Goblet cells, we also found NPL uptake in Paneth cells, to a lesser extent. Additionally, one cannot exclude the involvement of paracellular pathways in NPL transportation, that indeed occur with dietary antigens in the intestine [185]. To address this point, an imaging technique offering higher resolution, as transmission electron microscopy, could be of interest.

5.2.2 Direct sampling of NPL by CX$_3$CR1$^+$ macrophages

The second mechanism taking place in the uptake of NPL is the direct acquisition by CX$_3$CR1$^+$ cells. We have found that these cells in PP extend trans-epithelial dendrites across the FAE and sample NPL from the lumen. In the intestinal lamina propria, both CX$_3$CR1^{int} and CX$_3$CR1^{high} macrophages also contained NPL. However, direct sampling by these cells in the villi could not be confirmed, as trans-epithelial dendrites were not visualized by confocal microscopy and the presence of NPL$^+$ CX$_3$CR1$^+$ cells may be the result of NPL uptake after Goblet cell-dependent transcytosis. It would be interesting to determine if NPL uptake by CX$_3$CR1$^+$ cells in the villi also occurs through trans-epithelial acquisition, at least partially, by comparing the percentage of NPL$^+$ CX$_3$CR1$^+$ cells in the intestines of *Cx3cr1*$^{GFP/+}$ and *Cx3cr1*$^{GFP/GFP}$ mice, as the homozygous strain, having both CX$_3$CR1 alleles replaced by GFP, do not express the chemokine receptor and fail to extend protrusions [49].

5.2.3 Delivery and presentation of antigen formulated with NPL

Our results also show that, when formulated with NPL, OVA can be released in the lamina propria still conjugated with the vaccine vector, but also alone. Both forms of OVA were also visualized within intestinal epithelial cells. Dombu and colleagues studied the intracellular delivery of OVA in human airway epithelial cells by NPL [182]. Their results show that NPL are quickly taken up in this model and accumulate in clathrin vesicles and early endosomes. Here, they observed a gradual release of OVA from NPL and that these nanoparticles facilitate the escape of OVA from endosomes, which is apparently due to the charge of this protein at acidic pH. Their results may explain what we observed in the mouse intestine, as this mechanism of OVA release might also occur within the intestinal epithelial cells (previously identified as Goblet cells) that transport NPL into the lamina propria and subsequently release at least part of the antigen dissociated from the vaccine vector.

Another important aspect to consider when developing a new mucosal vaccine, is to trigger protection upon vaccination with low doses of antigen. To understand whether NPL are advantageous as a vaccine vector in the induction of an immune response, we compared OVA-specific responses in lymphoid organs when the antigen was delivered alone or loaded in NPL. We observed an increased proliferation of adoptively transferred OVA-specific CD4$^+$ T cells in mLN and spleen upon OVA:NPL immunization, which is encouraging for the use of NPL as vaccine carriers. This increase was not found in PP, though, meaning that antigen presentation in this tissue occurred similarly when the antigen was free or formulated. This could reflect that, at this level, the amount of antigen that is taken up is not enhanced by NPL delivery or even a different mechanism of epithelial/trans-epithelial transportation takes place. Noteworthy, high proliferation of antigen-specific CD4$^+$ T cells in mLN and PP was expected, but the finding that comparable proliferation occurred in spleens was surprising. This strong response in the spleen can be the result of recirculation of T lymphocytes that egress from lymphoid organs close to the site of induction, where antigen recognition and T cell activation occurs. Another hypothesis is that, as we observed by imaging analysis revealing the localization of NPL throughout the lamina propria, the vaccine vector might be able to cross the intestinal endothelium and end up in the bloodstream, where it can then spread systemically and reach the spleen. This needs to be further investigated, for instance by measuring the fluorescence intensity in the serum of mice injected with fluorescently-labeled NPL in the intestine or by *in vivo* imaging, tracking the NPL fluorescence over time and following their eventual accumulation in distant organs.

Also encouraging was the fact that, despite the increase of OVA delivery and presentation when formulated with NPL, this was not translated in induction of OVA-specific Tregs in any of the analyzed organs, as tolerance induction is a major concern when dealing with oral vaccines. Interestingly, McDole and colleagues found that antigens transported through Goblet cell-associated passages are directly delivered to CD103$^+$ DCs in the lamina propria, a subset closely linked to the establishment of oral tolerance [92]. Additionally, it was reported that mucus taken up by APCs can act as a modulatory signal,

imprinting a tolerogenic phenotype on these cells and leading to enhanced oral tolerance [10]. Nevertheless, this was not verified in our study, even though CD103⁺ DCs were able to take up NPL. One can speculate that this is due to the fact that the antigen loaded in NPL was not presented by this subset of APCs in the GALT. Another possibility is the absence of mucus uptake when NPL are internalized, preventing the assimilation of this tolerogenic signal. The Th1 and Th2 responses were also evaluated and we found that OVA:NPL induces a higher percentage of OVA-specific IFNγ-producing CD4⁺ T cells in PP, but not in mLN and spleen. Whether this is due to antigen presentation and CD4⁺ T cell priming by different subsets of APCs, which in turn imprint on these cells different phenotypes, is still an open question.

5.2.4 Starvation as a potential modulator of adaptive immune responses after oral immunization

The circadian clock is perceived by molecular machineries and allows regulation of different physiological processes according to variations in the environment [186]. We realized, from preliminary results on the advantage of NPL formulation, that mice in the same treatment group (OVA:NPL) presented variable responses and we hypothesized that the different immunization timing across the group could be the cause of such variability. Indeed, recently it was shown that lymphocyte trafficking in lymph and lymph nodes fluctuates throughout the day and this process is dependent on circadian clocks that trigger lymphocyte homing and egress [187]. Consequently, immunizations occurring at different time of the day shape different adaptive immune responses. We therefore investigated the impact of OVA:NPL immunization at distinct times, but our results showed that comparable immune responses were obtained and the circadian rhythm was not playing a role in this matter.

Our alternative hypothesis was the contribution of starvation. In fact, it was shown that also the intestinal microbiota can undergo diurnal oscillations, leading to different compositional and functional microbiota profiles throughout the day that are influenced by

feeding patterns [188]. Different periods of starvation can consequently shape the microbiota profile, which in turn may alter the intestinal homeostasis and its immune component. We evaluated the individual role of starvation in OVA-induced CD4$^+$ T cell proliferation after OVA:NPL immunization, as well as in combination with immunization occurring at different time of the day, and confirmed that mice undergoing a longer period of starvation (even only 3 more hours) presented a better response, independently of immunization time. Whether this effect relies on the fasting itself (as lack of food could trigger a compensatory mechanism that enhances nutrient absorption and this is reflected by an increase in the uptake of NPL formulation) or on microbiota-related alterations (that shape the immune response according to their numbers and composition under starvation), remains to be clarified.

5.2.5 Instability of NPL formulations in the stomach

Finally, we addressed the capacity of NPL to protect the loaded antigen from stomach degradation by immunizing mice with OVA:NPL through intragastric administration and comparing their OVA-specific response with mice in which immunization bypasses the stomach. We concluded that the effect of NPL as a vaccine vector was compromised when it was administered in the stomach, showed by lower responses to OVA. According to Dombu et al., acidic conditions, as found in the stomach, favor interaction of NPL-loaded OVA with proteases, by diminishing OVA attraction to the cationic nanoparticle and inducing its release, and consequently increasing its exposure to degradation [182]. Although NPL might survive through the GI tract, its oral delivery might compromise an immune response, as the antigen is no longer associated to the vaccine carrier. Neutralization of stomach acidity with sodium bicarbonate, which is a commonly used buffer for oral administrations, did not enhance vaccine effectiveness. Nevertheless, we confirmed the role of the stomach pH in the modification of OVA:NPL formulation by increasing the stomach pH to levels found at steady-state in the duodenum. However, manipulation of stomach pH with a proton pump inhibitor was only transient, which might have lead only to a partial amelioration of OVA:NPL stability, as the transit time from the

stomach to the small intestine might be longer than the effect of the drug. Protection from the stomach acidity is an important issue to take into consideration when developing an oral vaccine delivery system. Nevertheless, for the use in humans, this problem can be easily solved by loading NPL formulations in pH-resistant capsules, whereas for studies in animals, particularly mice, the dimensions of commercially available capsules are not adequate for them.

In conclusion, we have shown that, while the influenza vaccine candidate CTA1-3M2e-DD is retained in the intestinal lumen for a long period, NPL as vaccine vectors are indeed able to deliver the loaded antigen, to cross the intestinal barrier with Goblet cells as an important gateway and to be taken up by different intestinal APCs, with no apparent induction of tolerance and a Th1 response to the delivered antigen in PP. Moreover, the effect of starvation on the immune response in this setting was recognized. Further experiments are underway to characterize the ability of NPL to induce DCs activation after phagocytosis and the modulation of cytokine production, as well as to determine their potential to induce *in vivo* antigen-specific IgA and IgG following sequential immunizations in the intestine.

6 REFERENCES

1 Eberl G (2010) A new vision of immunity: homeostasis of the superorganism. *Mucosal Immunol.* **3**, 450–460.

2 Hooper LV & Macpherson AJ (2010) Immune adaptations that maintain homeostasis with the intestinal microbiota. *Nat. Rev. Immunol.* **10**, 159–169.

3 McGuckin MA, Lindén SK, Sutton P & Florin TH (2011) Mucin dynamics and enteric pathogens. *Nat. Rev. Microbiol.* **9**, 265–278.

4 Johansson MEV, Phillipson M, Petersson J, Velcich A, Holm L & Hansson GC (2008) The inner of the two Muc2 mucin-dependent mucus layers in colon is devoid of bacteria. *Proc. Natl. Acad. Sci.* **105**, 15064–15069.

5 Ouwerkerk JP, De Vos WM & Belzer C (2013) Glycobiome: Bacteria and mucus at the epithelial interface. *Best Pract. Res. Clin. Gastroenterol.* **27**, 25–38.

6 Van der Sluis M, De Koning BAE, De Bruijn ACJM, Velcich A, Meijerink JPP, Van Goudoever JB, Büller HA, Dekker J, Van Seuningen I, Renes IB & Einerhand AWC (2006) Muc2-deficient mice spontaneously develop colitis, indicating that MUC2 is critical for colonic protection. *Gastroenterology* **131**, 117–129.

7 Bergstrom KSB, Kissoon-Singh V, Gibson DL, Ma C, Montero M, Sham HP, Ryz N, Huang T, Velcich A, Finlay BB, Chadee K & Vallance BA (2010) Muc2 protects against lethal infectious colitis by disassociating pathogenic and commensal bacteria from the colonic mucosa. *PLoS Pathog.* **6**, e1000902.

8 Zarepour M, Bhullar K, Montero M, Ma C, Huang T, Velcich A, Xia L & Vallance BA (2013) The mucin muc2 limits pathogen burdens and epithelial barrier dysfunction during salmonella enterica serovar typhimurium colitis. *Infect. Immun.* **81**, 3672–3683.

9 Velcich A (2002) Colorectal cancer in mice genetically deficient in the mucin Muc2.

Science **295**, 1726–1729.

10 Shan M, Gentile M, Yeiser JR, Walland AC, Bornstein VU, Chen K, He B, Cassis L, Bigas A, Cols M, Comerma L, Huang B, Blander JM, Xiong H, Mayer L, Berin C, Augenlicht LH, Velcich A & Cerutti A (2013) Mucus enhances gut homeostasis and oral tolerance by delivering immunoregulatory signals. *Science* **342**, 447–453.

11 Brown EM, Sadarangani M & Finlay BB (2013) The role of the immune system in governing host-microbe interactions in the intestine. *Nat. Immunol.* **14**, 660–667.

12 Ayabe T, Satchell DP, Wilson CL, Parks WC, Selsted ME & Ouellette AJ (2000) Secretion of microbicidal alpha-defensins by intestinal Paneth cells in response to bacteria. *Nat. Immunol.* **1**, 113–118.

13 Vaishnava S, Behrendt CL, Ismail AS, Eckmann L & Hooper LV. (2008) Paneth cells directly sense gut commensals and maintain homeostasis at the intestinal host-microbial interface. *Proc. Natl. Acad. Sci.* **105**, 20858–20863.

14 Bevins CL & Salzman NH (2011) Paneth cells, antimicrobial peptides and maintenance of intestinal homeostasis. *Nat. Rev. Microbiol.* **9**, 356–368.

15 Pütsep K, Axelsson LG, Boman A, Midtvedt T, Normark S, Boman HG & Andersson M (2000) Germ-free and colonized mice generate the same products from enteric prodefensins. *J. Biol. Chem.* **275**, 40478–40482.

16 Kobayashi KS, Chamaillard M, Ogura Y, Henegariu O, Inohara N, Nuñez G & Flavell RA (2005) Nod2-dependent regulation of innate and adaptive immunity in the intestinal tract. *Science* **307**, 731–734.

17 Farin HF, Karthaus WR, Kujala P, Rakhshandehroo M, Schwank G, Vries RGJ, Kalkhoven E, Nieuwenhuis EES & Clevers H (2014) Paneth cell extrusion and release of antimicrobial products is directly controlled by immune cell–derived IFN-γ. *J. Exp. Med.* **211**, 1393–1405.

18 Wilson CL, Ouellette AJ, Satchell DP, Ayabe T, López-Boado YS, Stratman JL, Hultgren SJ, Matrisian LM & Parks WC (1999) Regulation of intestinal alpha-defensin

activation by the metalloproteinase matrilysin in innate host defense. *Science* **286**, 113–117.

19 Salzman NH, Hung K, Haribhai D, Chu H, Karlsson-Sjöberg J, Amir E, Teggatz P, Barman M, Hayward M, Eastwood D, Stoel M, Zhou Y, Sodergren E, Weinstock GM, Bevins CL, Williams CB & Bos NA (2010) Enteric defensins are essential regulators of intestinal microbial ecology. *Nat. Immunol.* **11**, 76–82.

20 Salzman NH, Ghosh D, Huttner KM, Paterson Y & Bevins CL (2003) Protection against enteric salmonellosis in transgenic mice expressing a human intestinal defensin. *Nature* **422**, 522–526.

21 Macpherson AJ & Slack E (2007) The functional interactions of commensal bacteria with intestinal secretory IgA. *Curr. Opin. Gastroenterol.* **23**, 673–678.

22 Macpherson AJ (2004) Induction of protective IgA by intestinal dendritic cells carrying commensal bacteria. *Science* **303**, 1662–1665.

23 Rescigno M, Urbano M, Valzasina B, Francolini M, Rotta G, Bonasio R, Granucci F, Kraehenbuhl JP & Ricciardi-Castagnoli P (2001) Dendritic cells express tight junction proteins and penetrate gut epithelial monolayers to sample bacteria. *Nat. Immunol.* **2**, 361–367.

24 Macpherson AJ, Geuking MB, Slack E, Hapfelmeier S & McCoy KD (2012) The habitat, double life, citizenship, and forgetfulness of IgA. *Immunol. Rev.* **245**, 132–146.

25 Mora JR, Iwata M, Eksteen B, Song S-Y, Junt T, Senman B, Otipoby KL, Yokota A, Takeuchi H, Ricciardi-Castagnoli P, Rajewsky K, Adams DH & von Andrian UH (2006) Generation of gut-homing IgA-secreting B cells by intestinal dendritic cells. *Science* **314**, 1157–1160.

26 Peterson DA, McNulty NP, Guruge JL & Gordon JI (2007) IgA response to symbiotic bacteria as a mediator of gut homeostasis. *Cell Host Microbe* **2**, 328–339.

27 Fagarasan S, Muramatsu M, Suzuki K, Nagaoka H, Hiai H & Honjo T (2002) Critical

roles of activation-induced cytidine deaminase in the homeostasis of gut flora. *Science* **298**, 1424–1427.

28 Suzuki K, Meek B, Doi Y, Muramatsu M, Chiba T, Honjo T & Fagarasan S (2004) Aberrant expansion of segmented filamentous bacteria in IgA-deficient gut. *Proc. Natl. Acad. Sci.* **101**, 1981–1986.

29 Goto Y & Kiyono H (2012) Epithelial barrier: An interface for the cross-communication between gut flora and immune system. *Immunol. Rev.* **245**, 147–163.

30 Iliev ID, Matteoli G & Rescigno M (2007) The yin and yang of intestinal epithelial cells in controlling dendritic cell function. *J. Exp. Med.* **204**, 2253–2257.

31 Lavelle EC, Murphy C, O'Neill LAJ & Creagh EM (2010) The role of TLRs, NLRs, and RLRs in mucosal innate immunity and homeostasis. *Mucosal Immunol.* **3**, 17–28.

32 Geijtenbeek TBH & Gringhuis SI (2009) Signalling through C-type lectin receptors: Shaping immune responses. *Nat. Rev. Immunol.* **9**, 465–479.

33 Artis D (2008) Epithelial-cell recognition of commensal bacteria and maintenance of immune homeostasis in the gut. *Nat. Rev. Immunol.* **8**, 411–420.

34 Rakoff-Nahoum S, Paglino J, Eslami-Varzaneh F, Edberg S & Medzhitov R (2004) Recognition of commensal microflora by toll-like receptors is required for intestinal homeostasis. *Cell* **118**, 229–241.

35 Gewirtz AT, Navas TA, Lyons S, Godowski PJ & Madara JL (2001) Cutting edge: Bacterial flagellin activates basolaterally expressed TLR5 to induce epithelial proinflammatory gene expression. *J. Immunol.* **167**, 1882–1885.

36 Lee J, Mo JH, Katakura K, Alkalay I, Rucker AN, Liu YT, Lee HK, Shen C, Cojocaru G, Shenouda S, Kagnoff M, Eckmann L, Ben-Neriah Y & Raz E (2006) Maintenance of colonic homeostasis by distinctive apical TLR9 signalling in intestinal epithelial cells. *Nat. Cell Biol.* **8**, 1327–1336.

37 Cario E, Gerken G & Podolsky DK (2007) Toll-like receptor 2 controls mucosal

inflammation by regulating epithelial barrier function. *Gastroenterology* **132**, 1359–1374.

38 Fukata M (2005) Toll-like receptor-4 is required for intestinal response to epithelial injury and limiting bacterial translocation in a murine model of acute colitis. *AJP Gastrointest. Liver Physiol.* **288**, G1055–G1065.

39 Vijay-Kumar M, Sanders CJ, Taylor RT, Kumar A, Aitken JD, Sitaraman S V., Neish AS, Uematsu S, Akira S, Williams IR & Gewirtz AT (2007) Deletion of TLR5 results in spontaneous colitis in mice. *J. Clin. Invest.* **117**, 3909–3921.

40 Iliev ID, Mileti E, Matteoli G, Chieppa M & Rescigno M (2009) Intestinal epithelial cells promote colitis-protective regulatory T-cell differentiation through dendritic cell conditioning. *Mucosal Immunol.* **2**, 340–350.

41 Iliev ID, Spadoni I, Mileti E, Matteoli G, Sonzogni A, Sampietro GM, Foschi D, Caprioli F, Viale G & Rescigno M (2009) Human intestinal epithelial cells promote the differentiation of tolerogenic dendritic cells. *Gut* **58**, 1481–1489.

42 Rimoldi M, Chieppa M, Salucci V, Avogadri F, Sonzogni A, Sampietro GM, Nespoli A, Viale G, Allavena P & Rescigno M (2005) Intestinal immune homeostasis is regulated by the crosstalk between epithelial cells and dendritic cells. *Nat. Immunol.* **6**, 507–514.

43 Mowat AM (2003) Anatomical basis of tolerance and immunity to intestinal antigens. *Nat. Rev. Immunol.* **3**, 331–341.

44 Schulz O, Jaensson E, Persson EK, Liu X, Worbs T, Agace WW & Pabst O (2009) Intestinal CD103+, but not CX3CR1+, antigen sampling cells migrate in lymph and serve classical dendritic cell functions. *J. Exp. Med.* **206**, 3101–3114.

45 Varol C, Vallon-Eberhard A, Elinav E, Aychek T, Shapira Y, Luche H, Fehling HJ, Hardt WD, Shakhar G & Jung S (2009) Intestinal lamina propria dendritic cell subsets have different origin and functions. *Immunity* **31**, 502–512.

46 Varol C, Zigmond E & Jung S (2010) Securing the immune tightrope: mononuclear

phagocytes in the intestinal lamina propria. *Nat. Rev. Immunol.* **10**, 415–426.

47 Muehlhoefer A, Saubermann LJ, Gu X, Luedtke-Heckenkamp K, Xavier R, Blumberg RS, Podolsky DK, MacDermott RP & Reinecker H-C (2000) Fractalkine is an epithelial and endothelial cell-derived chemoattractant for intraepithelial lymphocytes in the small intestinal mucosa. *J. Immunol.* **164**, 3368–3376.

48 Kim KW, Vallon-Eberhard A, Zigmond E, Farache J, Shezen E, Shakhar G, Ludwig A, Lira SA & Jung S (2011) In vivo structure/function and expression analysis of the CX 3C chemokine fractalkine. *Blood* **118**, 156-167.

49 Niess JH, Brand S, Gu X, Landsman L, Jung S, McCormick BA, Vyas JM, Boes M, Ploegh HL, Fox JG, Littman DR & Reinecker HC (2005) CX3CR1-mediated dendritic cell access to the intestinal lumen and bacterial clearance. *Science* **307**, 254–258.

50 Chieppa M, Rescigno M, Huang AYC & Germain RN (2006) Dynamic imaging of dendritic cell extension into the small bowel lumen in response to epithelial cell TLR engagement. *J. Exp. Med.* **203**, 2841–2852.

51 Hapfelmeier S, Müller AJ, Stecher B, Kaiser P, Barthel M, Endt K, Eberhard M, Robbiani R, Jacobi CA, Heikenwalder M, Kirschning C, Jung S, Stallmach T, Kremer M & Hardt WD (2008) Microbe sampling by mucosal dendritic cells is a discrete, MyD88-independent step in DeltainvG S. Typhimurium colitis. *J. Exp. Med.* **205**, 437–450.

52 Mowat AM & Bain CC (2011) Mucosal macrophages in intestinal homeostasis and inflammation. *J. Innate Immun.* **3**, 550–564.

53 Bogunovic M, Ginhoux F, Helft J, Shang L, Hashimoto D, Greter M, Liu K, Jakubzick C, Ingersoll MA, Leboeuf M, Stanley ER, Nussenzweig M, Lira SA, Randolph GJ & Merad M (2009) Origin of the lamina propria dendritic cell network. *Immunity* **31**, 513–525.

54 Rivollier A, He J, Kole A, Valatas V & Kelsall BL (2012) Inflammation switches the differentiation program of Ly6Chi monocytes from antiinflammatory macrophages to

inflammatory dendritic cells in the colon. *J. Exp. Med.* **209**, 139–155.

55 Medina-Contreras O, Geem D, Laur O, Williams IR, Lira SA, Nusrat A, Parkos CA & Denning TL (2011) CX3CR1 regulates intestinal macrophage homeostasis, bacterial translocation, and colitogenic Th17 responses in mice. *J. Clin. Invest.* **121**, 4787–4795.

56 Niess JH & Adler G (2010) Enteric flora expands gut lamina propria CX3CR1+ dendritic cells supporting inflammatory immune responses under normal and inflammatory conditions. *J. Immunol.* **184**, 2026–2037.

57 Cerovic V, Houston SA, Scott CL, Aumeunier A, Yrlid U, Mowat AM & Milling SWF (2013) Intestinal CD103− dendritic cells migrate in lymph and prime effector T cells. *Mucosal Immunol.* **6**, 104–113.

58 Diehl GE, Longman RS, Zhang J-X, Breart B, Galan C, Cuesta A, Schwab SR & Littman DR (2013) Microbiota restricts trafficking of bacteria to mesenteric lymph nodes by CX3CR1hi cells. *Nature* **494**, 116–120.

59 Arques JL, Hautefort I, Ivory K, Bertelli E, Regoli M, Clare S, Hinton JCD & Nicoletti C (2009) Salmonella induces flagellin- and MyD88-dependent migration of bacteria-capturing dendritic cells into the gut lumen. *Gastroenterology* **137**, 579–587.

60 Chang SY, Song JH, Guleng B, Cotoner CA, Arihiro S, Zhao Y, Chiang H Sen, O'Keeffe M, Liao G, Karp CL, Kweon MN, Sharpe AH, Bhan A, Terhorst C & Reinecker HC (2013) Circulatory antigen processing by mucosal dendritic cells controls CD8+ T cell activation. *Immunity* **38**, 153–165.

61 Denning TL, Wang Y, Patel SR, Williams IR & Pulendran B (2007) Lamina propria macrophages and dendritic cells differentially induce regulatory and interleukin 17–producing T cell responses. *Nat. Immunol.* **8**, 1086–1094.

62 Hadis U, Wahl B, Schulz O, Hardtke-Wolenski M, Schippers A, Wagner N, Müller W, Sparwasser T, Förster R & Pabst O (2011) Intestinal tolerance requires gut homing and expansion of FoxP3+ regulatory T cells in the lamina propria. *Immunity* **34**, 237–

246.

63 Siddiqui KRR, Laffont S & Powrie F (2010) E-cadherin marks a subset of inflammatory dendritic cells that promote T cell-mediated colitis. *Immunity* **32**, 557–567.

64 Platt AM, Bain CC, Bordon Y, Sester DP & Mowat AM (2010) An independent subset of TLR expressing CCR2-dependent macrophages promotes colonic inflammation. *J. Immunol.* **184**, 6843–6854.

65 Kostadinova FI, Baba T, Ishida Y, Kondo T, Popivanova BK & Mukaida N (2010) Crucial involvement of the CX3CR1-CX3CL1 axis in dextran sulfate sodium-mediated acute colitis in mice. *J. Leukoc. Biol.* **88**, 133–143.

66 Geissmann F, Manz MG, Jung S, Sieweke MH & Ley K (2010) Development of monocytes, macrophages and dendritic cells. *Science* **327**, 656–661.

67 Dogan A, Wang ZD & Spencer J (1995) E-cadherin expression in intestinal epithelium. *J. Clin. Pathol.* **48**, 143–146.

68 Jaensson E, Uronen-Hansson H, Pabst O, Eksteen B, Tian J, Coombes JL, Berg PL, Davidsson T, Powrie F, Johansson-Lindbom B & Agace WW (2008) Small intestinal CD103+ dendritic cells display unique functional properties that are conserved between mice and humans. *J. Exp. Med.* **205**, 2139–2149.

69 Coombes JL, Siddiqui KRR, Arancibia-Cárcamo CV, Hall J, Sun CM, Belkaid Y & Powrie F (2007) A functionally specialized population of mucosal CD103+ DCs induces Foxp3+ regulatory T cells via a TGF-β– and retinoic acid–dependent mechanism. *J. Exp. Med.* **204**, 1757–1764.

70 Sun CM, Hall JA, Blank RB, Bouladoux N, Oukka M, Mora JR & Belkaid Y (2007) Small intestine lamina propria dendritic cells promote de novo generation of Foxp3 T reg cells via retinoic acid. *J. Exp. Med.* **204**, 1775–1785.

71 Johansson-Lindbom B, Svensson M, Pabst O, Palmqvist C, Marquez G, Förster R & Agace WW (2005) Functional specialization of gut CD103+ dendritic cells in the regulation of tissue-selective T cell homing. *J. Exp. Med.* **202**, 1063–73.

72 Annacker O, Coombes JL, Malmstrom V, Uhlig HH, Bourne T, Johansson-Lindbom B, Agace WW, Parker CM & Powrie F (2005) Essential role for CD103 in the T cell–mediated regulation of experimental colitis. *J. Exp. Med.* **202**, 1051–1061.

73 Jaensson-Gyllenbäck E, Kotarsky K, Zapata F, Persson EK, Gundersen TE, Blomhoff R & Agace WW (2011) Bile retinoids imprint intestinal CD103+ dendritic cells with the ability to generate gut-tropic T cells. *Mucosal Immunol.* **4**, 438–447.

74 Matteoli G, Mazzini E, Iliev ID, Mileti E, Fallarino F, Puccetti P, Chieppa M & Rescigno M (2010) Gut CD103+ dendritic cells express indoleamine 2,3-dioxygenase which influences T regulatory/T effector cell balance and oral tolerance induction. *Gut* **59**, 595–604.

75 Fujimoto K, Karuppuchamy T, Takemura N, Shimohigoshi M, Machida T, Haseda Y, Aoshi T, Ishii KJ, Akira S & Uematsu S (2011) A new subset of CD103+ CD8+ dendritic cells in the small intestine expresses TLR3, TLR7, and TLR9 and induces Th1 response and CTL activity. *J. Immunol.* **186**, 6287–6295.

76 Ginhoux F, Liu K, Helft J, Bogunovic M, Greter M, Hashimoto D, Price J, Yin N, Bromberg J, Lira SA, Stanley ER, Nussenzweig M & Merad M (2009) The origin and development of nonlymphoid tissue CD103+ DCs. *J. Exp. Med.* **206**, 3115–3130.

77 Uematsu S, Fujimoto K, Jang MH, Yang BG, Jung YJ, Nishiyama M, Sato S, Tsujimura T, Yamamoto M, Yokota Y, Kiyono H, Miyasaka M, Ishii KJ & Akira S (2008) Regulation of humoral and cellular gut immunity by lamina propria dendritic cells expressing Toll-like receptor 5. *Nat. Immunol.* **9**, 769–776.

78 Laffont S, Siddiqui KRR & Powrie F (2010) Intestinal inflammation abrogates the tolerogenic properties of MLN CD103+ dendritic cells. *Eur. J. Immunol.* **40**, 1877–1883.

79 Kinnebrew MA, Buffie CG, Diehl GE, Zenewicz LA, Leiner I, Hohl TM, Flavell RA, Littman DR & Pamer EG (2012) Interleukin 23 production by intestinal CD103+ CD11b+ dendritic cells in response to bacterial flagellin enhances mucosal innate

immune defense. *Immunity* **36**, 276–287.

80 Mabbott NA, Donaldson DS, Ohno H, Williams IR & Mahajan A (2013) Microfold (M) cells: important immunosurveillance posts in the intestinal epithelium. *Mucosal Immunol.* **6**, 666–77.

81 Schulz O & Pabst O (2013) Antigen sampling in the small intestine. *Trends Immunol.* **34**, 155–161.

82 Chabot S, Wagner JS, Farrant S & Neutra MR (2006) TLRs regulate the gatekeeping functions of the intestinal follicle-associated epithelium. *J. Immunol.* **176**, 4275–4283.

83 Hase K, Ohshima S, Kawano K, Hashimoto N, Matsumoto K, Saito H & Ohno H (2005) Distinct gene expression profiles characterize cellular phenotypes of follicle-associated epithelium and M cells. *DNA Res.* **12**, 127–137.

84 Hase K, Kawano K, Nochi T, Pontes GS, Fukuda S, Ebisawa M, Kadokura K, Tobe T, Fujimura Y, Kawano S, Yabashi A, Waguri S, Nakato G, Kimura S, Murakami T, Iimura M, Hamura K, Fukuoka SI, Lowe AW, Itoh K, Kiyono H & Ohno H (2009) Uptake through glycoprotein 2 of FimH+ bacteria by M cells initiates mucosal immune response. *Nature* **462**, 226–230.

85 Nakato G, Fukuda S, Hase K, Goitsuka R, Cooper MD & Ohno H (2009) New approach for M-Cell-specific molecules screening by comprehensive transcriptome analysis. *DNA Res.* **16**, 227–235.

86 Nakato G, Hase K, Suzuki M, Kimura M, Ato M, Hanazato M, Tobiume M, Horiuchi M, Atarashi R, Nishida N, Watarai M, Imaoka K & Ohno H (2012) Cutting edge: Brucella abortus exploits a cellular prion protein on intestinal M cells as an invasive receptor. *J. Immunol.* **189**, 1540–1544.

87 Kim SH, Jung DI, Yang IY, Kim J, Lee KY, Nochi T, Kiyono H & Jang YS (2011) M cells expressing the complement C5a receptor are efficient targets for mucosal vaccine delivery. *Eur. J. Immunol.* **41**, 3219–3229.

88 Mantis NJ, Cheung MC, Chintalacharuvu KR, Rey J, Corthesy B & Neutra MR (2002)

Selective adherence of IgA to murine Peyer's patch M cells: Evidence for a novel IgA receptor. *J. Immunol.* **169**, 1844–1851.

89 Kadaoui KA & Corthesy B (2007) Secretory IgA mediates bacterial translocation to dendritic cells in mouse Peyer's patches with restriction to mucosal compartment. *J. Immunol.* **179**, 7751–7757.

90 Kujala P, Raymond CR, Romeijn M, Godsave SF, van Kasteren SI, Wille H, Prusiner SB, Mabbott NA & Peters PJ (2011) Prion uptake in the gut: Identification of the first uptake and replication sites. *PLoS Pathog.* **7**, e1002449.

91 Yoshida M, Kobayashi K, Kuo TT, Bry L, Glickman JN, Claypool SM, Kaser A, Nagaishi T, Higgins DE, Mizoguchi E, Wakatsuki Y, Roopenian DC, Mizoguchi A, Lencer WI & Blumberg RS (2006) Neonatal Fc receptor for IgG regulates mucosal immune responses to luminal bacteria. *J. Clin. Invest.* **116**, 2142–2151.

92 McDole JR, Wheeler LW, McDonald KG, Wang B, Konjufca V, Knoop KA, Newberry RD & Miller MJ (2012) Goblet cells deliver luminal antigen to CD103+ dendritic cells in the small intestine. *Nature* **483**, 345–349.

93 Pabst O & Mowat AM (2012) Oral tolerance to food protein. *Mucosal Immunol.* **5**, 232–239.

94 Lelouard H, Fallet M, De Bovis B, Méresse S & Gorvel J (2012) Peyer's patch dendritic cells sample antigens by extending dendrites through M cell-specific transcellular pores. *Gastroenterology* **142**, 592–601.

95 Spahn TW, Fontana A, Faria AMC, Slavin AJ, Eugster H Pietro, Zhang X, Koni PA, Ruddle NH, Flavell RA, Rennert PD & Weiner HL (2001) Induction of oral tolerance to cellular immune responses in the absence of Peyer's patches. *Eur. J. Immunol.* **31**, 1278–1287.

96 Worbs T (2006) Oral tolerance originates in the intestinal immune system and relies on antigen carriage by dendritic cells. *J. Exp. Med.* **203**, 519–527.

97 Fujihashi K, Dohi T, Rennert PD, Yamamoto M, Koga T, Kiyono H & McGhee JR

(2001) Peyer's patches are required for oral tolerance to proteins. *Proc. Natl. Acad. Sci.* **98**, 3310–3315.

98 Enders G, Gottwald T & Brendel W (1986) Induction of oral tolerance in rats without Peyer's patches. *Immunology* **58**, 311–314.

99 Kagnoff MF (1978) Effects of antigen-feeding on intestinal and systemic immune responses. III. Antigen-specific serum-mediated suppression of humoral antibody responses after antigen feeding. *Cell. Immunol.* **40**, 186–203.

100 Qian J, Hashimoto T, Fujiwara H & Hamaoka T (1985) Studies on the induction of tolerance to alloantigens. I. The abrogation of potentials for delayed-type-hypersensitivity response to alloantigens by portal venous inoculation with allogeneic cells. *J. Immunol.* **134**, 3656–3661.

101 Macpherson AJ & Smith K (2006) Mesenteric lymph nodes at the center of immune anatomy. *J. Exp. Med.* **203**, 497–500.

102 Melamed D & Friedman A (1993) Direct evidence for anergy in T lymphocytes tolerized by oral administration of ovalbumin. *Eur. J. Immunol.* **23**, 935–942.

103 Chen Y, Inobe J, Marks R, Gonnella P, Kuchroo V, K., Weiner H & L. (1995) Peripheral deletion of antigen-reactive T cells in oral tolerance. *Nature* **376**, 177–180.

104 Chen Y, Kuchroo VK, Inobe J, Hafler DA & Weiner HL (1994) Regulatory T cell clones induced by oral tolerance: suppression of autoimmune encephalomyelitis. *Science* **265**, 1237–1240.

105 Chen W, Jin W, Hardegen N, Lei K, Li L, Marinos N, McGrady G & Wahl SM (2003) Conversion of peripheral CD4+ CD25− naive T cells to CD4+ CD25+ regulatory T cells by TGF-β induction of transcription factor Foxp3. *J. Exp. Med.* **198**, 1875–1886.

106 Murai M, Turovskaya O, Kim G, Madan R, Karp CL, Cheroutre H & Kronenberg M (2009) Interleukin 10 acts on regulatory T cells to maintain expression of the transcription factor Foxp3 and suppressive function in mice with colitis. *Nat. Immunol.* **10**, 1178–1184.

107 Almond JW (2007) Vaccine renaissance. *Nat. Rev. Microbiol.* **5**, 478–481.

108 Plotkin SA (2009) Vaccines: The fourth century. *Clin. Vaccine Immunol.* **16**, 1709–1719.

109 Neutra MR & Kozlowski PA (2006) Mucosal vaccines: the promise and the challenge. *Nat. Rev. Immunol.* **6**, 148–158.

110 Lycke N (2012) Recent progress in mucosal vaccine development: potential and limitations. *Nat. Rev. Immunol.* **12**, 592–605.

111 Webster RG & Govorkova EA (2014) Continuing challenges in influenza. *Ann. N. Y. Acad. Sci.* **1323**, 115–139.

112 McLean KA, Goldin S, Nannei C, Sparrow E & Torelli G (2016) The 2015 global production capacity of seasonal and pandemic influenza vaccine. *Vaccine* **34**, 5410–5413.

113 Agren LC, Ekman L, Löwenadler B & Lycke NY (1997) Genetically engineered nontoxic vaccine adjuvant that combines B cell targeting with immunomodulation by cholera toxin A1 subunit. *J. Immunol.* **158**, 3936–3946.

114 Agren LC, Ekman L, Löwenadler B, Nedrud JG & Lycke NY (1999) Adjuvanticity of the cholera toxin A1-based gene fusion protein, CTA1-DD, is critically dependent on the ADP-ribosyltransferase and Ig-binding activity. *J. Immunol.* **162**, 2432–2440.

115 Simmons CP, Mastroeni P, Fowler R, Ghaem-maghami M, Lycke N, Pizza M, Rappuoli R & Dougan G (1999) MHC class I-restricted cytotoxic lymphocyte responses induced by enterotoxin-based mucosal adjuvants. *J. Immunol.* **163**, 6502–6510.

116 Agren L, Sverremark E, Ekman L, Schön K, Löwenadler B, Fernandez C & Lycke N (2000) The ADP-ribosylating CTA1-DD adjuvant enhances T cell-dependent and independent responses by direct action on B cells involving anti-apoptotic Bcl-2- and germinal center-promoting effects. *J. Immunol.* **164**, 6276–6286.

117 Bemark M, Bergqvist P, Stensson A, Holmberg A, Mattsson J & Lycke NY (2011) A unique role of the cholera toxin A1-DD adjuvant for long-term plasma and memory B cell development. *J. Immunol.* **186**, 1399–1410.

118 Belyakov IM, Derby MA, Ahlers JD, Kelsall BL, Earl P, Moss B, Strober W & Berzofsky JA (1998) Mucosal immunization with HIV-1 peptide vaccine induces mucosal and systemic cytotoxic T lymphocytes and protective immunity in mice against intrarectal recombinant HIV-vaccinia challenge. *Proc. Natl. Acad. Sci.* **95**, 1709–1714.

119 Cunningham KA, Carey AJ, Lycke N, Timms P & Beagley KW (2009) CTA1-DD is an effective adjuvant for targeting anti-chlamydial immunity to the murine genital mucosa. *J. Reprod. Immunol.* **81**, 34–38.

120 McNeal MM, Basu M, Bean JA, Clements JD, Lycke NY, Ramne A, Löwenadler B, Choi AHC & Ward RL (2007) Intrarectal immunization of mice with VP6 and either LT(R192G) or CTA1-DD as adjuvant protects against fecal rotavirus shedding after EDIM challenge. *Vaccine* **25**, 6224–6231.

121 Eliasson DG, Bakkouri KE, Schön K, Ramne A, Festjens E, Löwenadler B, Fiers W, Saelens X & Lycke N (2008) CTA1-M2e-DD: A novel mucosal adjuvant targeted influenza vaccine. *Vaccine* **26**, 1243–1252.

122 Akhiani AA, Stensson A, Schön K & Lycke N (2006) The nontoxic CTA1-DD adjuvant enhances protective immunity against Helicobacter pylori infection following mucosal immunization. *Scand. J. Immunol.* **63**, 97–105.

123 Kolpe A, Schepens B, Fiers W & Saelens X (2016) M2-based influenza vaccines: recent advances and clinical potential. *Expert Rev. Vaccines* **16**, 123–136.

124 Liu W, Zou P, Ding J, Lu Y & Chen YH (2005) Sequence comparison between the extracellular domain of M2 protein human and avian influenza A virus provides new information for bivalent influenza vaccine design. *Microbes Infect.* **7**, 171–177.

125 Neirynck S, Deroo T, Saelens X, Vanlandschoot P, Jou WM & Fiers W (1999) A

universal influenza A vaccine based on the extracellular domain of the M2 protein. *Nat. Med.* **5**, 1157–1163.

126 De Filette M, Ramne A, Birkett A, Lycke N, Löwenadler B, Min Jou W, Saelens X & Fiers W (2006) The universal influenza vaccine M2e-HBc administered intranasally in combination with the adjuvant CTA1-DD provides complete protection. *Vaccine* **24**, 544–551.

127 Fiers W, De Filette M, Birkett A, Neirynck S & Min Jou W (2004) A "universal" human influenza A vaccine. *Virus Res.* **103**, 173–176.

128 Eliasson DG, Omokanye A, Schön K, Wenzel UA, Bernasconi V, Bemark M, Kolpe A, El Bakkouri K, Ysenbaert T, Deng L, Fiers W, Saelens X & Lycke N (2017) M2e-tetramer-specific memory CD4 T cells are broadly protective against influenza infection. *Mucosal Immunol.* **11**, 273–289.

129 Randolph GJ, Angeli V & Swartz MA (2005) Dendritic-cell trafficking to lymph nodes through lymphatic vessels. *Nat. Rev. Immunol.* **5**, 617–628.

130 Levine MM (2010) Immunogenicity and efficacy of oral vaccines in developing countries: lessons from a live cholera vaccine. *BMC Biol.* **8**, 129.

131 Mayer L & Shao L (2004) Therapeutic potential of oral tolerance. *Nat. Rev. Immunol.* **4**, 407–419.

132 Seong SY, Cho NH, Kwon IC & Jeong SY (1999) Protective immunity of microsphere-based mucosal vaccines against lethal intranasal challenge with Streptococcus pneumoniae. *Infect. Immun.* **67**, 3587–3592.

133 Baca-Estrada ME, Foldvari M, Babiuk SL & Babiuk LA (2000) Vaccine delivery: Lipid-based delivery systems. *J. Biotechnol.* **83**, 91–104.

134 Chabot S, Brewer A, Lowell G, Plante M, Cyr S, Burt DS & Ward BJ (2005) A novel intranasal Protollin™-based measles vaccine induces mucosal and systemic neutralizing antibody responses and cell-mediated immunity in mice. *Vaccine* **23**, 1374–1383.

135 McNeela EA, O'Connor D, Jabbal-Gill I, Illum L, Davis SS, Pizza M, Peppoloni S, Rappuoli R & Mills KHG (2000) A mucosal vaccine against diphtheria: Formulation of cross reacting material (CRM197) of diphtheria toxin with chitosan enhances local and systemic antibody and Th2 responses following nasal delivery. *Vaccine* **19**, 1188–1198.

136 Neutra MR, Mantis NJ & Kraehenbuhl JP (2001) Collaboration of epithelial cells with organized mucosal lymphoid tissues. *Nat. Immunol.* **2**, 1004–1009.

137 Frey A, Giannasca KT, Weltzin R, Giannasca PJ, Reggio H, Lencer WI & Neutra MR (1996) Role of the glycocalyx in regulating access of microparticles to apical plasma membranes of intestinal epithelial cells: implications for microbial attachment and oral vaccine targeting. *J. Exp. Med.* **184**, 1045–59.

138 Mantis NJ, Frey A & Neutra MR (2000) Accessibility of glycolipid and oligosaccharide epitopes on rabbit villus and follicle-associated epithelium. *Am. J. Physiol. Gastrointest. Liver Physiol.* **278**, G915–G923.

139 Lebre F, Hearnden CH & Lavelle EC (2016) Modulation of immune responses by particulate materials. *Adv. Mater.* **28**, 5525–5541.

140 Babiuch K, Gottschaldt M, Werz O & Schubert US (2012) Particulate transepithelial drug carriers: barriers and functional polymers. *RSC Adv.* **2**, 10427–10465.

141 Sahdev P, Ochyl LJ & Moon JJ (2014) Biomaterials for nanoparticle vaccine delivery systems. *Pharm. Res.* **31**, 2563–2582.

142 Verheul RJ, Slütter B, Bal SM, Bouwstra JA, Jiskoot W & Hennink WE (2011) Covalently stabilized trimethyl chitosan-hyaluronic acid nanoparticles for nasal and intradermal vaccination. *J. Control. Release* **156**, 50–56.

143 Singh M, Briones M & O'Hagan DT (2001) A novel bioadhesive intranasal delivery system for inactivated influenza vaccines. *J. Control. Release* **70**, 267–276.

144 Primard C, Poecheim J, Heuking S, Sublet E, Esmaeili F & Borchard G (2013) Multifunctional PLGA-based nanoparticles encapsulating simultaneously hydrophilic

antigen and hydrophobic immunomodulator for mucosal immunization. *Mol. Pharm.* **10**, 2996–3004.

145 Liu Z, Lv D, Liu S, Gong J, Wang D, Xiong M, Chen X, Xiang R & Tan X (2013) Alginic acid-coated chitosan nanoparticles loaded with legumain DNA vaccine: effect against breast cancer in mice. *PLoS One* **8**, e60190.

146 Zhu Q, Talton J, Zhang G, Cunningham T, Wang Z, Waters RC, Kirk J, Eppler B, Klinman DM, Sui Y, Gagnon S, Belyakov IM, Mumper RJ & Berzofsky JA (2012) Large intestine-targeted, nanoparticle-releasing oral vaccine to control genitorectal viral infection. *Nat. Med.* **18**, 1291–1296.

147 Moon JJ, Suh H, Bershteyn A, Stephan MT, Liu H, Huang B, Sohail M, Luo S, Ho Um S, Khant H, Goodwin JT, Ramos J, Chiu W & Irvine DJ (2011) Interbilayer-crosslinked multilamellar vesicles as synthetic vaccines for potent humoral and cellular immune responses. *Nat. Mater.* **10**, 243–251.

148 Moon JJ, Suh H, Li AV, Ockenhouse CF, Yadava A & Irvine DJ (2012) Enhancing humoral responses to a malaria antigen with nanoparticle vaccines that expand Tfh cells and promote germinal center induction. *Proc. Natl. Acad. Sci.* **109**, 1080–1085.

149 Demuth PC, Moon JJ, Suh H, Hammond PT & Irvine DJ (2012) Releasable layer-by-layer assembly of stabilized lipid nanocapsules on microneedles for enhanced transcutaneous vaccine delivery. *ACS Nano* **6**, 8041–8051.

150 Li AV, Moon JJ, Abraham W, Suh H, Elkhader J, Seidman MA, Yen M, Im EJ, Foley MH, Barouch DH & Irvine DJ (2013) Generation of effector memory T cell-based mucosal and systemic immunity with pulmonary nanoparticle vaccination. *Sci. Transl. Med.* **5**, 204ra130.

151 Zhuang Y, Ma Y, Wang C, Hai L, Yan C, Zhang Y, Liu F & Cai L (2012) PEGylated cationic liposomes robustly augment vaccine-induced immune responses: Role of lymphatic trafficking and biodistribution. *J. Control. Release* **159**, 135–142.

152 Cui Z, Han SJ, Vangasseri DP & Huang L (2005) Immunostimulation mechanism of

LPD nanoparticle as a vaccine carrier. *Mol. Pharm.* **2**, 22–28.

153 Reddy ST, Van Der Vlies AJ, Simeoni E, Angeli V, Randolph GJ, O'Neil CP, Lee LK, Swartz MA & Hubbell JA (2007) Exploiting lymphatic transport and complement activation in nanoparticle vaccines. *Nat. Biotechnol.* **25**, 1159–1164.

154 Thomas SN, van der Vlies AJ, O'Neil CP, Reddy ST, Yu SS, Giorgio TD, Swartz MA & Hubbell JA (2011) Engineering complement activation on polypropylene sulfide vaccine nanoparticles. *Biomaterials* **32**, 2194–2203.

155 Stano A, van der Vlies AJ, Martino MM, Swartz MA, Hubbell JA & Simeoni E (2011) PPS nanoparticles as versatile delivery system to induce systemic and broad mucosal immunity after intranasal administration. *Vaccine* **29**, 804–812.

156 Stano A, Scott EA, Dane KY, Swartz MA & Hubbell JA (2013) Tunable T cell immunity towards a protein antigen using polymersomes vs. solid-core nanoparticles. *Biomaterials* **34**, 4339–4346.

157 Jewell CM, Bustamante Lopez SC & Irvine DJ (2011) In situ engineering of the lymph node microenvironment via intranodal injection of adjuvant-releasing polymer particles. *Proc. Natl. Acad. Sci.* **108**, 15745–15750.

158 Rizwan SB, McBurney WT, Young K, Hanley T, Boyd BJ, Rades T & Hook S (2013) Cubosomes containing the adjuvants imiquimod and monophosphoryl lipid A stimulate robust cellular and humoral immune responses. *J. Control. Release* **165**, 16–21.

159 Ali OA, Huebsch N, Cao L, Dranoff G & Mooney DJ (2009) Infection-mimicking materials to program dendritic cells in situ. *Nat. Mater.* **8**, 151–158.

160 Uto T, Akagi T, Yoshinaga K, Toyama M, Akashi M & Baba M (2011) The induction of innate and adaptive immunity by biodegradable poly(γ-glutamic acid) nanoparticles via a TLR4 and MyD88 signaling pathway. *Biomaterials* **32**, 5206–5212.

161 Wegmann F, Gartlan KH, Harandi AM, Brinckmann SA, Coccia M, Hillson WR, Kok WL, Cole S, Ho LP, Lambe T, Puthia M, Svanborg C, Scherer EM, Krashias G,

Williams A, Blattman JN, Greenberg PD, Flavell RA, Moghaddam AE, Sheppard NC & Sattentau QJ (2012) Polyethyleneimine is a potent mucosal adjuvant for viral glycoprotein antigens. *Nat. Biotechnol.* **30**, 883–888.

162 Nakamura T, Yamazaki D, Yamauchi J & Harashima H (2013) The nanoparticulation by octaarginine-modified liposome improves α-galactosylceramide-mediated antitumor therapy via systemic administration. *J. Control. Release* **171**, 216–224.

163 Nakamura T, Moriguchi R, Kogure K & Harashima H (2013) Incorporation of polyinosine-polycytidylic acid enhances cytotoxic T cell activity and antitumor effects by octaarginine-modified liposomes encapsulating antigen, but not by octaarginine-modified antigen complex. *Int. J. Pharm.* **441**, 476–481.

164 Nakamura T, Moriguchi R, Kogure K, Shastri N & Harashima H (2008) Efficient MHC class I presentation by controlled intracellular trafficking of antigens in octaarginine-modified liposomes. *Mol. Ther.* **16**, 1507–1514.

165 Yuba E, Kojima C, Harada A, Tana, Watarai S & Kono K (2010) pH-Sensitive fusogenic polymer-modified liposomes as a carrier of antigenic proteins for activation of cellular immunity. *Biomaterials* **31**, 943–951.

166 Yuba E, Harada A, Sakanishi Y, Watarai S & Kono K (2013) A liposome-based antigen delivery system using pH-sensitive fusogenic polymers for cancer immunotherapy. *Biomaterials* **34**, 3042–3052.

167 Flanary S, Hoffman AS & Stayton PS (2009) Antigen delivery with poly(propylacrylic acid) conjugation enhances MHC-1 presentation and T-Cell activation. *Bioconjug. Chem.* **20**, 241–248.

168 Foster S, Duvall CL, Crownover EF, Hoffman AS & Stayton PS (2010) Intracellular delivery of a protein antigen with an endosomal-releasing polymer enhances CD8 T-cell production and prophylactic vaccine efficacy. *Bioconjug. Chem.* **21**, 2205–2212.

169 Wilson JT, Keller S, Manganiello MJ, Cheng C, Lee CC, Opara C, Convertine A & Stayton PS (2013) PH-responsive nanoparticle vaccines for dual-delivery of antigens

and immunostimulatory oligonucleotides. *ACS Nano* **7**, 3912–3925.

170 Su X, Fricke J, Kavanagh DG & Irvine DJ (2011) In vitro and in vivo mRNA delivery using lipid-enveloped pH-responsive polymer nanoparticles. *Mol. Pharm.* **8**, 774–787.

171 Van Der Vlies AJ, Oneil CP, Hasegawa U, Hammond N & Hubbell JA (2010) Synthesis of pyridyl disulfide-functionalized nanoparticles for conjugating thiol-containing small molecules, peptides, and proteins. *Bioconjug. Chem.* **21**, 653–662.

172 Reinhold SE, Desai KGH, Zhang L, Olsen KF & Schwendeman SP (2012) Self-healing microencapsulation of biomacromolecules without organic solvents. *Angew. Chemie - Int. Ed.* **51**, 10800–10803.

173 Desai KGH & Schwendeman SP (2013) Active self-healing encapsulation of vaccine antigens in PLGA microspheres. *J. Control. Release* **165**, 62–74.

174 Hu CMJ, Fang RH, Luk BT & Zhang L (2013) Nanoparticle-detained toxins for safe and effective vaccination. *Nat. Nanotechnol.* **8**, 933–938.

175 Jung S, Aliberti J, Graemmel P, Sunshine MJ, Kreutzberg GW, Sher A & Littman DR (2000) Analysis of fractalkine receptor CX(3)CR1 function by targeted deletion and green fluorescent protein reporter gene insertion. *Mol. Cell. Biol.* **20**, 4106–4114.

176 Barnden MJ, Allison J, Heath WR & Carbone FR (1998) Defective TCR expression in transgenic mice constructed using cDNA-based alpha- and beta-chain genes under the control of heterologous regulatory elements. *Immunol. Cell Biol.* **76**, 34–40.

177 Bernocchi B, Carpentier R, Lantier I, Ducournau C, Dimier-Poisson I & Betbeder D (2016) Mechanisms allowing protein delivery in nasal mucosa using NPL nanoparticles. *J. Control. Release* **232**, 42–50.

178 Paillard A, Passirani C, Saulnier P, Kroubi M, Garcion E, Benoît JP & Betbeder D (2010) Positively-charged, porous, polysaccharide nanoparticles loaded with anionic molecules behave as "stealth" cationic nanocarriers. *Pharm. Res.* **27**, 126–133.

179 Tsilingiri K, Barbosa T, Penna G, Caprioli F, Sonzogni A, Viale G & Rescigno M

(2012) Probiotic and postbiotic activity in health and disease: comparison on a novel polarised ex-vivo organ culture model. *Gut* **61**, 1007–1015.

180 Tsilingiri K, Sonzogni A, Caprioli F & Rescigno M (2013) A novel method for the culture and polarized stimulation of human intestinal mucosa explants. *J. Vis. Exp.* **75**, e4368.

181 Eriksson A & Lycke N (2003) The CTA1-DD vaccine adjuvant binds to human B cells and potentiates their T cell stimulating ability. *Vaccine* **22**, 185–193.

182 Dombu C, Carpentier R & Betbeder D (2012) Influence of surface charge and inner composition of nanoparticles on intracellular delivery of proteins in airway epithelial cells. *Biomaterials* **33**, 9117–9126.

183 Nikitas G, Deschamps C, Disson O, Niault T, Cossart P & Lecuit M (2011) Transcytosis of Listeria monocytogenes across the intestinal barrier upon specific targeting of goblet cell accessible E-cadherin. *J. Exp. Med.* **208**, 2263–2277.

184 Wallmark B (1989) Omeprazole: mode of action and effect on acid secretion in animals. *Scand. J. Gastroenterol. Suppl.* **166**, 12–18.

185 Ménard S, Cerf-Bensussan N & Heyman M (2010) Multiple facets of intestinal permeability and epithelial handling of dietary antigens. *Mucosal Immunol.* **3**, 247–259.

186 Mohawk JA, Green CB & Takahashi JS (2012) Central and peripheral circadian clocks in mammals. *Annu. Rev. Neurosci.* **35**, 445–462.

187 Druzd D, Matveeva O, Ince L, Harrison U, He W, Schmal C, Herzel H, Tsang AH, Kawakami N, Leliavski A, Uhl O, Yao L, Sander LE, Chen CS, Kraus K, de Juan A, Hergenhan SM, Ehlers M, Koletzko B, Haas R, Solbach W, Oster H & Scheiermann C (2017) Lymphocyte circadian clocks control lymph node trafficking and adaptive immune responses. *Immunity* **46**, 120–132.

188 Thaiss CA, Zeevi D, Levy M, Zilberman-Schapira G, Suez J, Tengeler AC, Abramson L, Katz MN, Korem T, Zmora N, Kuperman Y, Biton I, Gilad S, Harmelin A, Shapiro

H, Halpern Z, Segal E & Elinav E (2014) Transkingdom control of microbiota diurnal oscillations promotes metabolic homeostasis. *Cell* **159**, 514–529.